การวิเคราะห์โครงสร้างทางธรณีวิทยาในแอ่งเมอร์กุยตอนใต้ ทะเลอันดามัน

นางสาวนิรมล ตินตกร

วิทยานิพนธ์นี้เป็นส่วนหนึ่งของการศึกษาตามหลักสูตรปริญญาวิทยาศาสตรมหาบัณฑิต
สาขาวิชาธรณีวิทยา ภาควิชาธรณีวิทยา
คณะวิทยาศาสตร์ จุฬาลงกรณ์มหาวิทยาลัย
ปีการศึกษา 2554

ANALYSIS OF GEOLOGICAL STRUCTURES IN THE SOUTHERN MERGUI BASIN, ANDAMAN SEA

Miss Niramol Tintakorn

A Thesis Submitted in Partial Fulfillment of the Requirements

for the Degree of Master of Science Program in Geology

Department of Geology

Faculty of Science

Chulalongkorn University

Academic Year 2011

CHAPTER I
INTRODUCTION

1.1 General backgrounds

The demand for natural resources, especially oil and gas are increasing every year, as a result, the price of oil and gas has increased continuouly. Therefore, the petroleum exploration is necessary and important to a developing country to minimize the amount of petroleum imported in the near future. The discovery and development of local petroleum resources from both onshore and offshore areas, such as the Fang oil field, the Sirikit oil field, the Kamphaeng Saen and U-Thong oil field etc (Figure 1.1). As most petroleum fields in Thailand are located in shallow water which will become exhausted in the future. Thus, there is a need for petroleum exploration in area with deep water setting, and the Andaman Sea region, is one of the prime prospect. The Andaman Sea consists of the largest Tertiary basin in Thailand (Mahatanachai, 1996). Two separated basins are recognized in the Andaman Sea, including the Andaman Basin and the Mergui Basin (Figure 1.2) (Polachan, 1988).

The Mergui basin in the Andaman region is located in the offshore of western peninsular Thailand (Figure 1.2). This area is very important because of the discovery of gas traces from few drilling wells and has continuous accumulation of sediments with the thickness of more traces than 8,000 meters (Department of Mineral Resouces, 2007) in the Tertiary and Quaternary time. Petroleum found in the basin is very deep and exploratory wells contain petroleum-bearing sediment layers between 1,700 and 4,200 meters (from sea surface) (Department of Mineral Resources, 1996). The petroleum reservoirs in the basin is considered to be mainly controlled by geological structure (Department of Mineral Resources, 1996).

This study concerns with analyzing geological structures by using investigated results of seismic interpretation in conjunction with previous core–log and biostratigraphic reports to interprete evolution of structures. The study result may be useful in applications for the petroleum potential in the study area.

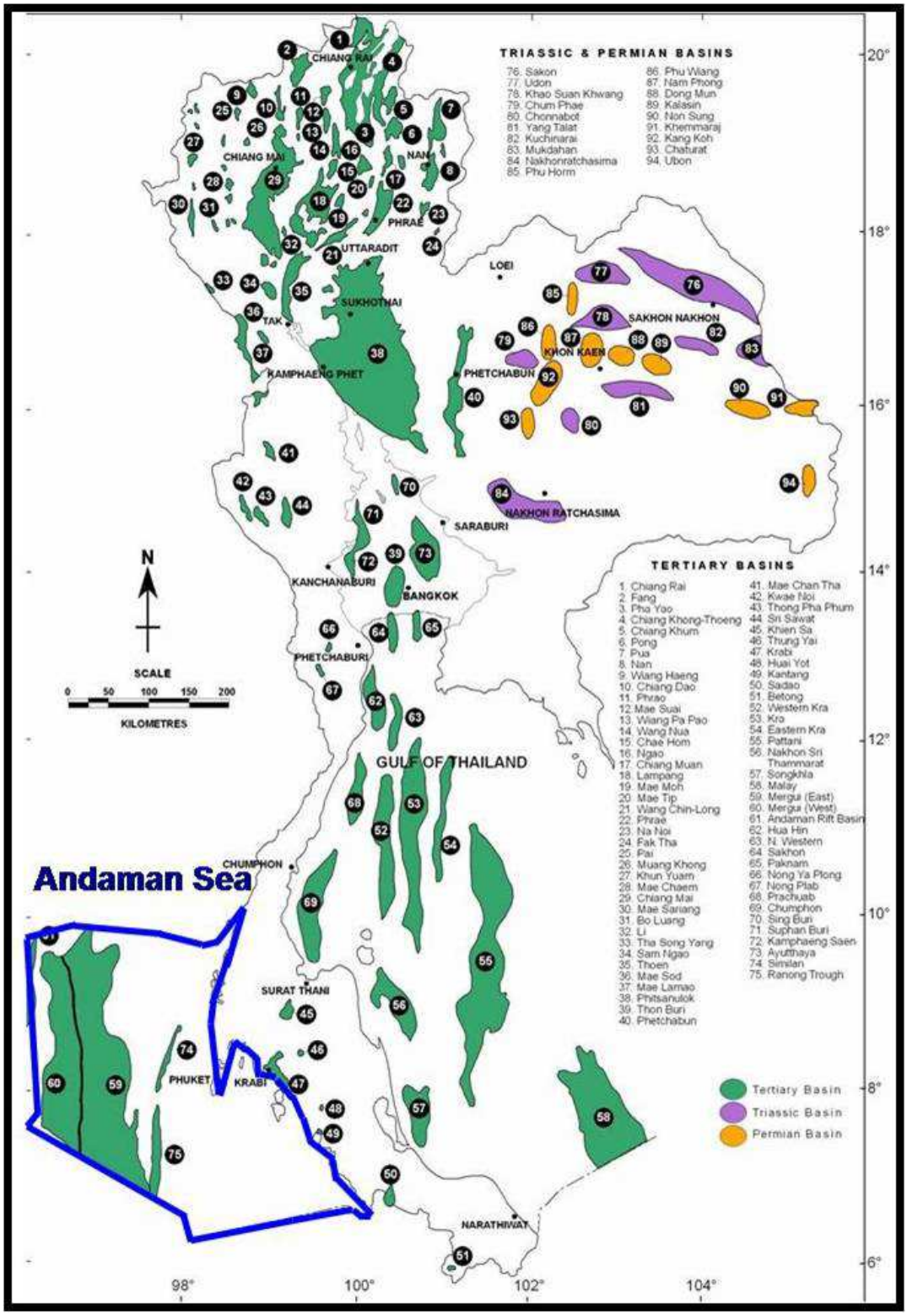

Figure 1.1 A map showing petroleum basins of Thailand. The blue-colored outline represents the Tertiary Mergui basin in the Andaman region (modified from Srikulwong, 2005).

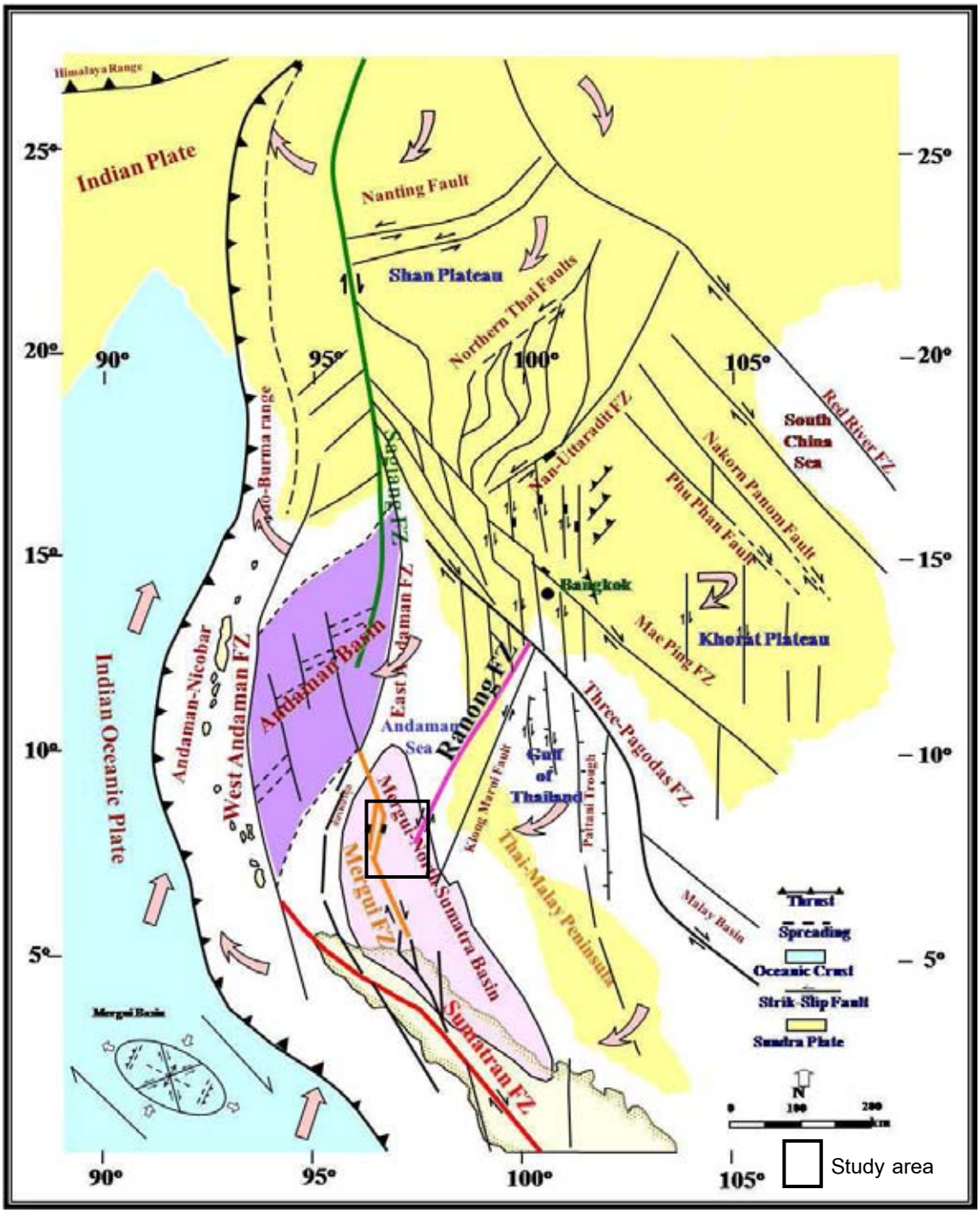

Figure 1.2 Plate motions and simplified structural framework of Cenozoic basins in the Gulf of Thailand and the Andaman Sea (modified after Polachan, 1988 and Mahatanachai, 1996).

1.2 Purpose of study

The objective of this research is to study geological structure style and describe in evolution of the southern Mergui basin.

1.3 Location and study area

The study area is located within the deep water offshore (Mahatanachai, 1996) of the Andaman Sea at the western peninsula Thailand with the water depth deeper than 200 meters (Figure 1.3) The study area is bounded by the Myanmar border to the north and by the Nicobar Islands of India to the west and Malaysia and Indonesia borders to the south (Department of Mineral Fuels, 2006). It is located between latitudes 7°0'22" N to 8 °31'27" N and longitudes 96°2'05" E to 97°33'45" E. The area covers about 22,000 square kilometers and lies within concession block W9/38 and W8/38 (A4/43).

1.4 Exploration History

Petroleum exploration history in the Andaman Sea began in 1971 – 1972 with the result of the 1st and 2nd Petroleum concession bidding round in Thailand (Mahatanachai,1996) but no exploration was conducted. In 1974, the government amended the petroleum law and promote the petroleum exploration and production in sea-water deeper than 200 meters (Department of Mineral Resouces or DMR, 2006) which leads to subsequent petroleum activities in Thailand, including the Andaman Sea. In 1974, the Union Oil Company of Thailand and collaborating companies drilled 6 exploration wells in the W8 block concession and traces of gas were found by in the Merqui-1 well (Figure 1.4).

After that the Esso Exploration and Production Thailand Inc. drilled five exploration wells in the concession exploration of W9 block, and gas shows were found (Department of Mineral Resouces or DMR, 2006). However, the activities in the Andaman Sea has continued to the 10th round concession bidding in 1987. Placid Oil Company drilled 2 wells in the block W8 concession in water depth of 618-655 meters and minor gas was found in the Yala-1 well (Figure 1.4). For the 14th round concession bidding in 1995, the Unocal Bangkok Co. obtained the concessions of W8/38 and W9/38 blocks and has seismic survey of 11,737 line-kilometers were lunched and three wells in

W8/38 block and the other 2 wells in W9/38 block were drilled subsequently, but no petroleum was discovered. During the 16th round concession bidding in 1997, the Kerr-Mcgee (Thailand) Co. Ltd. obtained the concession of W7/38 block and drilled the Manora-1 well, but no petroleum was discovered (Figure 1.4).

The petroleum discovered in this region was derived from the marine source rocks which were wildly distributed in the basin. Thus it is still considered to be a high potential area for petroleum exploration in the future (Department of Mineral Fuels or DMR, 2006).

1.5 Literature Reviews on the study area

1.5.1 Geologic setting and Geologic Structures.

The Andaman Sea is located along the eastern side of the Indian Ocean between the Malay Peninsula and the Andaman and Nicobar Islands (Global Ocean Associates, 2002). The area covers about 114,000 square kilometers in the Thai territory. The seafloor characterized a stream terrace descended down from the coast to centre of basin (Department of Mineral Resouces, 2006). In the Andaman Sea consist the biggest Tertiary-age basin such as the Andaman Basin and the Mergui Basin. The Mergui Basin can be subdivided into 2 sub-basins, the Western Mergui Basins blocked by Mergui fault zone and the Eastern Mergui Basins are divided by the Central High (Polachan, 1988) (Figure 1.5 and Figure 1.6). From study of Morley (2002) suggested Mae Ping (MPFZ), Three Pagodas (TPFZ) and Ranong and Klong Marui faults related rift systems that developed of the Andaman Sea and the Mergui during the Tertiary period.

1.5.2 Stratigraphy.

Hutchison (1975, 1977), Suensilpong (1977), Suensilpong et al. (1981) and Beckinsale et al. (1979) reported that granitic rocks of the Thai-Malay Peninsula form the principal crystalline basement to the Mergui Basin. Cretaceous - Early Tertiary granitic rocks represent the magmatic arc resulting from the subduction of the Indian Oceanic crust beneath the southern margin of the SE Asian plate, which consistent with studied by Garson and Mitchell (1970), Ridd (1971) Koch (1973) and Suensilpong, (1977)

suggested granitic rocks have been faulted, jointed and offset by tensional stresses related to the movement of the Ranong-Klong Marui and Three Pagodas Faults.

The regional stratigraphy of the Mergui Basin has been based on geological data from ten wells and have been studied by Nakanart and Mantajit (1983) suggested informally divided the Tertiary sequences into several formations, stratigraphic relationships or thicknesses, which consistent with studied by Polachan and Racey (1994) suggested stratigraphic sequence of the Mergui Basin can be subdivided into 9 formations on the basis which the formation was deposited in a very shallow marine environment to deep marine environment.

Srikulwong (1986) suggested sedimentation of the area began in early Late Oligocene as the shallow marine environment which then rapidly change to deep marine environment. And from studied by Tananchai (2004) can be identified seismic facies consist of the Basement Seismic Facies, the Carbonate Seismic Facies, the Deep Marine Seismic Facies, and the Clinoform Seismic Facies and suggest that the depositional environments of seismic package vary between shallow water, or shoreface, and deep marine. According to Andmason et al. (1997), hydrocarbons are primarily being generated and migrating from the deep Eastern Mergui and Western Mergui Basin. Miocene reefs and Oligocene to Miocene fluvio-deltaics and turbidites constitute the major potential exploratory plays. The sediment deposited in this basin are more than 8,000 meters, the Pre-Tertiary Basement is covered by the Tertiary sediments (Department of Mineral Resouces, 2006).

1.5.3 Geotectonic and Tectonic Evolutions

The structural trend of the Barisan Range of northern Sumatra and the Burma Range can be linked through the Andaman Sea (Peter et al., 1966). The linear structural belts on land were traced through the Andaman. The structural development of the island arc system from east to west, by Weeks et al. (1967) suggested the island arc system includes foredeep, outer sedimentary island arc, interdeep, inner volcanic arc (and rift valley), and backdeep.

The continental margin and the Andaman-Nicobar Ridge were then rifted apart by Late Miocene to Recent movements produced dilational stress which opened up and formed the Andaman Basin as a rhombochasm (Rodolfo, 1969 and Shouls, 1973). The Mergui Basin may have opened as a result of a dextral shear couple bounded to the east by the NE-SW trending Ranong - Klong Marui Fault system and to the west by the Sagaing - Sumatra Fault System (Ridd, 1971 and Morley, 2002). According to Molnar and Tapponnier (1975), the Mergui Basin opened progressively northwards as a wedge-shaped gap, concurrently with strike-slip movements along the Ranong-Klong Marui and Sagaing-Sumatra Fault Systems in the Oligocene. However, Tapponnier et al., (1982, 1986) suggested explain the tectonics caused by the collision of India with Eurasia plate about 2,500-3,500 kilometers and displacements in excess of 1,000–1,500 kilometers, which the area is subduction beneath the Andaman-Nicobar ridge (Dain et al., 1984).

The geological evolution of the Mergui Basin SE. Andaman Sea, Thailand studied by Polachan (1988) suggested the basin overlies continental crust at the western edge of Sundaland association with a major subduction zone which extends along the west coast of Sumatra. The time of reactivation of pre-existing fault fabrics can be related to the development of a series of NW-SE and NE-SW trending faults. Right-lateral wrench faults also formed along the western margin of the basin during the mid-Miocene due to the major regional compression, caused by the northwards movement of the Indian Plate.

Packham (1993) gave a global view on basin evolution and tectonics in the area. Plate tectonic reconstructions are illustrated four periods of time, i.e., in the Late Oligocene to Early Miocene, a Late Eocene to Oligocene rifting phase, the Middle Miocene and the present regime of oblique subduction and partial coupling of the combined Australia-India Plate to the Southeast Asian part of the Eurasia Plate was initiated in the Middle Eocene.

Curray et al. (2004) suggested active sea-floor spreading in the Andaman Sea and rifting of the Mergui-North Sumatra Basin may be related to the displacement of crustal blocks along these faults. The Mergui Basin starting at 32 Ma.

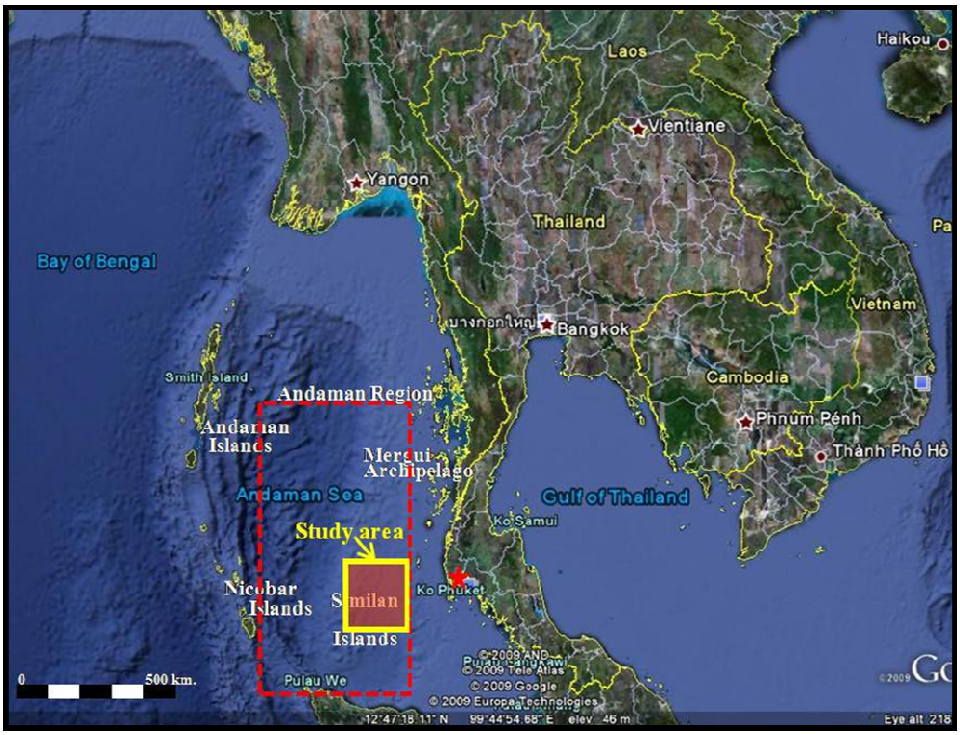

Figure 1.3 Location of the study area (yellow square) in the Andaman Region (red square) (on Google map).

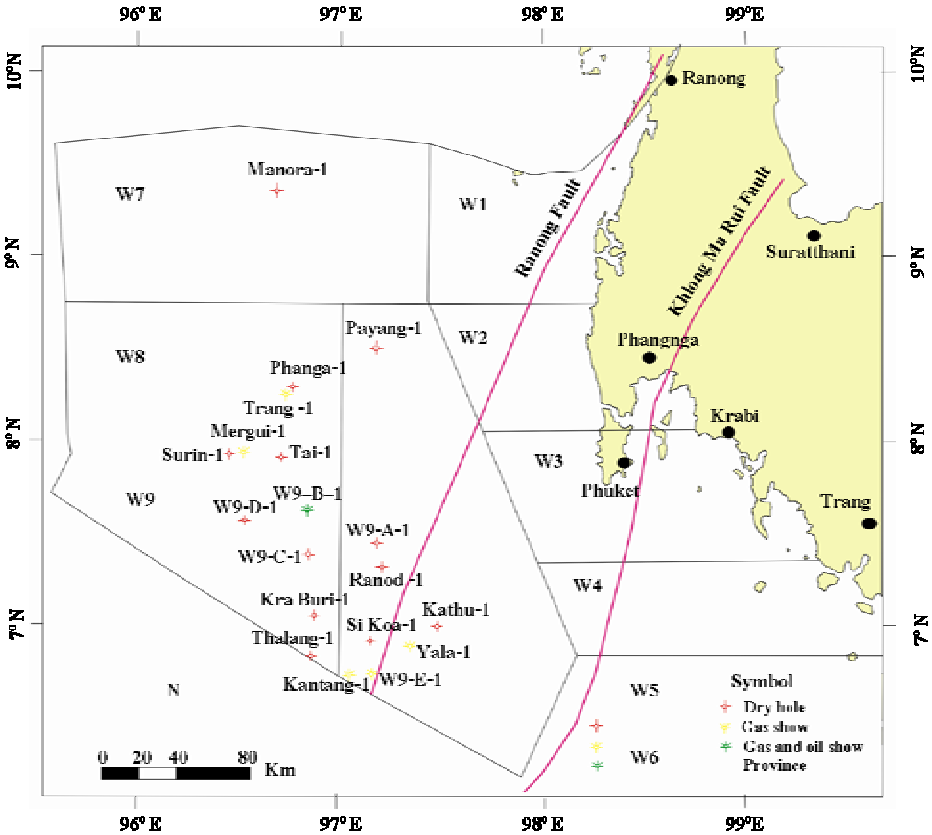

Figure 1.4 Well-locations and outline of blocks W-1 to W-9 in the Mergui Basin (modified from Polachan and Racey, 2005 and Department of Mineral Fuels, 2006).

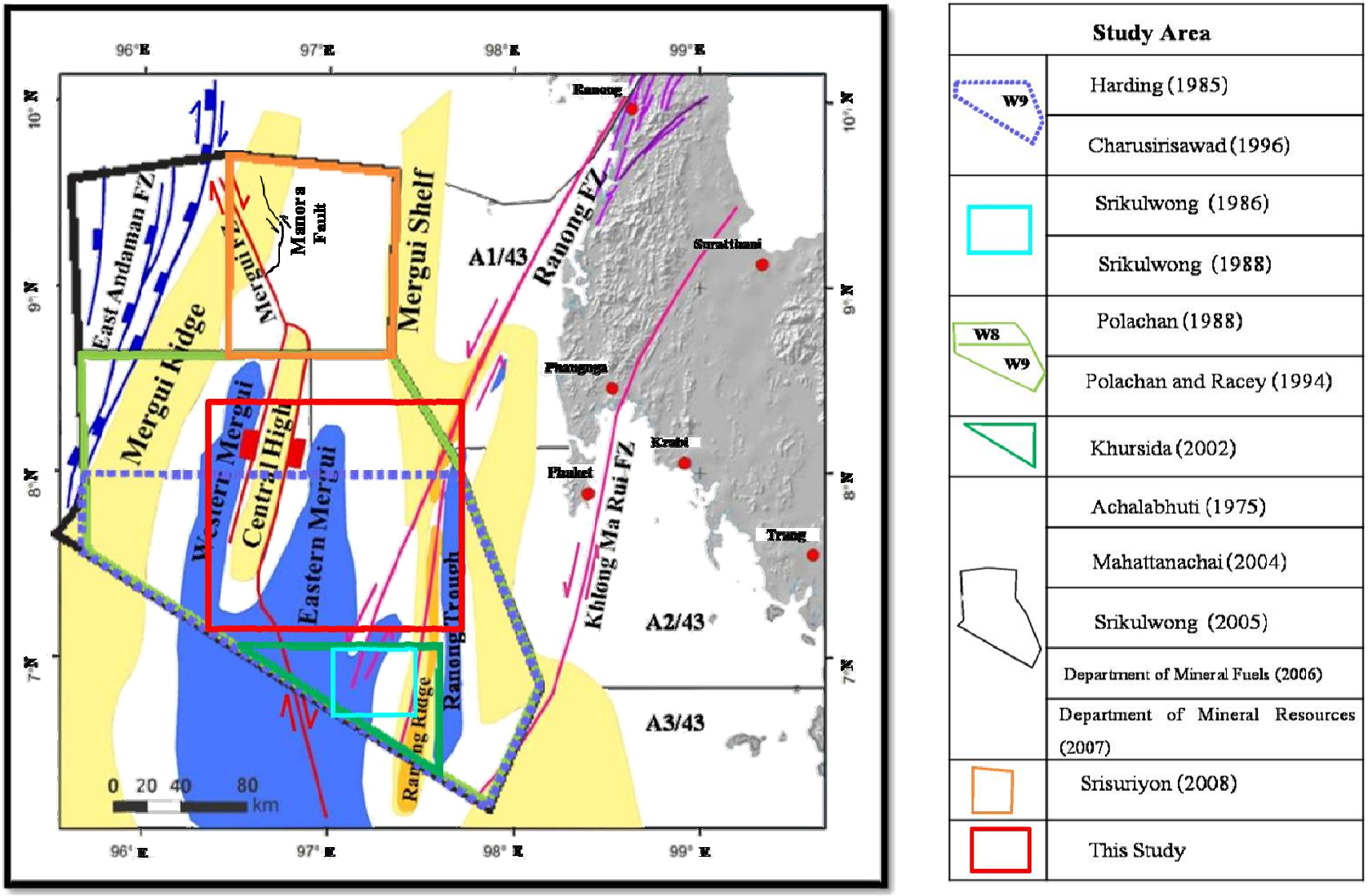

Figure 1.5 Locations of the previous and present studies in the Mergui Basin, Andaman Sea, (modified after, Mahatanachai, 1996 and Thipyopass, 2010).

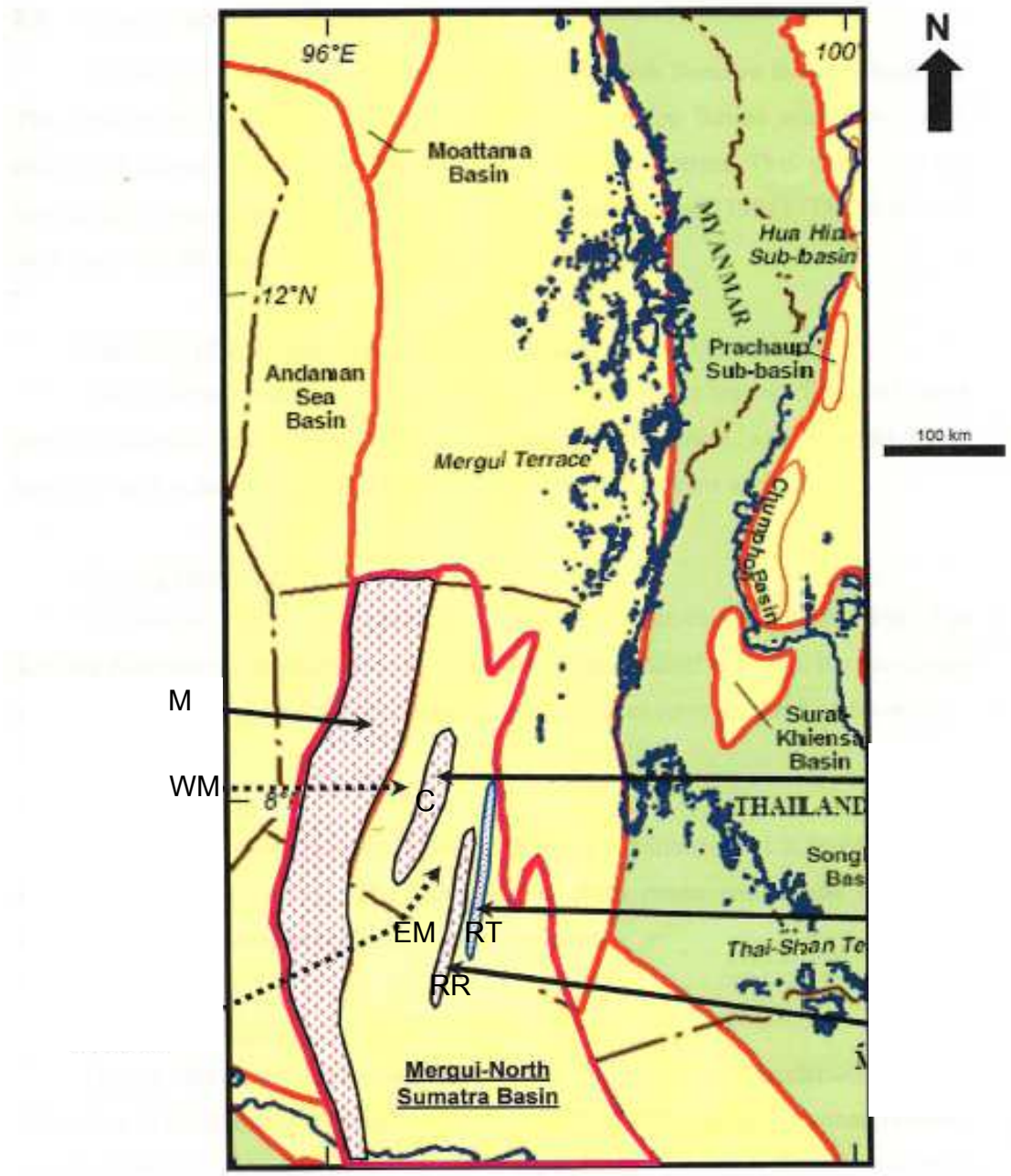

Figure 1.6 Map of the Andaman Sea showing major geological provinces of the Mergui Basin; M = Mergui Ridge, WM = West Mergui sub-basin, EM = East Mergui sub-basin, C = Central High, RT = Ranong Trough and RR = Ranong Ridge (modified Polachan and Racey, 1994, Srisuriyon, 2008).

Recently, Srisuriyon (2008) studied structural style and evolution of the northern Mergui basin, Northern Mergui Basin shows a series of NNW-SSE strike-slip and NE-SW extensional faults. The NNW-SSE faults display distribution of compressional and extensional features at fault tips, and restraining and releasing bends consistent with dextral motion, faults fit with to regional tectonic regime characterised by dextral motion along (N-S trending) Sagiang fault and high displacement during Oligocene-Middle Miocene (syn-rift) and less in Late Miocene to Pliocene (post-rift, passive margin stage).

1.5.4 Geochemistry and Petroleum Assessment.

Geochemical results (Achalabhuti, 1975) in the Tertiary strata revealed that the Tertiary source beds are mainly immature. Tertiary sediments have a low potential for hydrocarbon accumulations. Biostratigraphic studied indicate that the depositional environment changed occasionally from Oligocene to Present (Achalabhuti, 1975). Geochemicals analysis by Khursida (2002) indicates both oil and gas prone types. The sandstone and reefal limestones are of fair to good quality reservoir. The marine claystone, siltstone and shale are effective hydrocarbon seal, which petroleum generation might have been the oil generation at a depth below the oldest sedimentary unit, 1,000 meters in Kantang-1a well and 1,200 to 1,300 meters in Kraburi-1 well.

Exploration area can be divided into 2 areas based on water depth, i.e., a shallow water with the water depth less than 200 meters and the deep water with a depth water deeper than 200 meters. Traces of gas have been recorded in well nos. W9-B-1, Trang-1, Mergui-1, W9-E-1, Yala-1, and Kantang-1 (see Figure 1.4) Such discovery allows D). The type of petroleum traps can be divided into 3 types, i.e., the structural traps, the stratigraphic traps and the combination traps (Department of Mineral Fuels, 2006).

1.6 Methodology

The flow chart (Figure 1.7) showing sequences of work and methodology used in this study can be divided into 7 steps including:

1.6.1 Literature reviews, the first step, including collecting data for supporting further steps and several previous works on regional geology, stratigraphy, geomorphology, geological structures geotectonics and biostratigraphic reports etc.;

1.6.2 Wireline log data collection based on work by ESSO (1976) and interpretation including compilation and interpretation of 4 wells using gamma ray log (GR) and sonic log (DT), from well no. W9D-1, W9B-1, W9A-1 and W9C-1. Listhostratigraphy and deposition environments have been done on the basis of wireline log interpretation

1.6.3 Selection and enhancement of seismic data and interpretation from section provided by Department of Mineral Fuel (DMF) using Kingdom 8.4 suite enhancement software program. Seismic data used in this study consistes of 10 lines of the 2D seismic reflection surveys in digital format. Geologic structures in this area have been determined based on the seismic interpretation.

1.6.4 Comparison of the results of seismic data with those of the wire-line log data to describe stratigraphic sequences and structures;

1.6.5 Interpretation geological structures for determining fault displacement (see Appendix C) tectonic setting and evolution of the basin;

1.6.6 Discussion on sequences of faulting, geological structures, and geotectonic evolution; and

1.6.7 Conclusion of the results of this research.

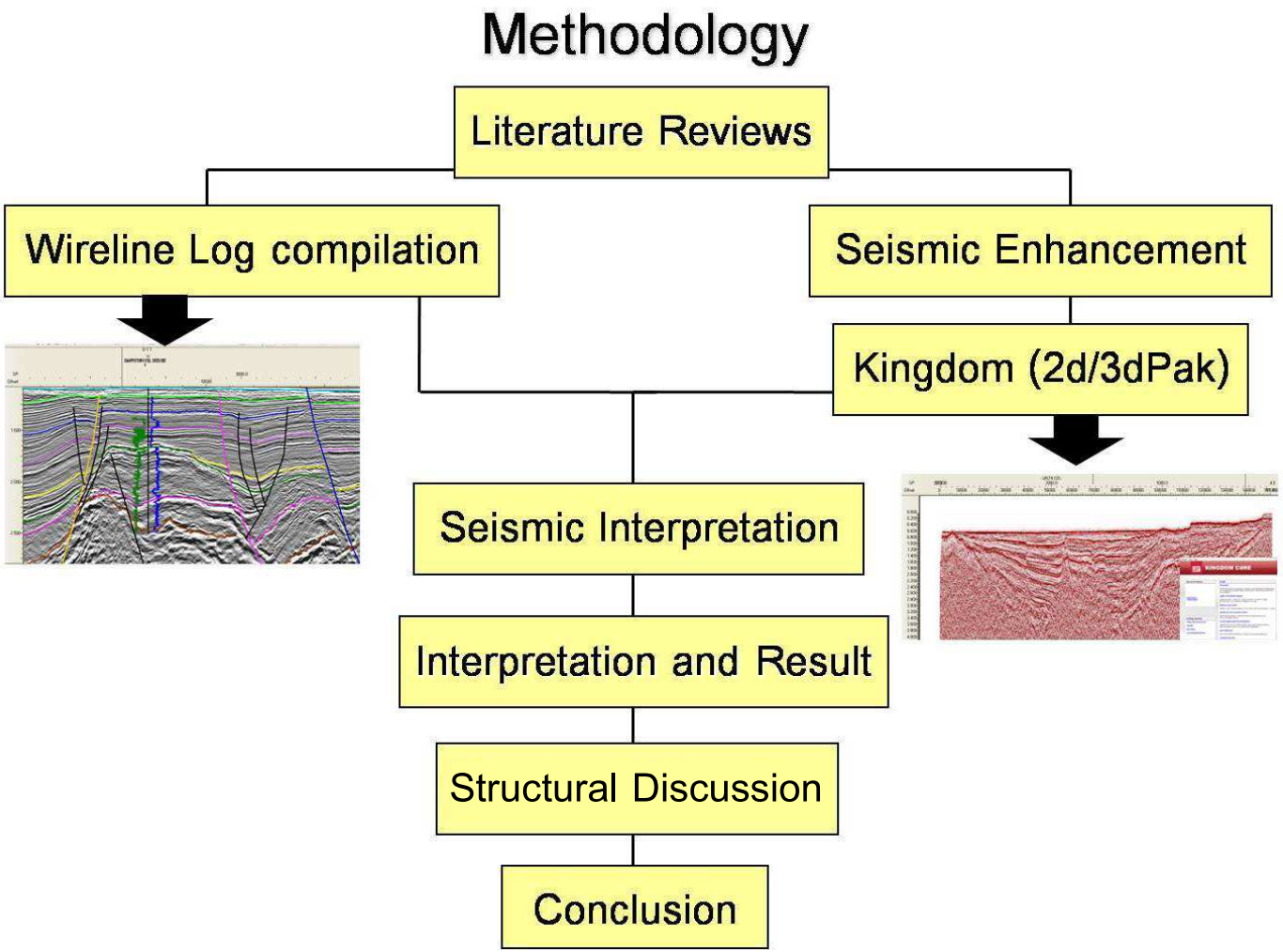

Figure 1.7 Flow chart showing the methodology used in this study.

CHAPTER II
GENERAL GEOLOGY

2.1 Regional Framework

The Andaman Sea located at the edge of the Sundaland Craton, is a complex tectonic region, which the Indian oceanic crust collision with the Eurasian Plate at about 59 Ma (Curray, 2005). The Indian oceanic crust has been subducted to the NNE below the Eurasian Plate at a rate of 6-7 cm/year in Early Tertiary (Tapponier et al., 1982; Polachan et al., 1988). The Andaman Sea has a spreading center to the west and Peninsular Thailand to the east and it opens in a NNW-SSE direction at a rate of 3.72 cm/yr spreading axes which are offset by a series of NNW trending right-lateral transform faults which connect to the Sumatra Fault System (Curray et al., 1979). The oblique opening by a succession of extensional episodes, which extension normal to the trend of the subduction zone combined with strike-slip faulting. During the collision of India with Asia, the alignment of the Sunda subduction zone gradually rotated in a clockwise direction (Figures 2.1 and 2.2).

The Indian Plate moved continuously to the north (between 44 Ma and 32 Ma), causing several large faults, e.g., the Sumatran Fault, Eastern and Western Andaman Faults, and Sagiang Fault, which GPS data recorded the rate of Sagiang Fault movement at about 20 mm/yr (Curray, 2005). As these faults were increasingly intensified, the basins had been rifted and subsequently subjected to continuous subsidence as transtensional deformation in the North Sumatra and Mergui Basin, which occurred the Central Andaman Basin. The faulting moved onshore from the Mentawai Fault to the Sumatra Fault System in the Cenozoic (about 32 Ma). Between 23 Ma to 15 Ma, the area extended as a result of clockwise rotation and bending of the northern and western Sunda Arc (Curray, 2005) (Figure 2.2), the rate of India plate motion is about 15 mm/yr during 2.5 Ma to 2Ma age. The Andaman Sea formed at the NE-SW trending spreading centre at the rate of 16 mm/yr. and speed up to 38 mm/yr. (Curray, 2005) in the present day time.

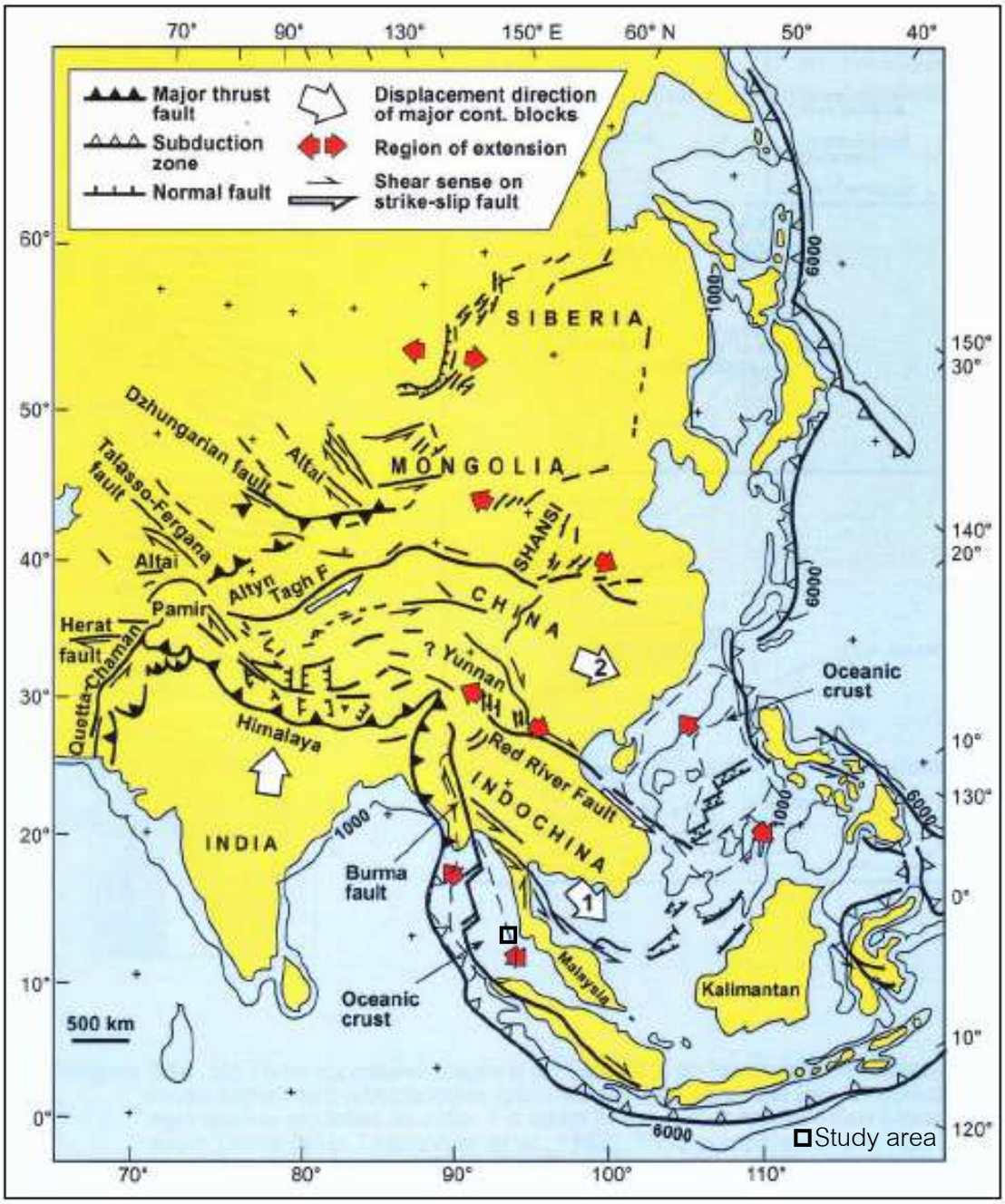

Figure 2.1 Tectonic map of the south and the east Asia illustrating 'extrusion' model and its relationship with Cenozoic structures in the region, including the Andaman Sea and the study are. Numbers in white arrows indicate the relative order in which certain continental blocks were extruded toward the southeast (after Tapponnier et al., 1982).

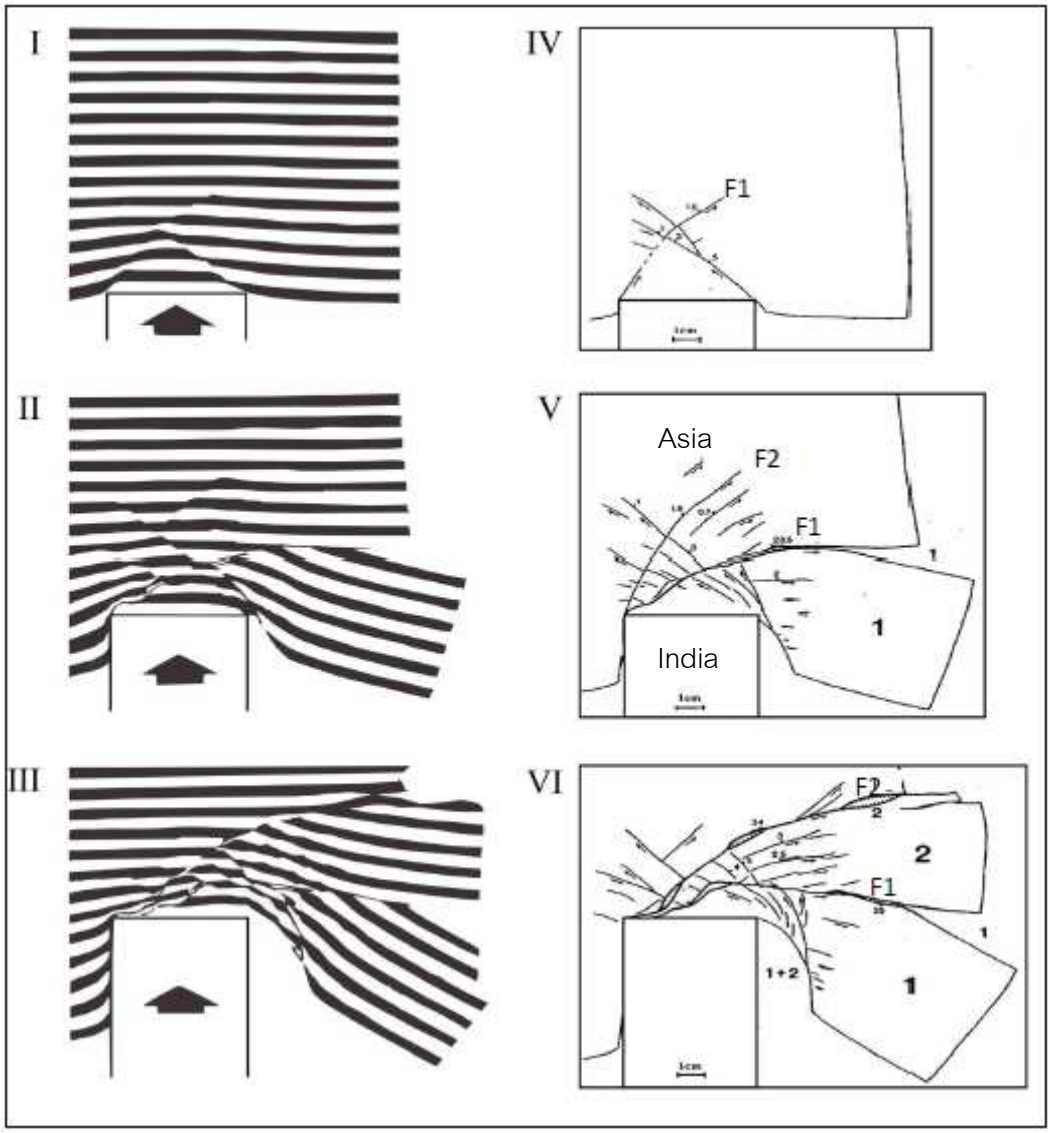

Figure 2.2 Three successive stages (I to III) and extrusion-tectonic model (IV to VI) with plasticine experiment (plain view). In unilaterally confined experiment, two major faults (F1 and F2) guide successive extrusion of two blocks. In stage VI, blocks 1 and 2 can be compared to Indochina and southern China, and open gap 1, 1+2, 2 to South China Sea, Andaman Sea, and northeastern China, respectively (Tapponnier et al., 1982).

The main normal fault in the area made the Andaman Basin and the Mergui Basin on the north-south direction (Srikulwong, 1986), which related the Mae Ping Fault, Three Pagodas Fault and Ranong-Khlong Marui Faults (Morley, 2002) (Figures 2.3 and 2.4).

Tectonic framework of this region consists of 4 different geological provinces: Indoburman Ranges; the Andaman Sea and Central Lowlands of Burma; the Mergui-North Sumatra Basin; and the Thai-Malay Peninsula (Polachan, 1988).

This Mergui Basin has a V-shaped geometry, underlain by thin continental crust on the western edge of Sundaland (Polachan, 1988). The basin stretched during the late Oligocene stage, the phase of opening is aborted probably in the early Miocene, and the present phase of opening started with formation of oceanic sea floor during middle Miocene (13 Ma) in a NW-SE direction (Curray et al., 1979, 1982; Lawver and & Curray, 1981) along a rectilinear plate edge, with short segments of spreading axis and transform faults.

2.2 Major Structures

2.2.1 Structural Geology

Andaman Sea consists of the large Tertiary basin 2 basins, i.e. the Andaman Basin and the Mergui Basin on the west and east respectively. Boths basins are separated by Mergui Ridge. The Mergui Ridge represents the western edge of the Sunda Craton (Curray et al., 1979) (Figure 2.5). The Mergui Basin constitutes the true Tertiary marine basin in Thailand. The area covers some 50,000 square kilometers, which the water depths of 200 to over 3,000 m (Polachan and Racey, 1994) can be further subdivided into 2 sub-basins, the Western Mergui Basins and the Eastern Mergui Basins. The Western Mergui Basins is located between the Mergui Ridge and the Central High (Figures 2.5). The eastern side of basin is bounded by the Mergui Fault Zone. The Eastern Mergui Basins is located between the Central High in the west and the Mergui Shelf in the northeast or the Ranong Fault Zone in the southeast (Polachan, 1988) (Figure 2.5). The Central High is a horst-block extending along the Mergui Fault Zone. The Mergui Shelf is a part of the mainland (Shan-Thai block of the Sunda Craton)

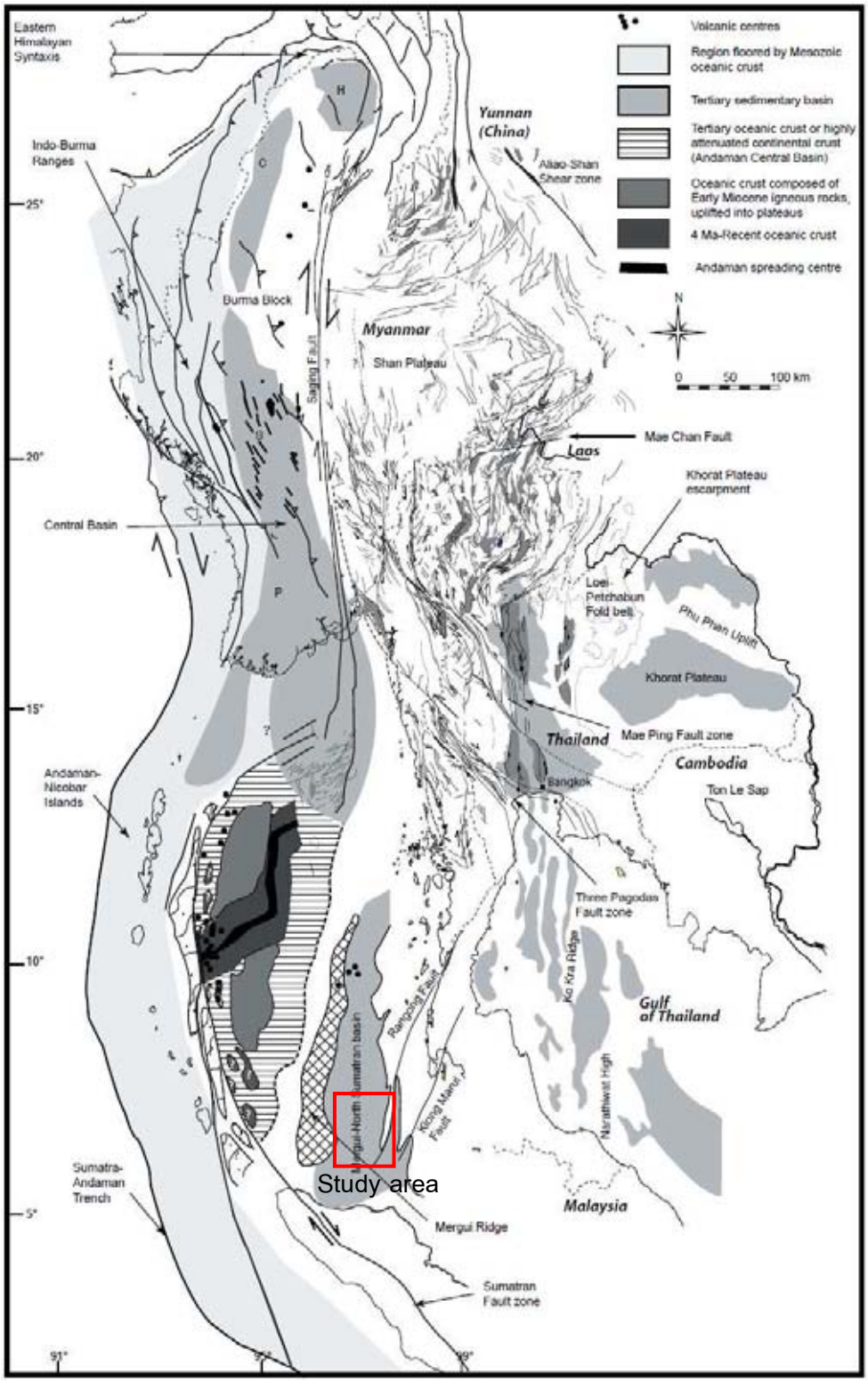

Figure 2.3 Main Cenozoic-Recent tectonic and structural features of the Myanmar-Western Thailand region of the back-arc mobile belt (Pivnik et al., 1998, Morley, 2004, and Curray, 2005).

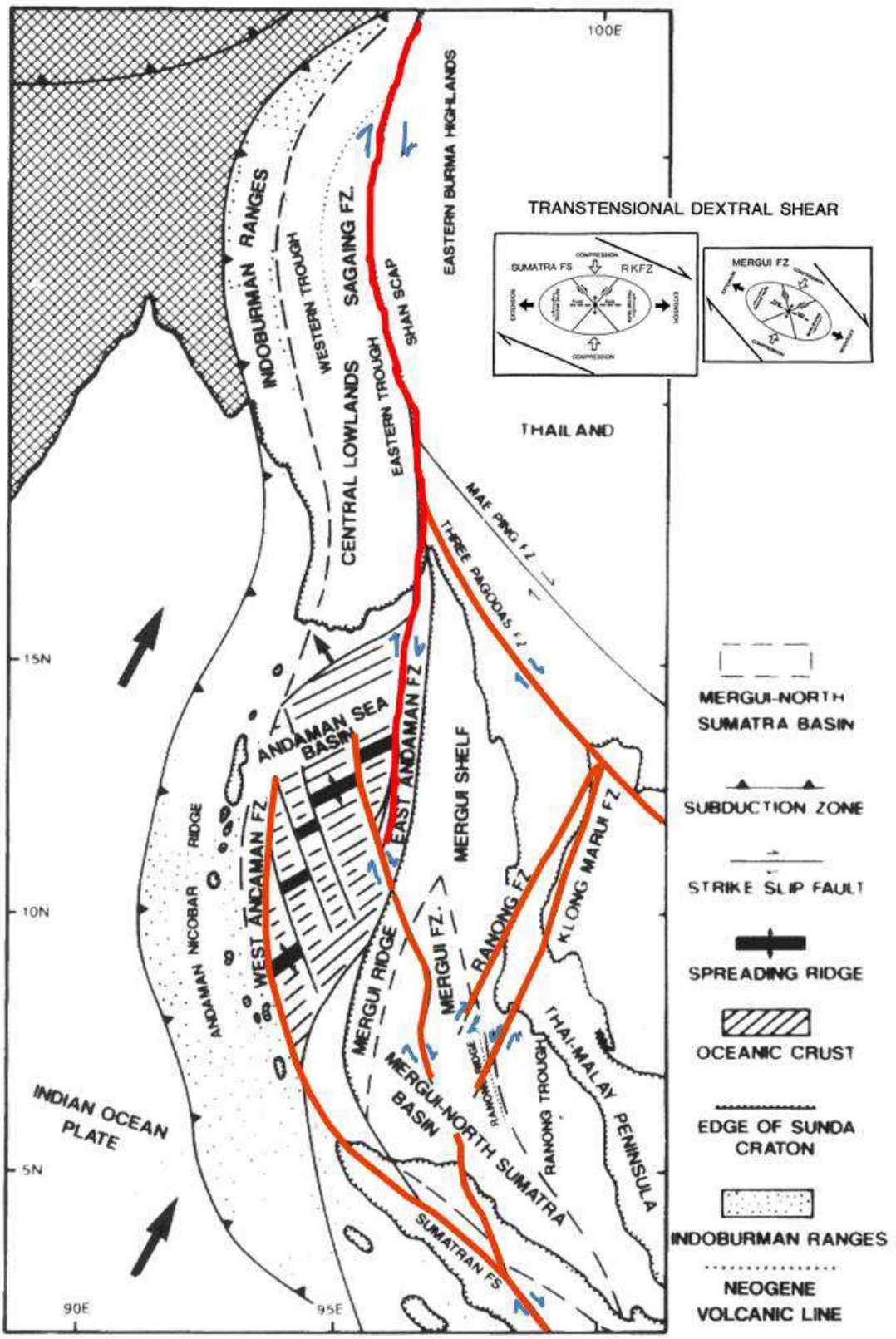

Figure 2.4 Tectonic map of the Mergui-North Sumatra and Andaman sea. The red-colored outline represents the major faults. (Polachan, 1988)

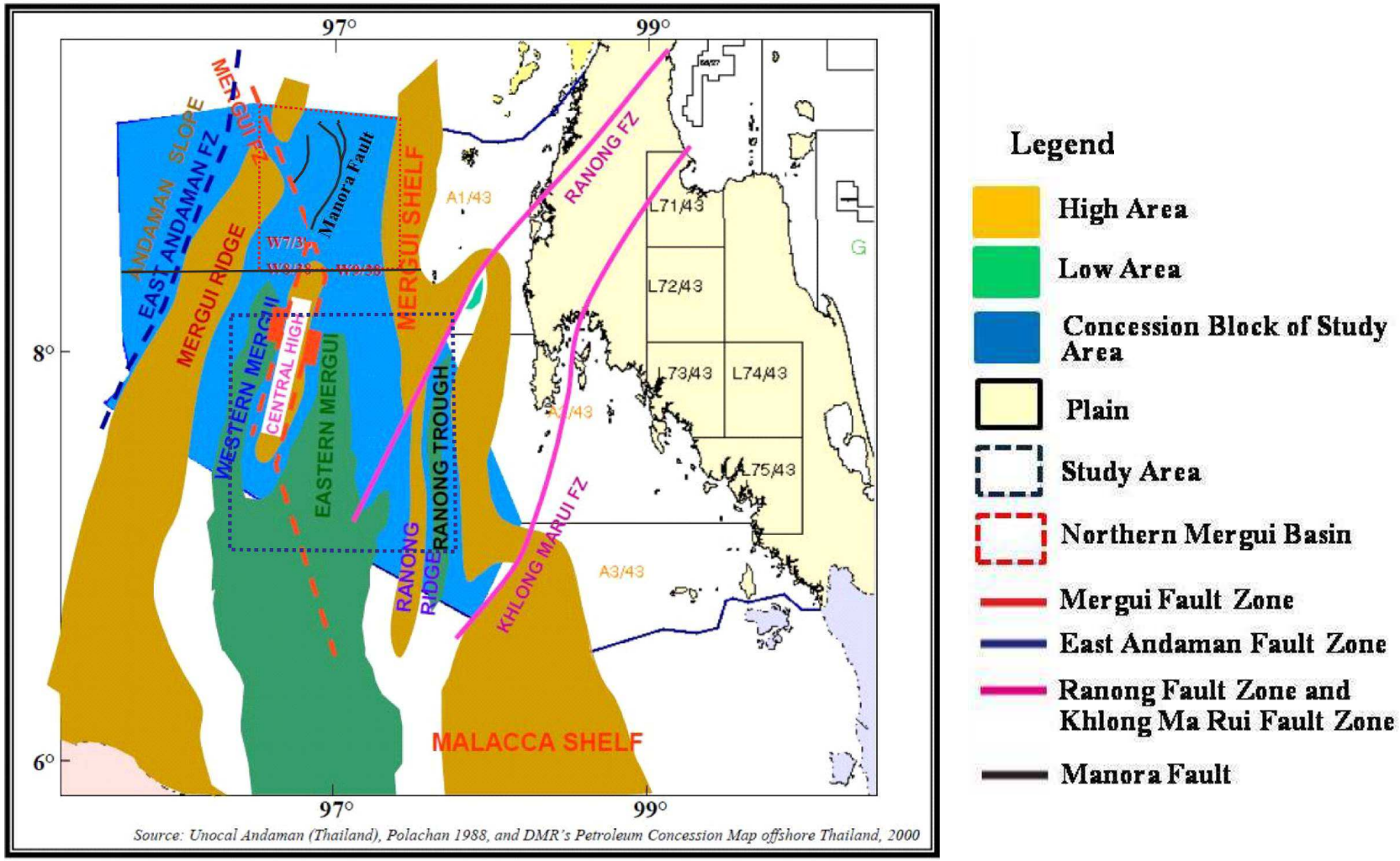

Figure 2.5 Physiographic map of the Mergui Basin, Andaman Sea (modified from Polachan, 1988, Mahatanachai,1996, Srikulwong, 2005 and Thipyopass, 2010).

(Figure 2.5) which is covered by a very thin Tertiary sediment overlying the Pre-Tertiary basement.

The east of the Mergui Basin is consisted of 2 basins, Ranong Trough and Similan Basin which are separate by the Ranong Ridge, is bounded to the west by N-S trending basement high. The Ranong Trough (or Ranong Basin) lies between the Ranong Ridge and the Mergui-Malacca Shelf (Figure 2.5). The trough is NE-SW trending along the Ranong Fault Zone and slopping to the east. The Similan sub-basin located in the north of the Ranong Basin and in the east of Ranong Fault Zone. (Figure 2.5) (Department of Mineral Fuel, 2006) All of these basins had been formed since Early Tertiary.

2.2.2 Faults in the Mergui Basin

The Tertiary Mergui basin in the Andaman Sea consists of 2 fault types, i.e. the strike-slip faults and the normal faults (Figure 2.4). The strike–slip fault in the Mergui Basin consisting 2 faults: the Mergui Fault trending NNW-SSE cuts across the N-S trending Mergui Basin (Figure 2.4) and the Ranong-Khlong Marui Faults are NNE-SSW trending wrench fault cutting obliquely across the Thai-Malay Peninsula (Figure 2.4), and having a significant left-lateral. The Ranong-Khlong Marui Faults is truncated in the north by the NW-SE trending Three Pagodas Fault Zone at the northwestern edge of the Gulf of Thailand (Polachan, 1988). The main normal fault in the area makes the Mergui Basin resulted in a north-south direction consisting 2 styles: the N-S trend controls the several basement highs with intervening half-graben to align in a NS direction (Department of Mineral Fuels, 2006) and the NNE-SSW trend developed mainly along the Mergui fault, but amount of movement along the faults is relatively small (Department of Mineral Fuels, 2006). The folds of the Andaman region consist into 2 styles as follows, i.e., the NW trending of en-echelon folds which developed obliquely along the Mergui Fault System, and N-S trending roll-overs developed on the hanging-walls of N-S faults (Polachan, 1988).

2.3 Stratigraphy

The stratigraphy of the Mergui Basin in the Andaman region (Figure 2.6) contains the Mergui group which can subdivided into 9 formations from the oldest to the

youngest, e.g., Ranong Formation, Yala Formation, Payang Formation, Tai Formation, Kantang Formation, Surin Formation, Trang Formation, Thalang Formation and Takua Pa Formation. (Figure 2.7) (Department of Mineral Fuels, 2006) can be described the followings:

Pre–Tertiary basement rocks in the Mergui Basin are composed largely of igneous and metamorphic rocks, e.g., slaty, quartzite, granite, shale, phyllite etc. basement are covered almost entirely by Tertiary sediments.

2.3.1 Ranong Formation (1,162 m thick) consists of mainly greyish red to black shales and sandstones. A depositional environment of the Ranong Formation was fluviatile–deltaic–shallow marine, deltaic shallow marine and prograding delta front (Polachan and Racey, 1994). The formation occurred in the Late Oligocence- Earliest Miocene.

2.3.2 Yala Formation comprises of shale bearing substantial glauconite, micaceous sandstone, siltstone, and some limestone. Yala Formation was deposited in a bathyal environment (Polachan and Racey, 1994), which is laterally related to the Ranong Formation. The formation is about 1,100-2,085 m thick and occurred in Late Oligocence- Earliest Miocene

2.3.3 Payang Formation is composed of sandstones which are commonly interbedded with shales accumulated at the delta front, front shelf or open shelf. The formation is about 603 m thick and occurred in the Earliest Miocene-end Early Miocene (Polachan and Racey, 1994)

2.3.4 Kantang Formation consists of the lower unit consists mainly of grey to brown-grey glauconitic shales, siltstone and sandy limestone. The middle part contains sandstone and the upper part comprises silty shale and glauconitic shale and the upper unit consists of grey, very silty, glauconitic shales interbedded with thin siltstones. This formation was deposited simultaneously with the Payang Formation. It is interpreted to have been deposited in a shallow marine environment (Polachan and Racey, 1994). The average thickness of this formation is 1,404 m.

2.3.5 Tai Formation is composed of dolomite, the coral-algal reef, and the calcarenite characterize the lower, the middle, and the upper parts of the formation

respectively. This formation was deposited simultaneously with the Payang Formation and Kantang Formation. A depositional environment of the lower, middle and upper unit of Tai Formation was deposited in saline lagoon, shallow marine and very deep marine, respectively (Polachan and Racey, 1994). The average thickness of this formation is 768 m.

2.3.6 Surin Formation consists of glauconitic sandstone containing carbonate and mica interbedded with shale and limestone. The formation was deposited in a very shallow marine environment (Polachan and Racey, 1994). The average thickness of this formation is 198 m and occurred in the Middle Miocene

2.3.7 Trang Formation is characterized by a sequence of glauconitic shale, glauconitic sandstone, and limestone. This formation was deposited simultaneously with the Surin Formation. This formation was deposited in a rather deep and bathyal environment. The average thickness of this formation is 732 m. (Polachan, 1988 and Polachan and Racey, 1994).

2.3.8 Thalang Formation is classified into 2 parts namely the upper and lower parts. The upper part of the formation consisted of siltstone, fine-grained glauconitic sandstone and shale. The lower part is consisted mainly of silty shale and some intercalations of fine-grained glauconitic sandstone. This formation was deposited in a deep marine environment and a lower bathyal zone (Polachan and Racey, 1994). The average thickness of this formation is 174 m. The Thalang Formation took place in the Late Miocene.

2.3.9 Takua Pa Formation consists significantly of glauconite and carbonaceous shale, with siltstone in some places. This formation was deposited in shallow marine environments (Polachan and Racey, 1994). The average thickness of this formation is 319.5 m and formation is occurred the Pliocene- Recent.

2.4 Petroleum System

Traces of gas and oil have been discovered in drilling wells in the Mergui Basin. In the Eastern Mergui Basin natural gas has been found at least 5 wells,i.e., W9B-1,

W9E-1, Yala-1, Ranod -1 and Kantang-1. In the Western Mergui Basin petroleum has been discovered in 2 wells,i.e., Trang -1 and Mergui-1. This makes both sub-basins having the appropriate structure (Srikulwong, 2005). Andmason et al. (1997) suggested that carbonate buildups within the Peutu and Belumai sequences (Early Miocene) are considered the most prospective exploratory play in the Mergui Basin. It is believed that Miocene reefs, and Oligocene to Miocene fluvio-deltaics and turbidites are the major exploratory plays.

According to the result of geochemical analysis by Khursida (2002), a potential source rock is marine shale in the Yala Formation and reef limestone in the Tai Formation, which is mature and vertical migration along faults. The reservoir rocks are largely sandstone in the Ranong Formation (ranging in age from Middle and Late Oligocene to earliest Miocene) reef limestones in the early Miocene Tai Formation, and sandstone in the Kantang, Payang, Trang, and Surin Formations of Early to Middle Miocene (Polachan and Racey, 1994). Potential traps can be divided into 3 types, i.e., the structural traps, the stratigraphic traps and the combination traps. The majority is found distributed along the faults and the folding axis (Department of Mineral Fuels, 2006). Hydrocarbons primarily move laterally from mature source areas updip along unconformities and/or via permeable carrier beds while faults tend to block and redirect vertical hydrocarbon migration. Hydrocarbons are primarily being generated and migrating from the deep Eastern Mergui and Western Mergui Basin (Andmason et al., 1997).

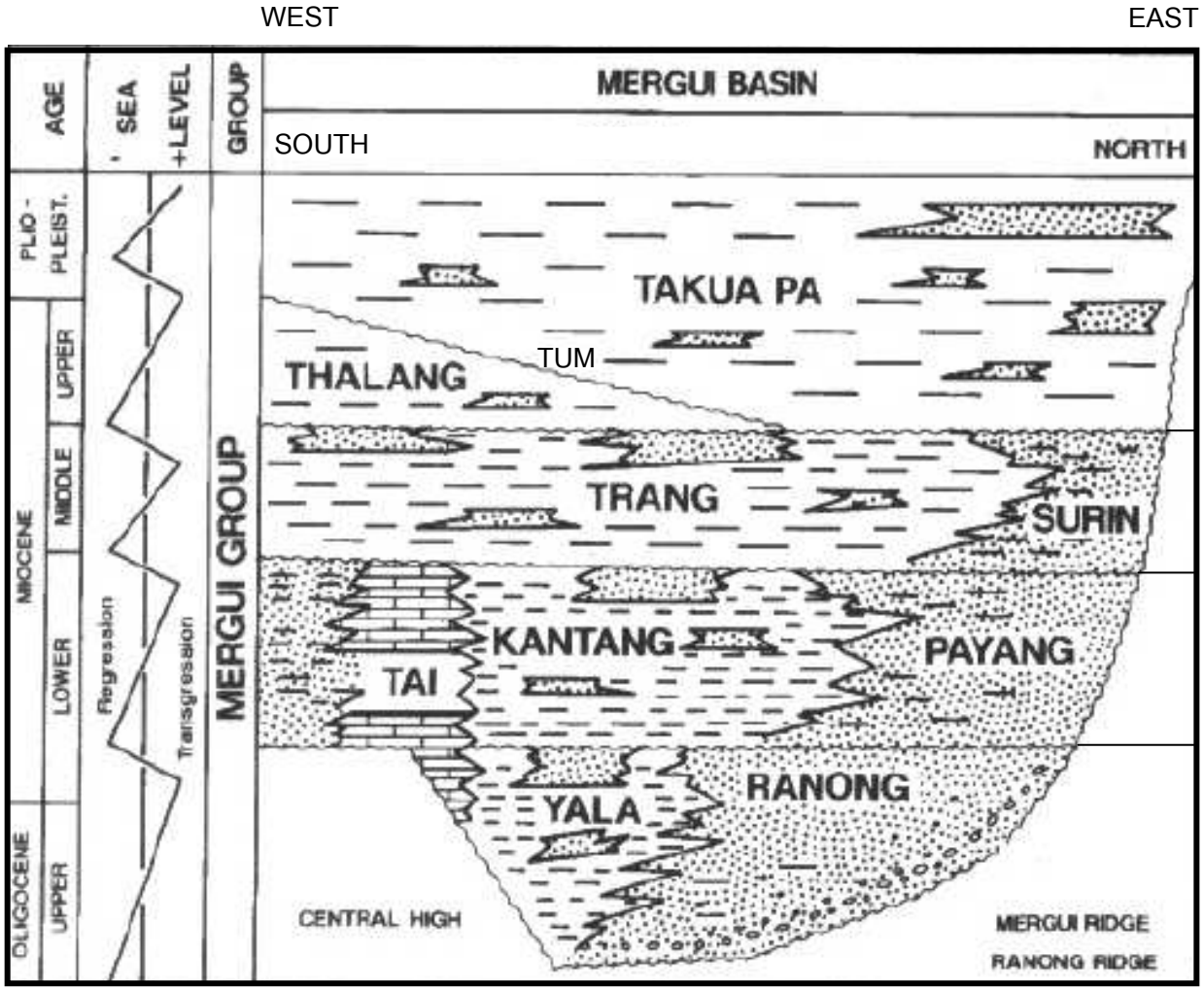

Figure 2.6 Stratigraphic Correlation of the southern Mergui Basin (modified Polachan,1988)

Chapter III
Methodology

3.1 Wireline Log compilation

Data from well correlation (Table 3.1 and Figure 3.1-3.3) provide understanding of the lithology and depositional environments and defining the boundaries of sedimentary sequences. 4 wells with wireline logs data included gamma ray log (GR) and sonic log (DT), W9D-1, W9B-1, W9A-1 and W9C-1, were used in this study.

3.1.1 Gamma ray log (GR)

The gamma ray log is the tool to detect radiated elements in rock formation. This is essentially related to the amount of clay. Among the sediments, shales commonly have the strongest radiation with high gamma ray values. In contrary, sandstones usually show low gamma ray values. Moreover, as shale content related to grain size, the gamma ray log could be also used to identify variation of the grain size through the formation.

The shape of the gamma-ray log are frequently used for interpreting sedimentary cycles or depositional facies. The five log trends (Figure 3.4) are bell shape (upwards increasing in gamma counts), funnel shape (upward decrease in gamma counts), boxcar or cylindrical (relatively consistent gamma readings), bow shape (systematic increase and decrease of gamma counts) and irregular trend (no systematic change in gamma values).

Therefore, the gamma ray log shapes could be used to characterized facies of depositional environment of sedimentary succession as the gamma ray correspond to grain size trends. For example, a bell shape with fining upward sequence could be interpreted as transgressive marine shelf sand, and a funnel shape specified coarsening upward sequence, which could be a deltaic progradation or a shallow marine progradation (Figure 3.5). Changing of the trends in gamma ray logs are used to identify the sequence boundaries within vertical session.

3.1.2 Sonic log (DT)

The sonic log measured an interval transit time (Δt) of compressional seismic wave through a formation. Transit time varied with lithology and rock texture (porosity-ø) and commonly decrease with depth. The total time that it takes, is proporotional to the amout of fluid in the pore space and the amount of rock matrix (Serra, 1985). The sonic log is a significant tool for calculating seismic velocity (sound) formation, and generally be used in generating synthetic seismograms. The changes of the slope in log trend is can also indicate the sequence boundaries.

Table 3.1 Detailed of Petroleum Exploratory Well, Andaman Region

Well	Operator	Date	TD (m)	WD (m)	Results	Wireline logs data
W9-A-1	Esso	15/12/75-01/03/76	2,408	583	dry	/
W9-B-1	Esso	04/03-22/05/76	3,634	802	oil gas show	/
Trang-1	Union Oil	11/03-24/05/76	3,944	512	gas show	-
W9-C-1	Esso	27/05-25/07/76	3,724	902	dry	/
Tai-1	Union Oil	28/05-30/06/76	1,775	603	dry	-
Phanga-1	Union Oil	01-13/07/76	1,389	494	dry	-
Mergui-1	Union Oil	16/07-30/08/76	3,810	621	gas show	-
W9-D-1	Esso	02-31/08/76	2,491	808	dry	/
Payang-1	Union Oil	02-19/09/76	1,597	410	dry	-
W9-E-1	Esso	05/09-20/11/76	4,278	1,055	gas show	-
Surin-1	Union Oil	20/09-2/10/76	830	618	dry	-
Yala-1	Placid Oil	28/01-18/02/87	1,762	665	gas show	-
Ranot-1	Placid Oil	14/06-05/06/87	2,591	617	dry	-
Thalang-1	Unocal	11-23/10/97	2,596	1,041	dry	-
Kantang-1	Unocal	25/10-5/11/97	2,090	1,062	gas show	-
Kra Buri-1	Unocal	9-24/11/97	3,152	1,041	dry	-
Si Koa-1	Unocal	26/11-03/12/97	1,732	1,017	dry	-

Table 3.1 (Cont).

Well	Operator	Date	TD (m)	WD (m)	Results	Wireline logs data
Kathu-1	Unocal	6-10/12/97	1,013	512	dry	-
Manora-1	Kerr McGee	22/02-13/03/00	2,311	400	dry	-

From: Department of Mineral Resources (2006)

3.2 Seismic Interpretation

3.2.1 Seismic Data

Seismic data provided by the Department of Mineral Fuels (DMF), consists of 10 lines of the 2D seismic reflection surveys in digital format (Figure 3.6). The Kingdom Suites program version (8.4) is the software largely used for seismic interpretation. The resolution of these migrated seismic data is poor to very good in this study area. These selected 10 seismic lines are AD1, AD2, AD3, AD4 AD5, AD6, AD7, AD8, AD9 and AD10 and are shown in Figure 3.6. The length of the seismic lines are between 80 to 260 kilometers and the spacing between seismic lines is about 3 to 40 kilometers.

Seismic data interpretation includes geological structural styles as well as depositional sequences and lithology. Interpretation of seismic reflection data has been done correlating seismic unit with known lithology from well data. Then the geological features, i.e., fault, unconformity, folding and reef are identified. A seismic sequence is a also identified on a seismic section. The sequence is bounded at its top and base by surfaces of discontinuity marked by reflection terminations which are interpreted as unconformities or the correlative conformities. The reflection termination i.e. onlap, downlap, toplap, erosional truncation etc. (Figure 3.7) and the reflection configuration are analyzed in order to define the seismic sequences boundaries.

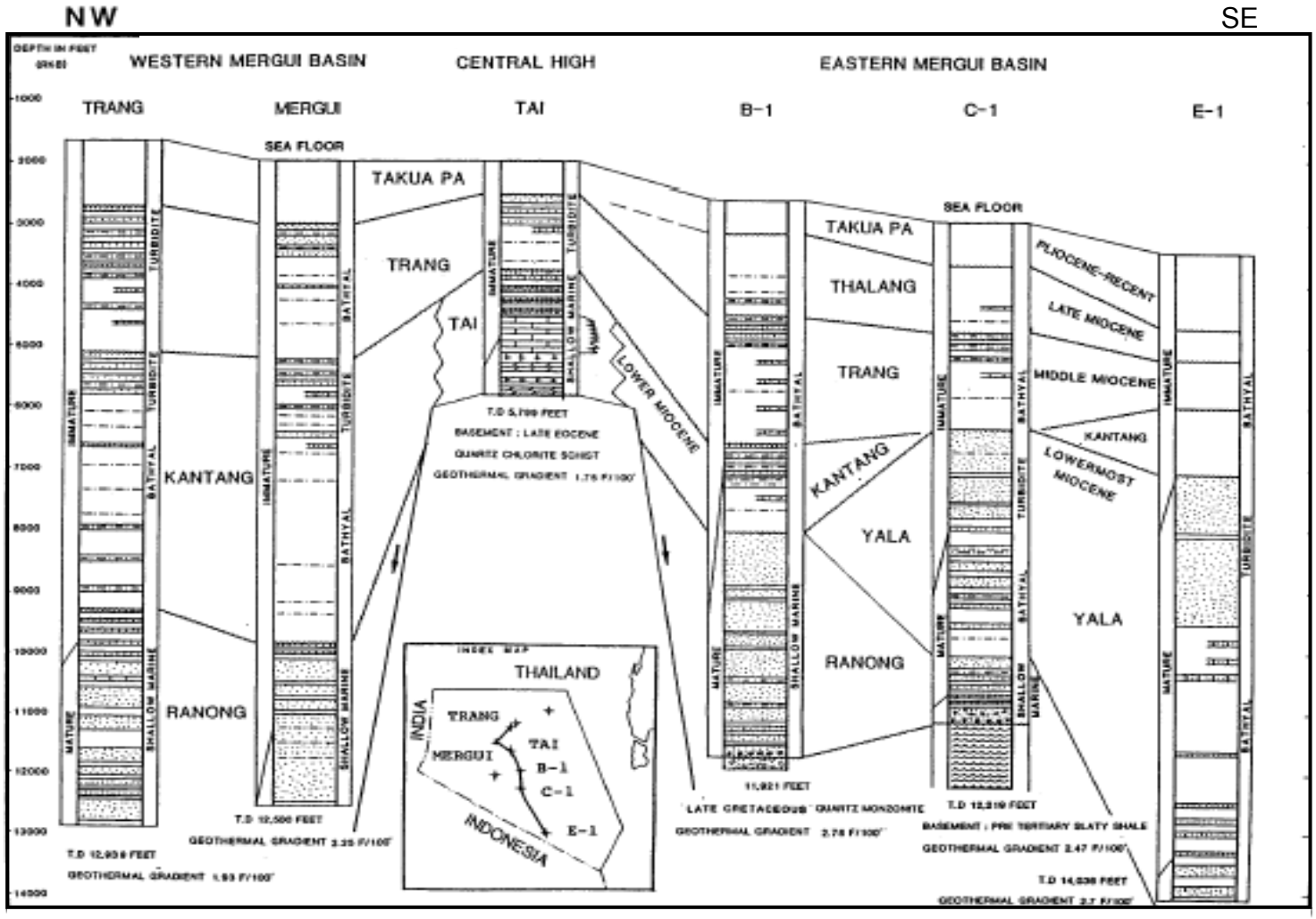

Figure 3.1 Well correlation Northwest-Southeast cross section in the Merguii Basin (Polachan, 1988).

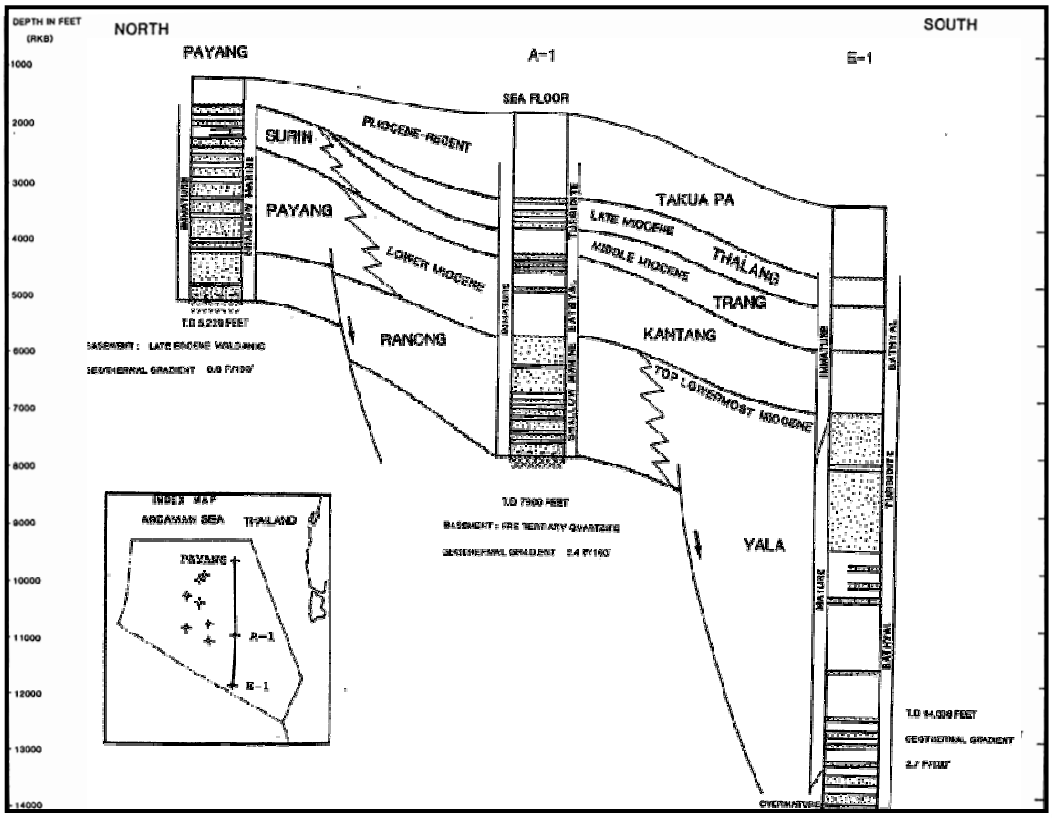

Figure 3.2 Well correlation Northt-South cross section in the Mergui Basin (Polachan, 1988).

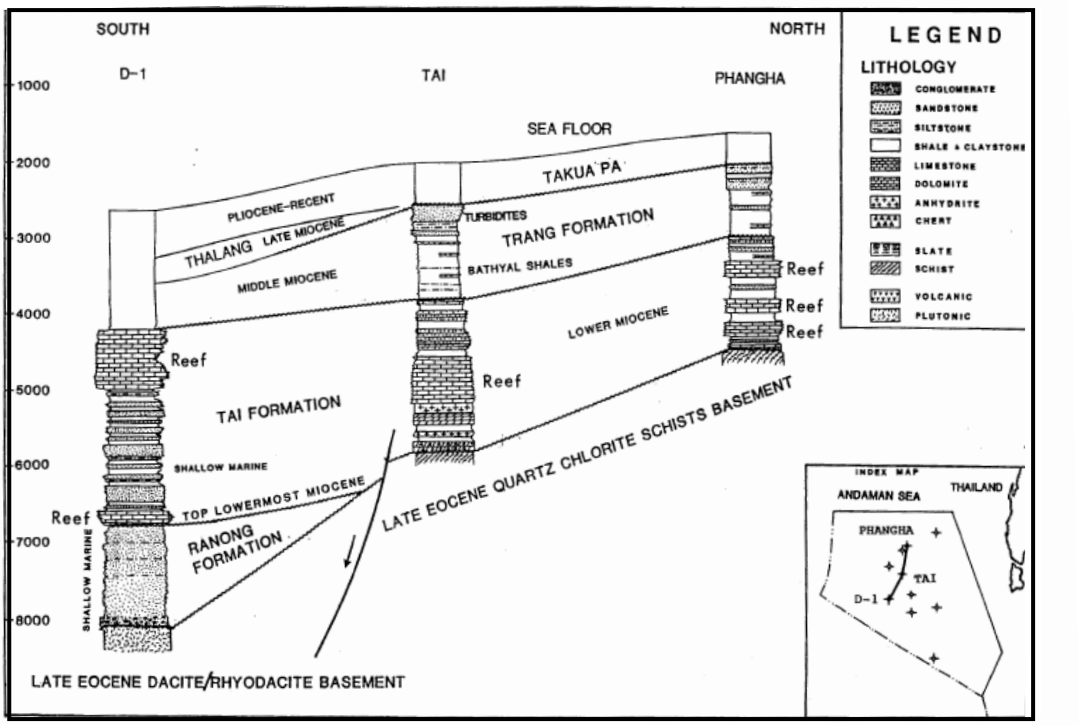

Figure 3.3 Well correlation across the Central High in the Mergui Basin (Polachan, 1988).

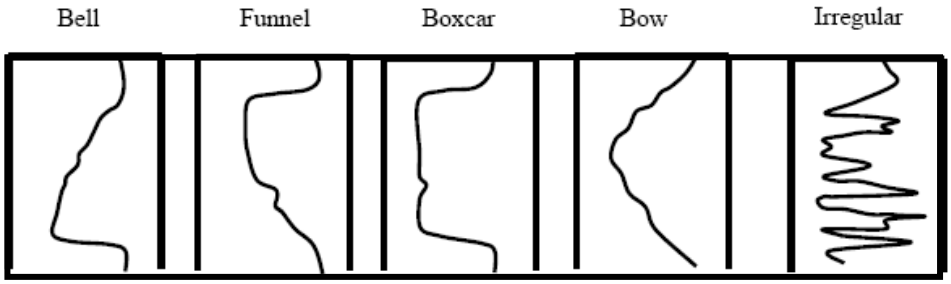

Figure 3.4 Idealized gamma-ray log trends (modified after Rider 1993).

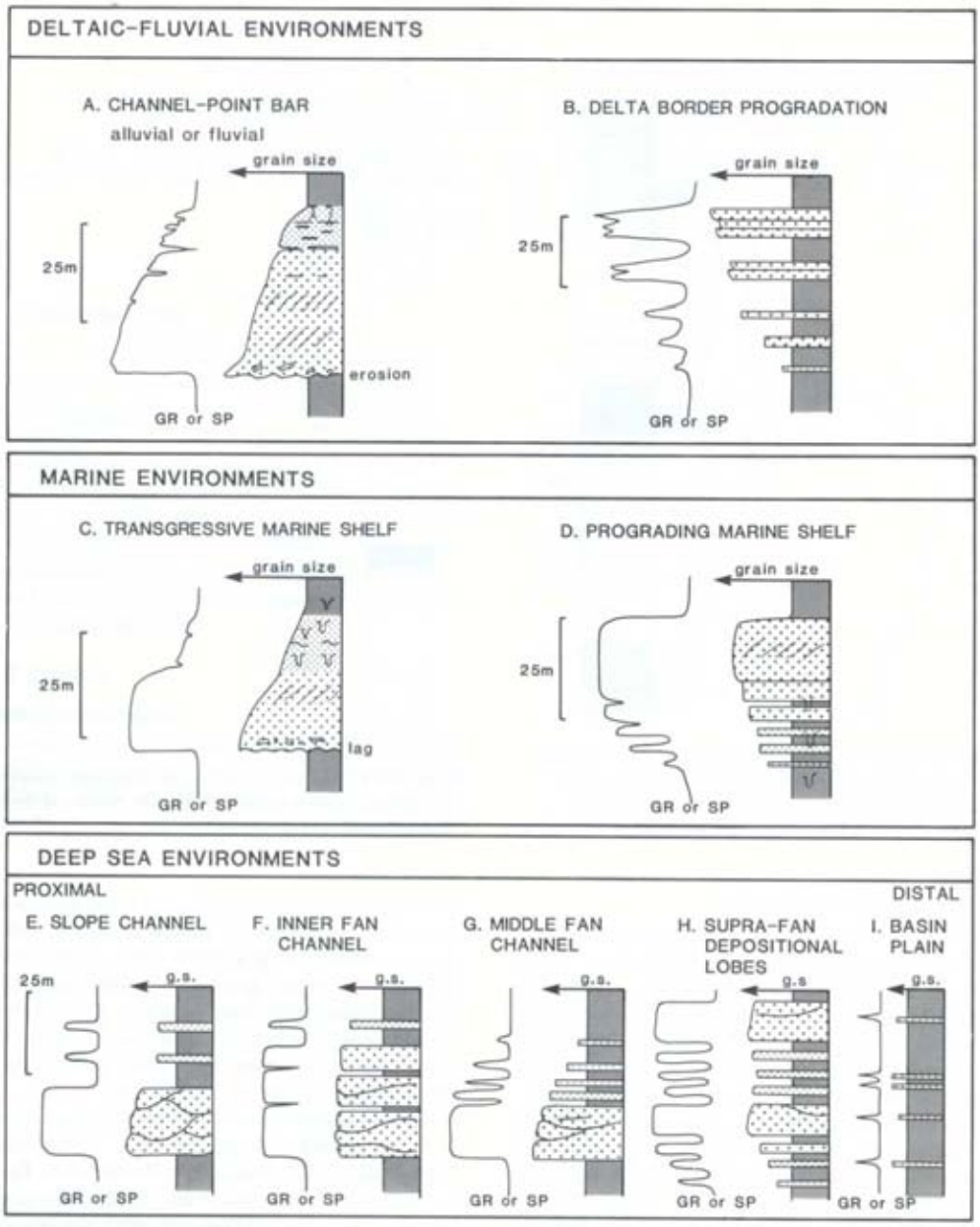

Figure 3.5 Depositional environment interpretation by using log Gamma ray patterns (Serra, 1972; Parker, 1977; Galloway and Hobday, 1983, and Rider, 1996).

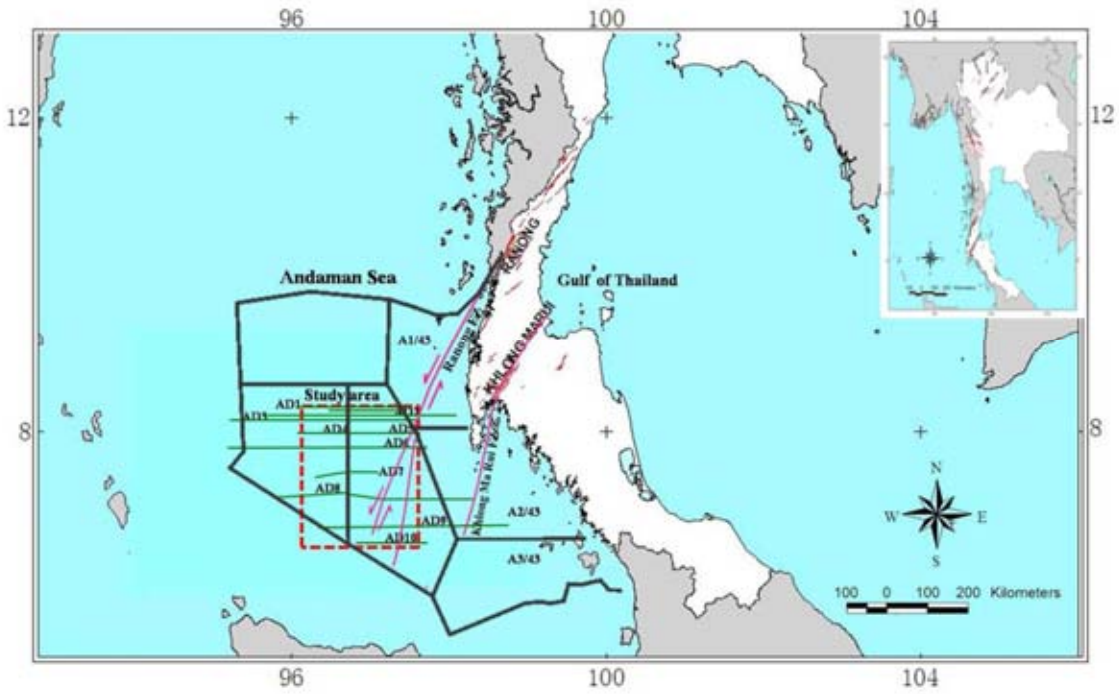

Figure 3.6 Map showing seismic survey lines (green) used in the study area (red block) within the Andaman Sea region of Thailand (black blocks) (modified from Charusiri et al., 2006).

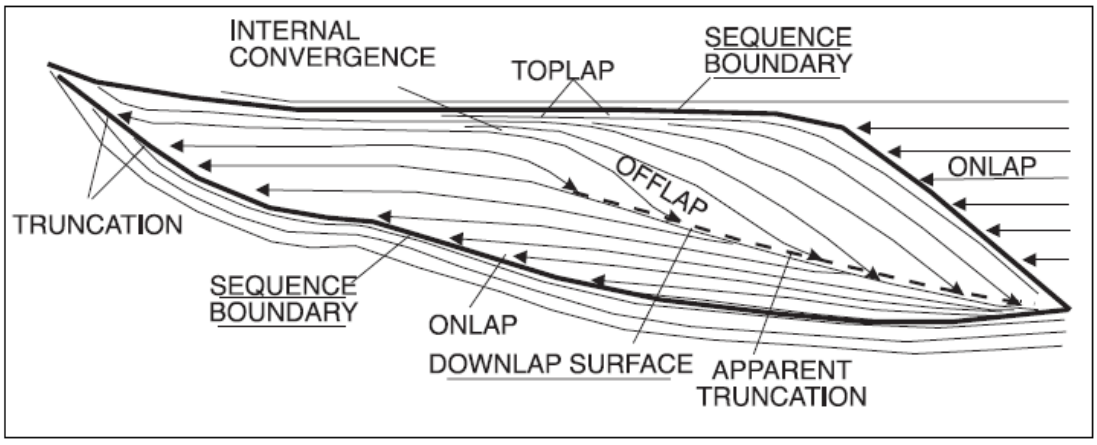

Figure 3.7 Seismic Stratigraphic reflection terminations and the associated discontinuity surfaces. HST is highstand systems tract, LST is lowstand systems tract, and TST is transgressive systems tract. (Vail, 1987).

3.2.2 Reflection Termination

The first step in the interpretation is to determine the vertical and horizontal scales of the section. To find out the header or the seismic data if the section has been migrated, and whether it is marine or land data. Seismic sequence boundaries are identified on the basis of termination of seismic reflectors against the surfaces (Table 3.2). These terminations include baselap (downlap and onlap on the lower depositional boundary), toplap, erosional truncation and concordance on upper depositional boundary. The following definitions of these terms are obtained from Octavian (2002).

Table 3.2 The seismic sequence analysis showing groups termination patterns of by position with respect to a discontinuity.

Reflection Termination Point	Pattern	Associated Discontinuity
Above a discontinuity	Onlap	Sequence boundary (unconformity)
	Downlap	Downlap surface (condensed section)
Below a discontinuity	Truncation	Sequence boundary
	Toplap	Sequence boundary
	Apparent Truncation	Downlap surface

From: Exploring for Stratigraphic Traps (Dolson J.C. et al., 2000).

Downlap is a base-discordant relation, which inclined strata terminate downdip against an initially horizontal or inclined surface and commonly seen at the base of prograding clinoforms and usually represent progradation of the basin margin.

Onlap is a base-discordant relation, which horizontal strata progressively terminate against an initially inclined surface and termination of low-angle reflections against a steeper seismic surface. It is generally associated with a marine transgression.

Toplap is the termination of strata against an overlying lower angle surface. Initially the lower strata such as forest beds and clinoforms get inclined due to some

tectonic movements. Sea level variations also form the toplap reflection patterns in shallow marine deposits, particularly in deltaic complexes.

Erosional truncation is the termination of strata against an overlying erosional surface. This implies the deposition of strata and their subsequent tilting and removal along an unconformity surface. This termination is the most reliable top discordant criterion of a sequence boundary. Such truncation can also be caused by termination against erosional surface, as for instance a channel.

3.2.3 Reflection Configuration

The principal strata configurations, which are gross stratification patterns identified on seismic records and generally indicative of depositional setting and later structural movement, are the patterns and relations of strata within stratigraphic unit. Four basic types of configurations are recognized (Figure 3.8):

Parallel patterns (Figure 3.8) include even or wavy patterns and is generated by strata that were probably deposited at uniform rates on a uniformly subsiding shelf or stable basin setting (Krishna, 2007).

Divergent configurations (Figure 3.8) are characterized by a wedge-shaped unit in which lateral thickening of individual reflection subunits within the main unit. It signifies lateral variations in rates of deposition or progressive tilting of the sedimentary surface during deposition (Krishna, 2007).

Prograding reflection configurations (Figure 3.8) are reflection patterns generated by strata that were deposited by lateral outbuilding or progradation to form gently sloping depositional surfaces called clinoforms. Prograding reflection configurations may have a variety of patterns including sigmoid, oblique, or hummocky (Krishna, 2007).

Chaotic reflection patterns (Figure 3.8) represent a disordered arrangement of reflection surfaces owing to softsediment deformation, or deposition of strata in a variable high-energy environment. Some chaotic reflections may also be related to over pressured zones. Reflection-free areas on seismic records may represent

homogeneous, nonstratified units such as igneous masses or thick salt deposits (Krishna, 2007).

3.2.4 Structural Geology

Interpretation of Fault, fold and inversion structure found in the seismic section has important for petroleum trap. Faults are of different types in term of which way the parts of the broken formations moved. In a normal fault, there has usually been some tensional force tending to pull the rocks apart. An intrusion may have bent the rock up over a greater length than it had occupied. So the rock breaks, and one part drops down lower than the other (Coffeen, 1984) (Figure 3.9). A reverse or thrust fault occurs when some compression force is pushing the rock together from the sides. The rock break and some slide up over the others. The fault trend to be low angle and the fault plane can curve steeply upward near the surface, in a sled-runner fault. The lower part may even be horizontal with one formation sliding over another for some distance (Coffeen, 1984) (Figure 3.9). A strike-slip fault, the movement is horizontal with one part moving sideways along the break. This type of fault is harder to detect from seismic data than the other two types, as the formations may still be at the same level where they meet on a section (Coffeen, 1984) (Figure 3.9).

A fault can be interpreted better even in interpreting just one horizon, if the breaks in other horizons are taken into account. The fault is a discontinuities in reflection (distorts reflection or reflection disappears) which divergence in dip not related to stratigraphy and seismic diffraction around faults (Murry, 2012).

Correlating across a fault is easier if the parts of the geologic section on the two sides happen to be equal in thickness. They are equal if the fault occurred after the sediments forming those parts of the section were all deposited. But if the fault is a growth fault, it occurred in stages and deposition went on between the times of movement.

Unconformities and truncations are reflections with widespread continuity but highly variable amplitude (especially if they exhibit angular relationships with reflections above or below). Unconformities are usually good reflectors and commonly separate rock units with different dips, which an unconformity is a surface of erosion or non

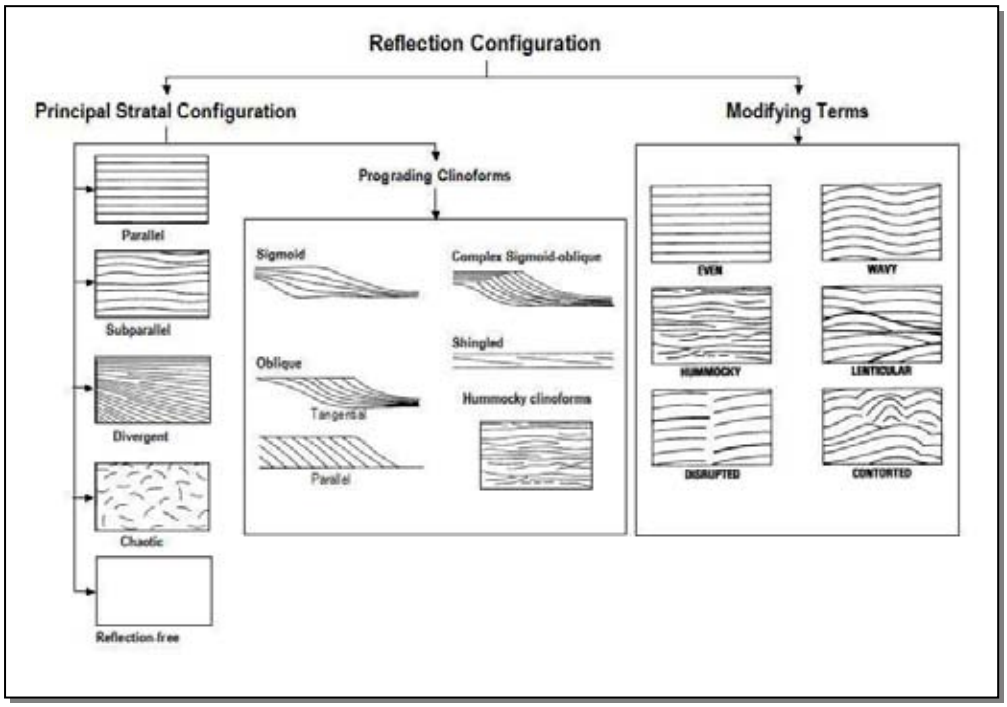

Figure 3.8 Seismic Stratigraphic reflection configuration (Mitchum et al., 1977).

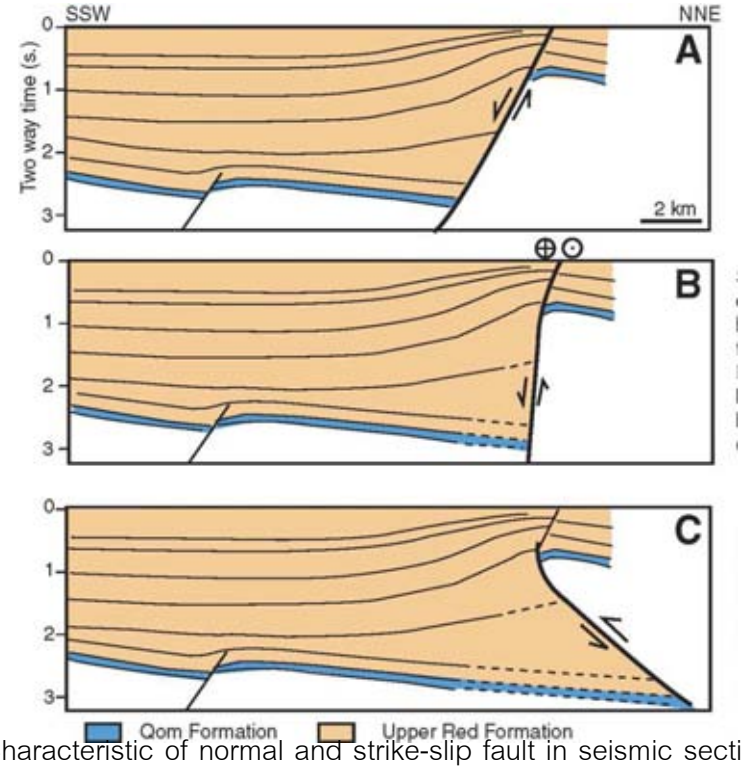

Figure 3.9 Characteristic of normal and strike-slip fault in seismic section. (A) Normal Fault showing lower wedge shaped expansion of section toward fault compatible with early extension. (B) Strike-slip fault showing requires a large component of extension, followed by later folding, and (C) Thrust or reverse fault does not explain switch from lower section expansion toward fault, to upper section folding (Morley et al., 2009).

deposition that separates younger strata from older rocks and represents a significant hiatus.

Unconformities and Truncations found in the seismic section are another type of unconformity called an angular unconformity (Figure 3.10) or structural unconformity. An angular unconformity is an unconformity where horizontally parallel strata of sedimentary rock are deposited on tilted and eroded layers, producing an angular discordance with the overlying horizontal layers. Figure 3.10 showing an angular unconformity is picked on onlap and erosional surface (red color) which relative sea level fall and uplift of the basin. This unconformity observed during in the Late Miocene.

3.3 Biostratigraphic data

Biostratigraphic data are summarized from the report by Exxon (1976). The data are from W9A-1 well, W9B-1 well, W9E-1 and Kantang-1. Age determination and paleoenvironments are mainly from fossil assemblages such as biozones of forams, calcareous nannofossils, palynomorphs.

3.3.1 W9A-1 well

Sediments of this well are at interval 2,255' to 7,900' feet. They are foraminiferal oozes, shale, sandstone, glauconitic sand and shale, calcareous sandstone, dolomite and limestone. The sediments (5,830'-7,900' ft) contain palynomorph assemblages (dinoflagellates and spore-pollen) of Oligocene in the shallow marine to brackish water. An unconformity (±3.5 Ma) is missing. The sediments (5,800'-2,255' ft) were deposited in the deep water to the shallow water (bathyal-brackish-marine environment). They are dominantly sands and silts. Fossil assemblages from this interval are Coccoliths (*Globorotalia siakensis*, *G. fohsi*, and *G. peripheroronda*), nannoplankton, forams (*Pulleniatina spectabilis*, *P. primalis* and *Sphaeroidinellopsis subdehiscens*), foraminiferal ooze, suggesting the age of Early Miocene to Pleistocene.

3.3.2 W9B-1 well

Sediments of this well are interval 3,758' to 11,921' feet. They are sandy silts and coarser grain clastics. Fossil assemblage include forams, calcareous nannoplankton,

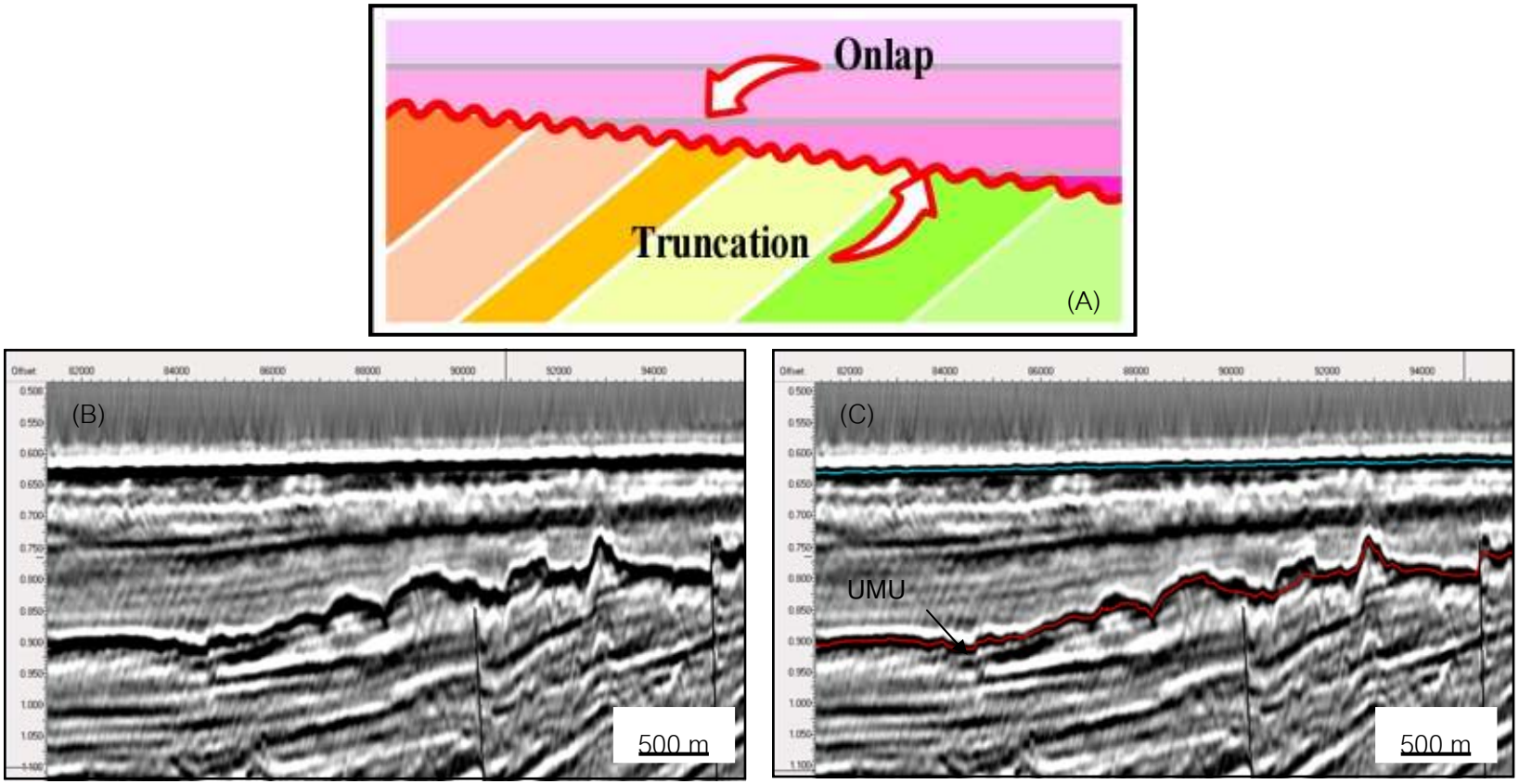

Figure 3.10 The angular unconformity or erosional surfaces on the seismic lines. (A) below and above strata or reflection terminations. Generally, such a surfaces are induced by relative sea level falls created by the combination of the subsidence (uplift). (B) Uninterpreted section showing erosional truncation of the Upper Miocene Unconformity (UMU), and (C) Interpreted section from seismic line AD1 in the southern Mergui Basin.

coccolith (*Globorotalia acostaensis*), and palynomorphs, suggesting the age of Late Miocene to Oligocene. The sediments were deposited in the deep water between 8,030' to 8,256' feet. Sediments were deposited in the very shallow marine to paludal environments and occurrence of mangrove pollen was a good age indicator.

3.3.3 W9E-1 well

This well, the analyzed interval is 5,480' to 7,520' feet. The sediments deposited from upper bathyal to middle bathyal (6,860'-7,400' ft) and from upper bathyal to middle bathyal (7,400' to 7,520' ft). Fossil assemblages found in the W9E-1 well are Nanofossils (*Discoaster braarudii, Discoaster exilis*, *Cyclicargolithus floridanus*, *Sphenolithus heteromorphus*, *Helicosphaera ampliaperta* and *Triquetrorhabdulus carinatus*) Forams (*Globorotalia peripheroacuta*, *Globorotalia praefohsi*). The age of these sediments are middle Miocene to late Oligocene.

3.3.4 Kantang-1 well

This well, the analyzed interval is 5,530' to 6,850' feet. Fossil assemblages are nanofossils (*Discoaster hamatus, Discoaster neohamatus, Discoaster kuglerii, Sphenolithus heteromorphus, Helicosphaera ampliaperta*) and planktonic forams (*Globorotalia* mayeri, *Globoquadrina baroemoenensis*, *Globoquadrina altispira globosa*, *Globoquadrina dehiscens*, *Globorotalia lobata*, *Globorotalia robusta*, *Globigerinoides* aff. *mitra*, *Sphaeroidinella subdehiscens, Globigerinoides sicanus*, *Globorotalia peripheroronda*, and *Praeorbulina glomerosa curva*). The age of these sediments are Middle Miocene to Early Miocene, possible Late Oligocene or Middle Eocene, and they were deposited in deep water (middle to upper bathyal).

CHAPTER IV
INTERPRETATION AND RESULT

Before describing geological structures of the southern Mergui Basin, it is important to understand clearly the succession of individual formations seen in the studied interpret on seismic sections. So in this chapter, several topics, including wireline log interpretation, seismic stratigraphy, structure, unconformity and structural development, are presented as the interpretation and results of the present study.

4.1 Wireline log interpretation

4 wells including W9D-1, W9B-1, W9A-1 and W9C-1 with the wireline logs data (gamma ray log: GR and sonic log: DT) were used to study and to correlate among wells. Most of the wells are located in the Southern Area as shown in Figure 4.1. The well markers picked are correlated to regional unconformities, which can be characterized by vertical changes in lithology and shape of wireline log motif. The well markers in this study consist of the Top Ranong Formation (Pink maker), Top Yala Formation (Blue maker), Top Kantang Formation (Gold maker), Top Tai Formation (Yellow maker), Top Trang Formation (Red maker) and Top Thalang Formation (Light green maker).

North of this study area found Surin and Payang Formations are quite consistent with those studied by Polachan (1988) suggested Surin and Payang Formations found in Payang-1 well are used in this study. All formations found in this study are described below.

4.1.1 Basement rock (Brown maker)

Basement rocks occur in the wells have different kinds of rock. The basement rocks in W9D-1 and Payang-1 wells included metamorphosed volcanic sediment (Polachan, 1988) at the depth is about 2,473 and 1,583 meters. In W9B-1 well basement rock consist quartz monzonite acid igneous rock (Polachan, 1988) at the depth of about 3,571 meters. Basement rocks present in the W9A-1 wells are quartzite (Polachan, 1988) at the depth of about 2,402 meters, and the W9C-1 wells found the most basement rock is mainly slaty shale showing low grad metamorphism (Polachan, 1988) at the depth

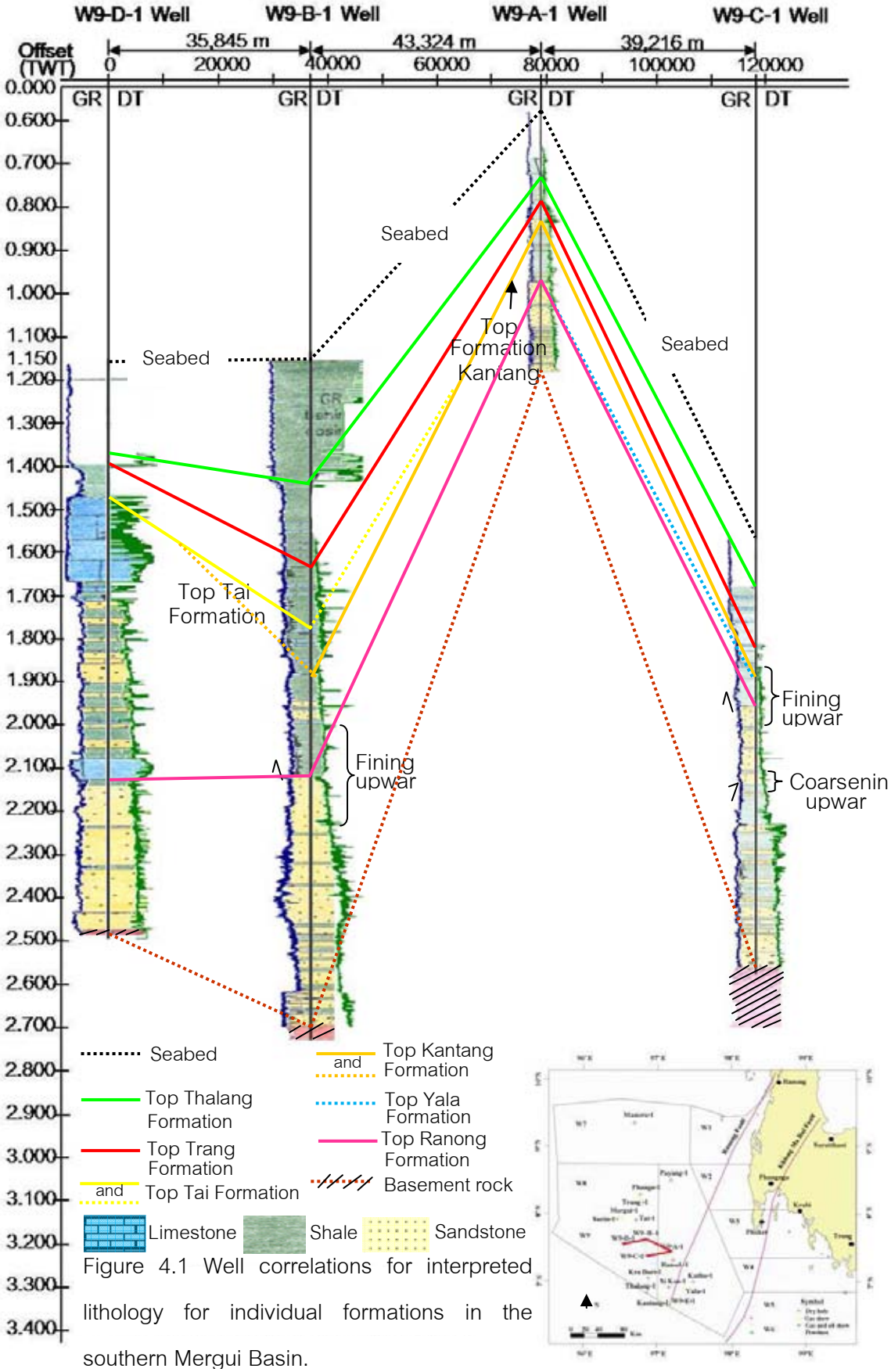

Figure 4.1 Well correlations for interpreted lithology for individual formations in the southern Mergui Basin.

of about 3,393 meters. The age of basement rock at W9D-1 well dated using K-Ar method to be late Eocene (± 41 Ma) (Polachan, 1988).

4.1.2 Ranong Formation (Pink maker)

Ranong Formation observed from wells comprises mainly sandstones. This formation occurs in the W9B-1 (Figure 4.2), W9A-1, W9C-1 (Figure 4.3) and W9D-1 wells and has characteristic of log motifs revealed the fining upward sequence in the basal unit. The most of middle unit consisted of sandstones interbeded with siltstones, shales and thin lignite (found only in W9B-1 well). The W9D-1 well (Figure 4.4) contains sandstone with minor siltstone, and shale, which consistent with those studied by Polachan (1988) who subdivided the Ranong Formation into 3 rock units, i.e. basal unit, middle unit and upper unit. The basal unit comprises massive or thick-bedded sandstones and conglomerates, which defined as an Alluvial fan deposit. The middle unit consists of interbedded green-grey sandstones, grey siltstones, dark grey shales and occasional thin coals, and the upper unit in W9B-1, W9C-1, and W9A1 wells has shape of the gamma-ray log are cylinder-shaped sequence of upper unit sands, comprises massive green-grey, very fine- to fine-grained, calcareous, micaceous, thick-bedded sandstones, subangular to subrounded clasts and poorly sorted and grade into changed downward to silty clay matrix conglomerates.

Ranong Formation in W9D-1, W9B-1, W9A-1 and W9C-1 are about 439 meters, 1193 meters, 635 meters and 338 meters thick, respectively. This formation is thinning to a minimum of about 229 m in the Payang-1 Well (Polachan, 1988). The depositional environment in the W9C-1 and W9A-1 well is considered to be basin plain deposit, while in W9B-1 well delta plain and distal fan deposit are suggested. The basal unit was deposited in alluvial fan and shoreface, and delta deposit in the upper unit of WD9-1 well (Polachan, 1988). This well maker can be correlated to the Top Ranong Formation in seismic marker, at the major unconformity near top of Ranong or Yala Formation (Polachan, 1988, and Polachan and Racey, 1994), which unconformably overlies Late Cretaceous quartz monzonite basement in the W9B-1 well, and overlies quartzite basement in the W9 A - 1 well and volcanic basement in the w9D-1 well and

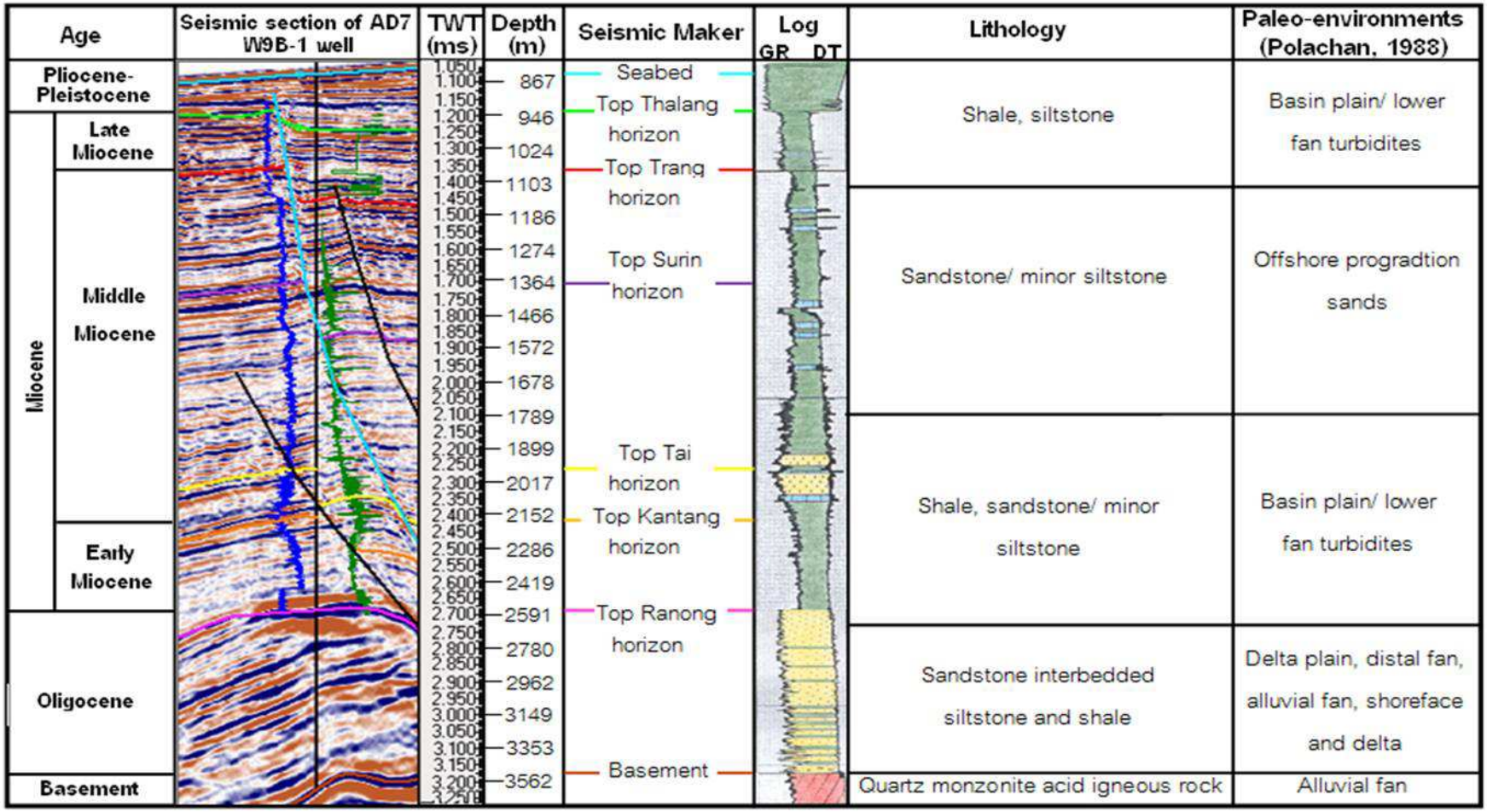

Figure 4.2 Seismic section of well AD7 in the southern Mergui Basin correlated with wireline log in well W9B-1 (modified from Mahattanachai, 1996).

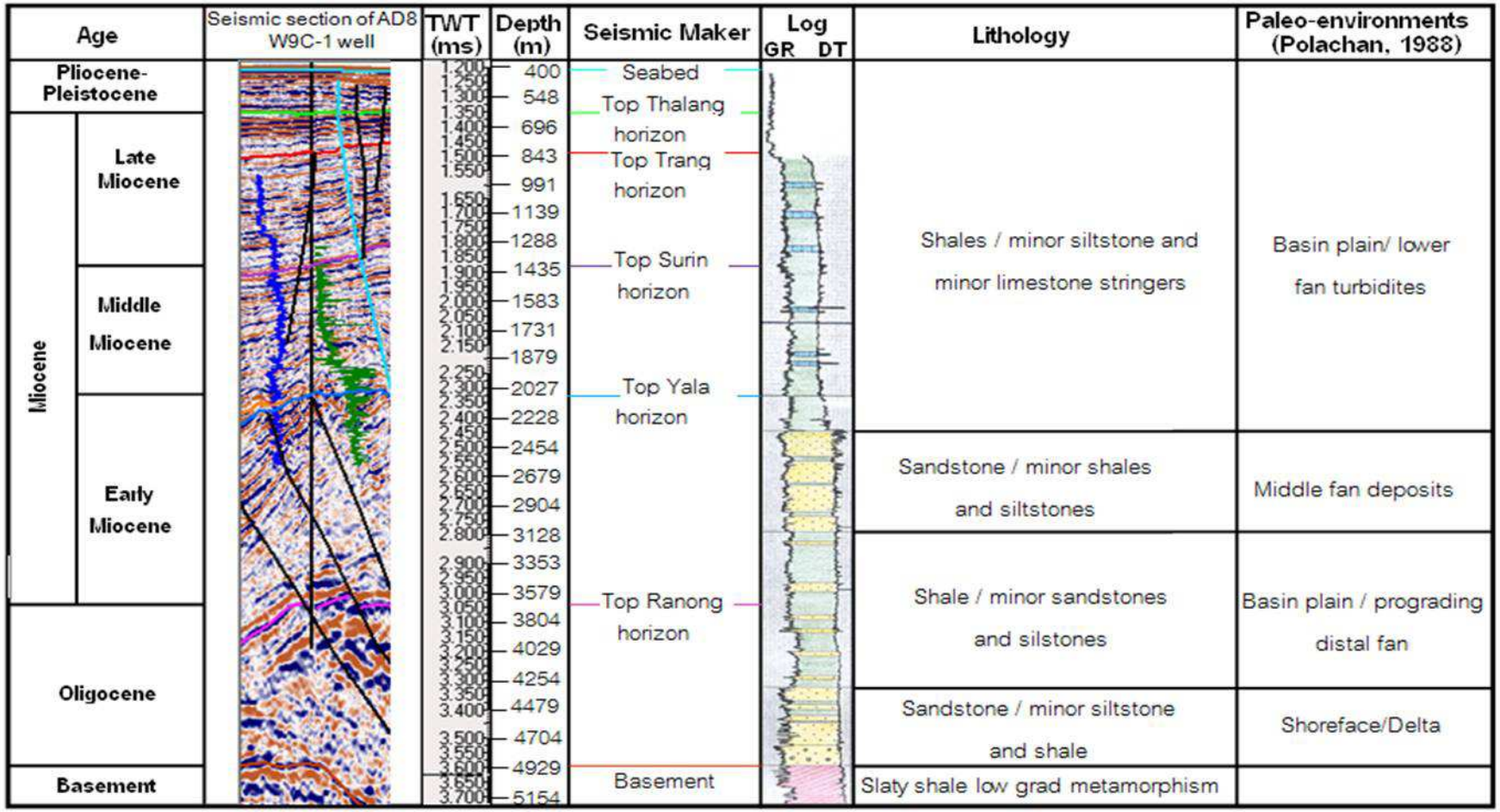

Figure 4.3 Seismic section of well AD8 in the southern Mergui Basin correlation with wireline log in well W9C-1 (modified from Mahattanachai, 1996).

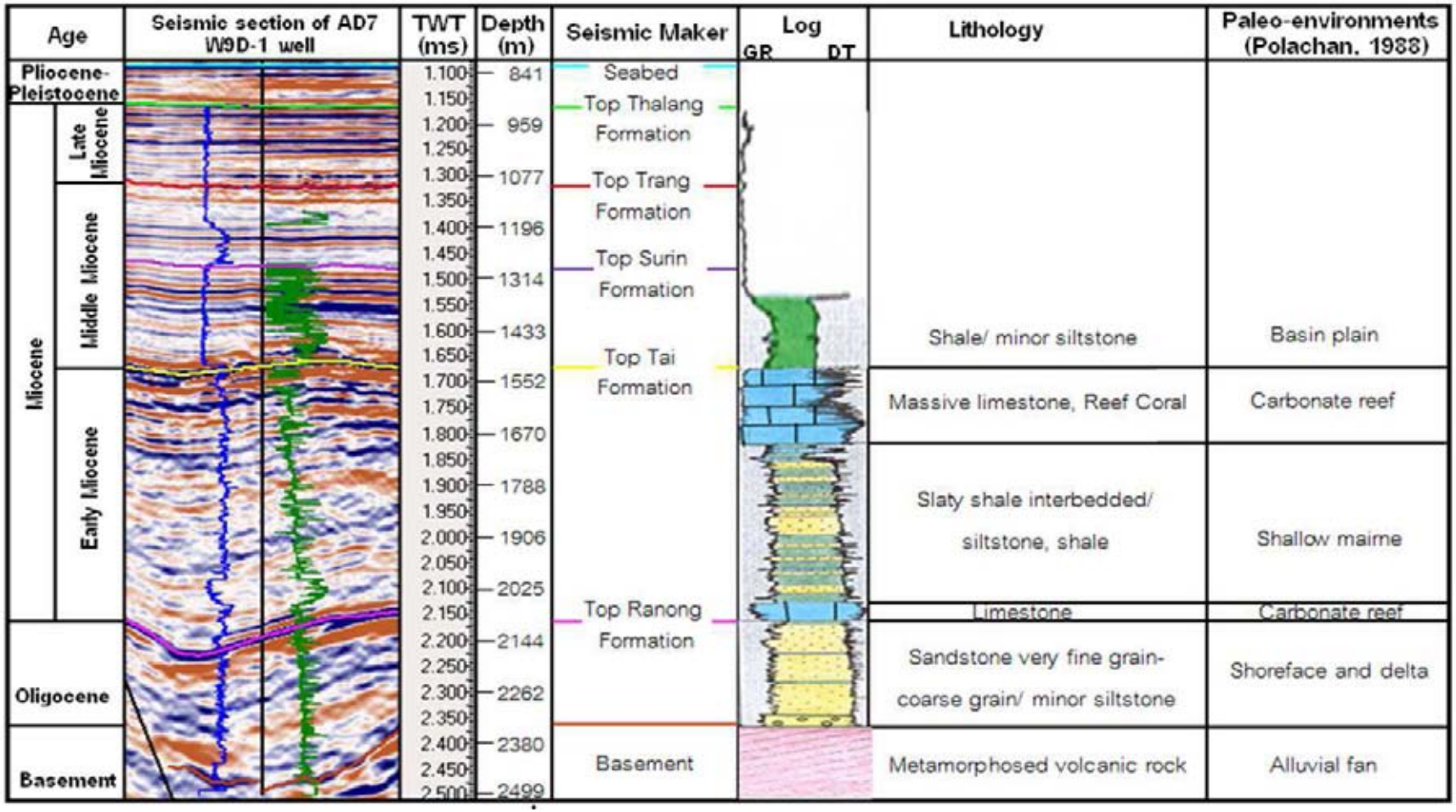

Figure 4.4 Seismic section of well AD7 in the southern Mergui Basin correlation with wireline log in well W9D-1 (modified from Mahattanachai, 1996).

Payang-1 well (Polachan, 1988), and slaty shale basement in the W9C-1 well. Exxon (1976) reported the age of the Ranong Formation is around Late Oligocene to Early Miocene.

4.1.3 Yala Formation (Blue maker)

Yala Formation observed from W9C-1 wells comprises mainly shales with thin sandstones. This formation in the W9C-1 well is 1,642 meter thick, which occurs overlies the Ranong Formation and is unconformably overlain by the Kantang Formation as shown by a sharp change of lithology from sands to shales in the gamma-ray and sonic-log motifs (Figure 4.1). This well maker can be correlated to the Top Yala Formation in Seismic Marker. The depositional environment in the W9C-1 well suggested basin plain deposit and prograding distal fan (Polachan, 1988). According to the study by Polachan (1988) the Yala Formation consists of two units, i.e. the lower unit comprising glauconitic shales with abundant planktonic foraminifera and thin calcareous and micaceous sandstones, siltstones and detrital limestones and the upper unit comprising glauconitic sandstones, containing abundant planktonic foraminifera and shell fragments.

The detailed biostratigraphic study by Pflum et al. (1977) shows that abundant deep-water planktonic and agglutinated benthic foraminifera, calcareous nannofossils and dinoflagellates, were found in sediments of the Ranong Formation and suggested the age of the Ranong Formation is around Late Oligocene to Early Miocene.

4.1.4 Kantang Formation (Gold maker)

Kantang Formation mainly comprises shales with minor sandstones. In the W9B-1 and W9A-1 wells this formation unconformably overlies the Ranong Formation. This formation in the W9B-1 well has characteristic of log motifs revealed the coarsening upward sequence with grading up from shale to sandstone. In the W9C-1 well thin fining upward sequence is found in the upper unit. Sediments in the upper unit in the W9A-1 well are grains of sands and silts coarse than sediments of the upper unit in the W9B-1 well. Polachan (1988) suggested that the Kantang Formation consists of two essential, i.e. the lower unit of grey to brown grey glauconitic shales with abundant planktonic foraminifera and occasional thin siltstones, fine grained glauconitic sandstones and

detrital limestones, and the upper unit of silty glauconitic shales usually interbeded with thin siltstones, fine grained glauconitic sandstones and occasional detrital limestones.

Horizons of the Kantang Formation in W9B-1, W9A-1 and W9C-1 well are 308 meters, 356 meters and 160 meters thick, respectively. The depositional environment this formation base on wire-line log data is basinal plain and lower fan turbidites. The Payang formation observed from Payang-1 well, lied unconformably over Ranong formation and can be correlated to the Kantang formation in the Southern area. The limestones of Tai Formation in some well are also included in the basinal plain. The unconformity between the Ranong formation and the Payang formation, as observed characteristic of log motifs, revealed the massive fining upward delta sand of the Ranong formation in the Payang-1 well (Polachan, 1988).

4.1.5 Tai Formation (Yellow maker)

Tai Formation observed from W9D-1 and W9B-1 wells comprises mainly limestone (carbonate reef). In the W9D-1 well carbonate rocks are white to light grey, recrystallised coral-algal boundstones and foraminiferal packstones to grainstones, consistent with studied by Polachan (1988), The Tai Formation consists of three units, i.e. the basal unit comprising microcrystalline dolomite interbedded with anhydrite, dark grey shales and sandstones, the middle unit consisting of white to light grey massive, coral-algal reef limestones, and the upper unit comprising limestone clasts interbedded with grey, silty shales and fine-grained glauconitic sandstones, suggesting the deposition of Reefal carbonate in high energy environment (Polachan, 1988). However, the limestone strata associated with dark gray shale in the deeper part of the basin are inferred to be the deep-water or basinal limestone.

Horizons of the Tai Formation observed in the W9D-1 and W9B-1 wells are 730 and 146 meters thick, respectively. K-Ar dating result (38±3.8 Ma) by Union Oil (1976) suggested the formation overlies late Eocene quartz-chlorite schist basement in the Phanga and Tai wells. In the W9D-1 wells observed unconformity between Ranong Formation and Tai Formation have characteristic of lithological change from sandstones to reef limestones.

4.1.6 Trang Formation (Red maker)

Trang Formation observed from wells comprises mainly fine-grained clastic sediments: i.e., shales. In the W9B-1 well characteristic of log motifs revealed the fining upward sequence. The depositional environment was basin plain deposit with lower fan turbidites. Top horizon of the Trang Formation can be correlated to Middle Miocene Unconformity (MMU) which occurred regionally in the Andaman and Southeast Asia. This formation in W9D-1, W9B-1, W9A-1 and W9C-1 well are 85 meters, 853 meters, 109 meters and 156 meters thick, respectively.

According to Polachan (1988), the Trang Formation consists of two units, i.e. the lower unit consisting grey to brown-grey glauconitic shales containing abundant planktonic foraminifera and occasional thin siltstones fine-grained glauconitic sandstones and limestone and the upper unit comprising grey glauconitic shales, containing abundant planktonic foraminifera, shell fragments and carbonaceous detritus interbedded with siltstones, fine-grained glauconitic sandstones and calcarenites.

4.1.7 Thalang Formation (Light green maker)

Thalang Formation observed from wells comprises mainly silty shales. This formation in W9D-1, W9B-1, W9A-1 and W9C-1 wells can be correlated to the Top Thalang Formation and Top Upper Miocene (TUM) in seismic marker. Characteristic of log motifs in the W9B-1, W9A-1 and W9C-1 wells is the fining upward sequence. This formation in W9D-1, W9B-1, W9A-1 and W9C-1 well are 29 meters, 115 meters, 396 meters and 30 meters thick, respectively. Log motifs in the W9B-1 well revealed the fining upward sequence. The depositional environment was basin plain deposit with lower fan turbidites. Top Trang Formation is considered herein to represent Middle Miocene Unconformity (MMU).

According to Polachan (1988), the Thalang Formation comprises silty, glauconitic shales containing abundant planktonic, agglutinating and benthonic foraminifera, shell fragments and carbonaceous detritus interbedded with siltstones and fine-grained glauconitic sandstones, which indicate a late Miocene age.

In summary, well correlations in this study (Figure 4.1), it is suggested that the Ranong Formation unconformably underlain by Pre-tertiary basement in W9D-1, W9B-1 and W9A-1 wells, which in W9C-1 well found the Ranong Formation subsequent Yala Formation unconformably underlain by Pre-tertiary basement and is unconformably overlain by the Kantang Formation in W9B-1, W9A-1 and W9c-1 wells. No representative of this formation was found in the W9D-1 well. W9D-1 well is located at the Central High consisted of the Ranong Formation is partly missing on top of the structure and the Tai Formation is developed above the Formation. The Kantang Formation unconformably overlain by the Tai and Trang Formations. The Tai Formation observed in W9D-1 and W9B-1 wells but not found this formation in W9A-1 and W9c-1 wells, and this formation is an unconformably overlain by the Trang Formation is a facies equivalent of the Surin Formation, which unconformably overlain by the Thalang Formation. W9D-1 well is located at the Central High at about 40 km NW of C-1 well, which it was drilled on a large basement high faulted on both sides (Department of Mineral Fuels, 2006). W9B-1 well is located at about 45 km NW of W9A-1. W9C-1 well is located at about 30 km south of W9B-1 well. The W9B-1 and W9C-1 wells are located on a crest of block separating the two deepest zones of the Eastern Mergui Basin and and W9A-1 well was drilled on the biggest structure covering an area over 420 sq km (Department of Mineral Fuels, 2006).

4.2 Seismic Stratigraphy

4.2.1 Seismic interpretation

In this study, stratigraphy of the southern Mergui Basin has been determined based mainly upon the nature of theirs uniform characteristics which include reflection termination, seismic facies parameters, and reflection configurations in conjunction with the compiled wireline-logging data and provious studies.

The stratigraphy of the southern Mergui Basin is subdivided into 9 formations from bottom to top, include Ranong, Yala, Payang, Tai, Kantang, Surin, Trang, Thalang and Takua Pa formations, which the Ranong Formation unconformably overlie the Pre-

Tertiary Basement. The Upper Miocene Unconformity (UMU) overlyies the upper Miocene sediment. The seismic characteristics of individual units are described below.

4.2.1.1 Basement

The Top Basement (Figures 4.5) represents an unconformity between the pre-Tertiary and Tertiary rocks. The formation shows seismic characteristic by high-amplitude reflections with good to poor continuity and low frequency. The reflection laterally changes in polarity and amplitude, and the characteristic of an angular unconformity that overlies multiple types of lithology. The Mergui ridge, the Mergui shelf, and the Central high are herein regarded as the basement high, which the Central High separated Western Mergui sub-basin from Eastern Mergui sub-basin. The high of the basement from the present sea level ranges from 736 m at seismic line AD1 to 1,512 m at seismic line AD7. It is found that in the study Southern Mergui Basin area, the basement rock became deeper to the west (up to the depth of 1,375 meters) than to the east (up to the depth of 1,300 meters) basin.

4.2.1.2 Ranong Formation

Top horizon of the Ranong Formation in the southern Mergui Basin is shown in pink color (Figure 4.6). This formation comprises sub-parallel reflection with moderately continuous reflection with moderate to high amplitude and moderate to good continuity. This formation lay onlapped onto the Basement rock. The top of the Ranong Formation is truncated into the Yala Formation. The Ranong Formation is assigned as Oligocene to Earliest Miocene based on microfossils (Polachan and Racey, 1994). Three lithologicall subunits are recognized by Srikulwong (2006) based on wireline-log data. The lower subunit is mainly coarse-grained sandstone with poor sorting and fining upward sequence. The middle subunit consists largely of greenish-gray sandstone, siltstone, and shale with thin coal seam. The upper subunit is sandstone and conglomerate. The formation thickness ranges from 1,400 meter to a minimum of about 300 meter toward the basement highs.

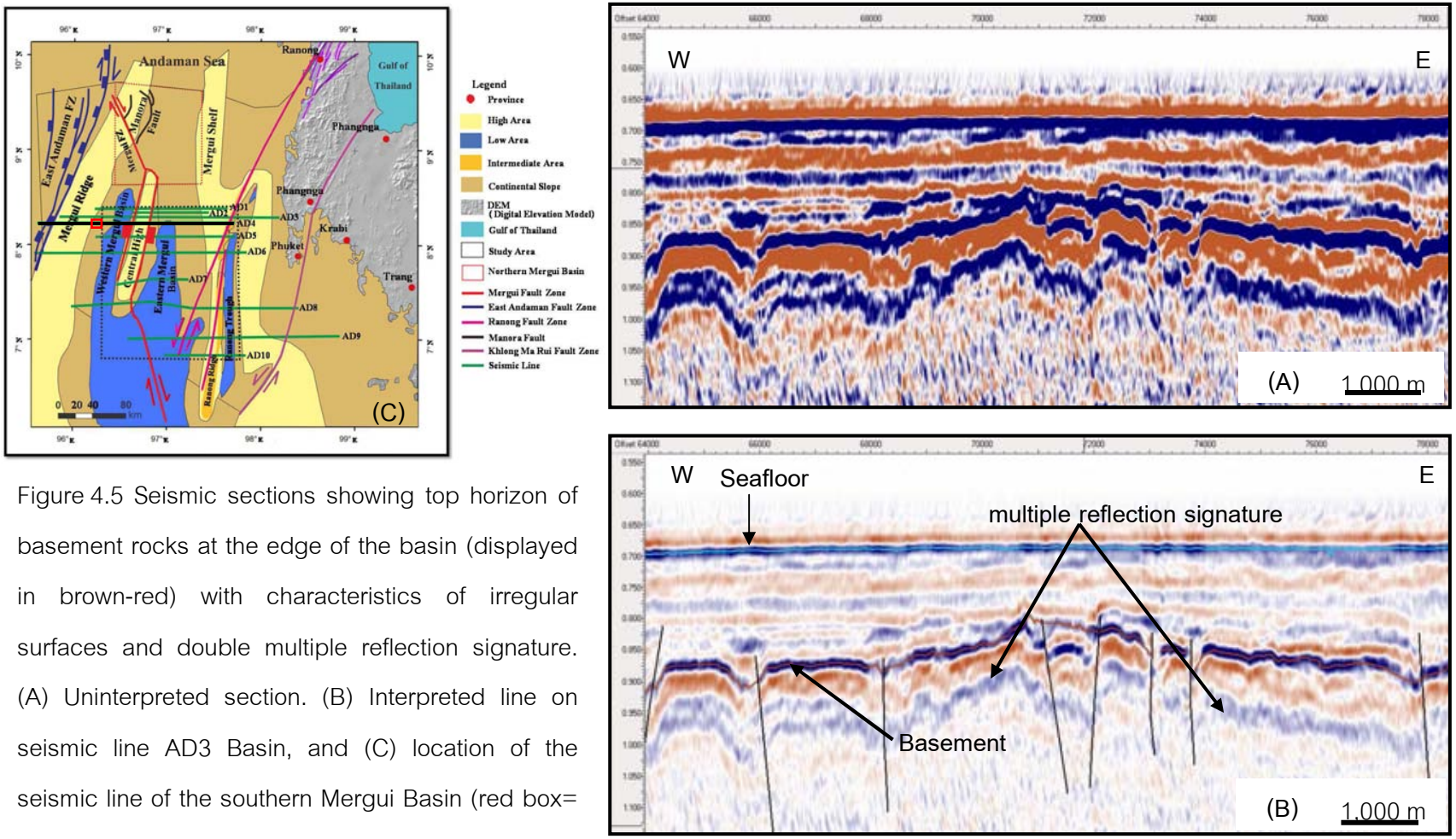

Figure 4.5 Seismic sections showing top horizon of basement rocks at the edge of the basin (displayed in brown-red) with characteristics of irregular surfaces and double multiple reflection signature. (A) Uninterpreted section. (B) Interpreted line on seismic line AD3 Basin, and (C) location of the seismic line of the southern Mergui Basin (red box= location of seismic section).

4.2.1.3 Yala Formation

Top horizon of the Yala Formation (blue color line in Figure 4.6) is recognized as an onlap surface, and is picked at the base of upper Oligocene sediment. This formation comprises sub-parallel reflection with moderate amplitude with low frequency and good continuity reflection. The Yala Formation is sitting over the Ranong Formation. The Yala formation from the well data, indicates a lateral facies change with the Ranong Formation and is found only within the southern area. The Yala Formation consists entirely of fine-grained clastic sediments including glauconite shale, micaceous fine-sandstone and siltstone, and few limestone (Srikulwong, 2006). The thickness of the Yala Formation varies from 1,120 meter to 2,120 meter.

4.2.1.4 Payang Formation

Top horizon of the Payang Formation (green color line in Figure 4.7) comprises sub-parallel reflection with moderate to high amplitudes and moderate continuity, which lay onlapped onto the Ranong Formation. Payang Formation is used herein for these Lower Miocene sandstones (Polachan, 1988) with its thickness ranging from 700 merter to 1,300 meter.

4.2.1.5 Kantang Formation

Top horizon of the Kantang Formation (gold color line in Figure 4.8) is represented by sub-parallel reflection. At the edge of basin (or the Mergui ridge) an erosion truncation is observed. The formation toplaps onto the Ranong formation with strong amplitudes and moderate to good continuity. This formation consists mainly of shales in lower and upper silty shales interbedded with sandstones. The Kantang Formation has a thickness ranging from 350 to 1,300 meter. Such a stratigraphic configuration suggests that basin subsidence during the deposition of the Kantang Formation with the termination of normal fault.

The Kantang Formation lies unconformably over the Ranong and Yala Formations and comprises sub-parallel relfections with strong to moderate amplitndes and good continuity. These reflections onlap onto Ranong Formation.

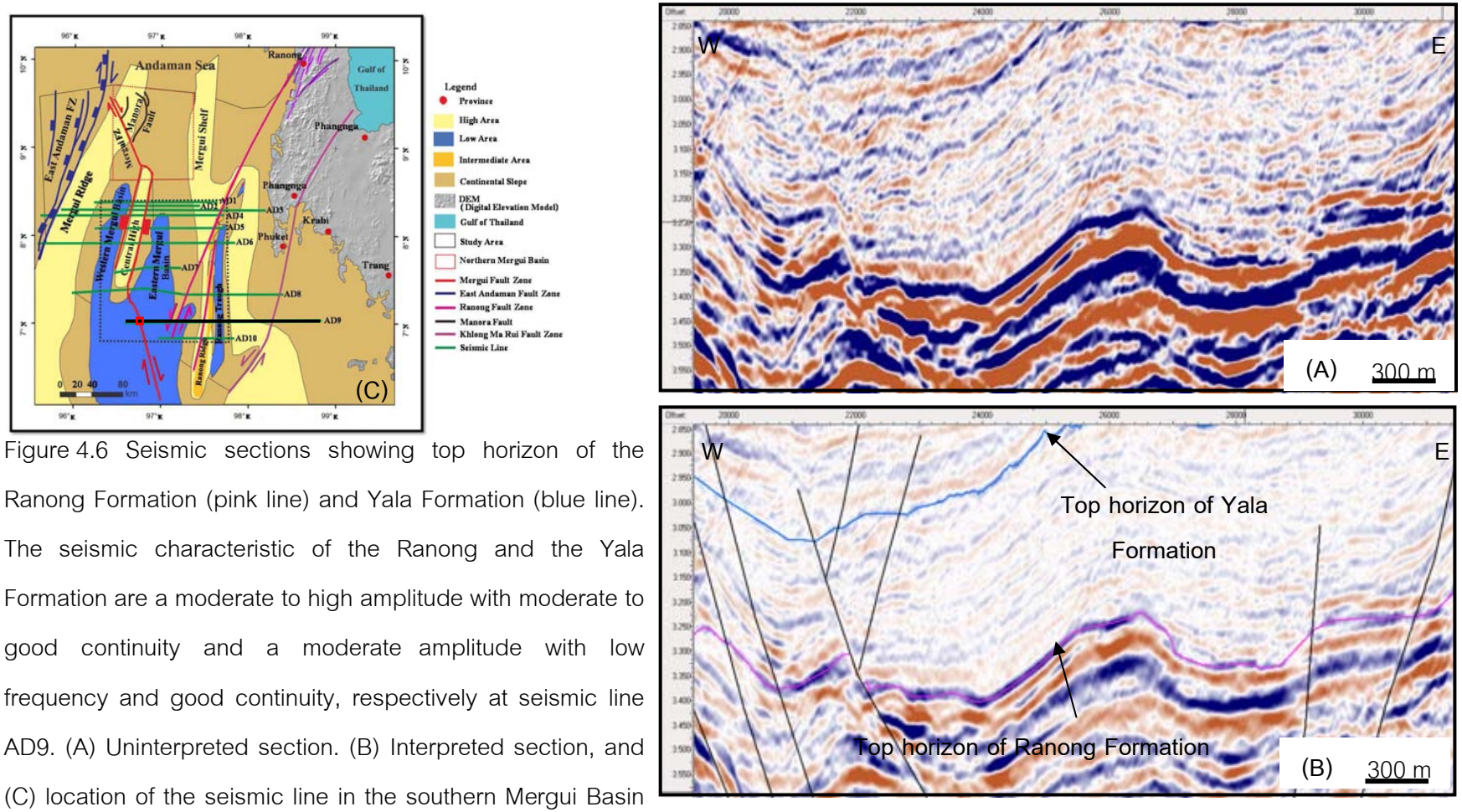

Figure 4.6 Seismic sections showing top horizon of the Ranong Formation (pink line) and Yala Formation (blue line). The seismic characteristic of the Ranong and the Yala Formation are a moderate to high amplitude with moderate to good continuity and a moderate amplitude with low frequency and good continuity, respectively at seismic line AD9. (A) Uninterpreted section. (B) Interpreted section, and (C) location of the seismic line in the southern Mergui Basin (red box= location of seismic section).

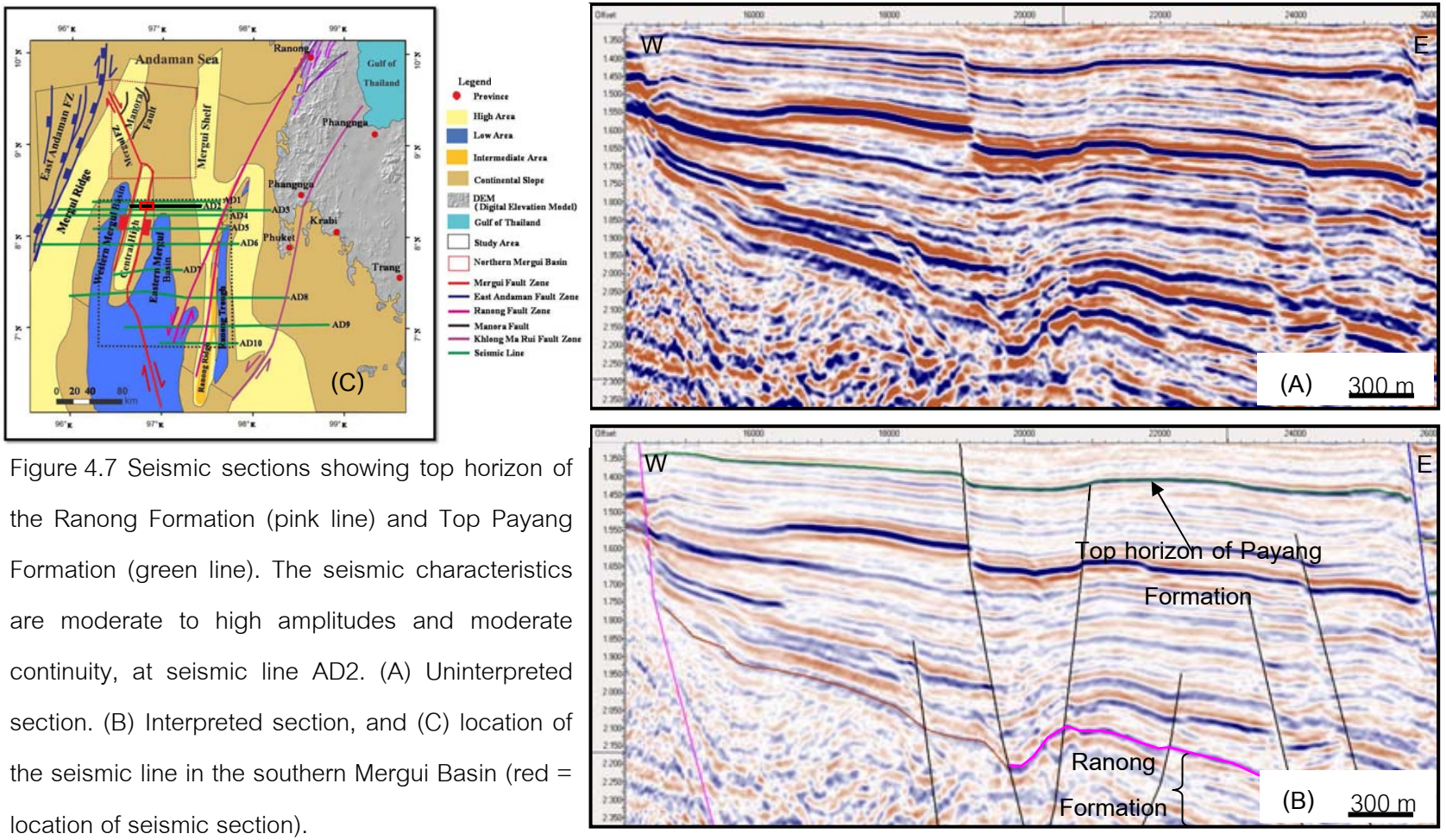

Figure 4.7 Seismic sections showing top horizon of the Ranong Formation (pink line) and Top Payang Formation (green line). The seismic characteristics are moderate to high amplitudes and moderate continuity, at seismic line AD2. (A) Uninterpreted section. (B) Interpreted section, and (C) location of the seismic line in the southern Mergui Basin (red = location of seismic section).

4.2.1.6 Tai Formation

Top horizon of the Tai Formation (yellow color line in Figure 4.9) is picked on the top of reefal carbonate formation observed in seismic line AD7 at the location of well W9-D1. The formation lies underneath an unconformable surface and can be found generally throughout the area under study. This formation comprises sub-parallel reflection with high amplitudes and moderate to good continuity and low frequency. This formation has the thickness ranging of 400 to 800 meter.

4.2.1.7 Surin Formation

Top horizon of the Surin Formation is shown as purple line (Figure 4.9 and 4.10) and consists of distinct sets west-dipping clinoforms and toplap. The clinoform vary from 420 to 794 meter. This formation is a truncation surface at certain locations. This formation comprises sub-parallel reflection with high-moderate amplitude and good continuity. The internal reflections vary in amplitudes and depicts typical of prograding shallow-marine (Polachan, 1988) with grain size decreasing away from the shoreline. The horizon was locally truncated by an erosional surface. The Surin formation has a thickness ranging from 200 to 730 meter, except in the southern part of the basin and at the edge of basin which the sediment supply was limited. The Surin formation has a wedge-shaped geometry.

4.2.1.8 Trang Formation

Top of the Trang Formation represents an erosional surface occurring during late Miocene time. This formation is seismic characterized by onlap surface, which is comprises sub-parallel reflection with very high amplitude and moderate to good continuity. In the Central Area, this formation was terminated by the Upper Miocene Unconformity-UMU horizon. In the southern area, this formation was appeared to the top of prograding clinoforms. The average thickness of this formation is 700 meters.

The Upper Miocene Unconformity (UMU) shown in red color is picked on onlap and erosional surface, overlying the Trang Formation and Thalang Formation.

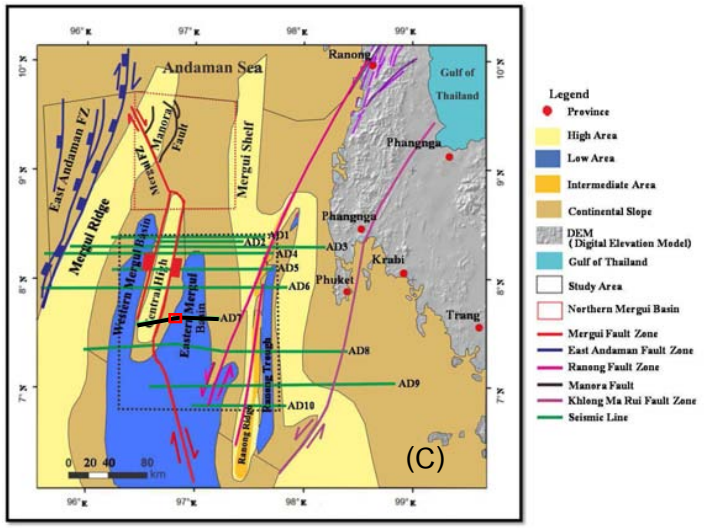

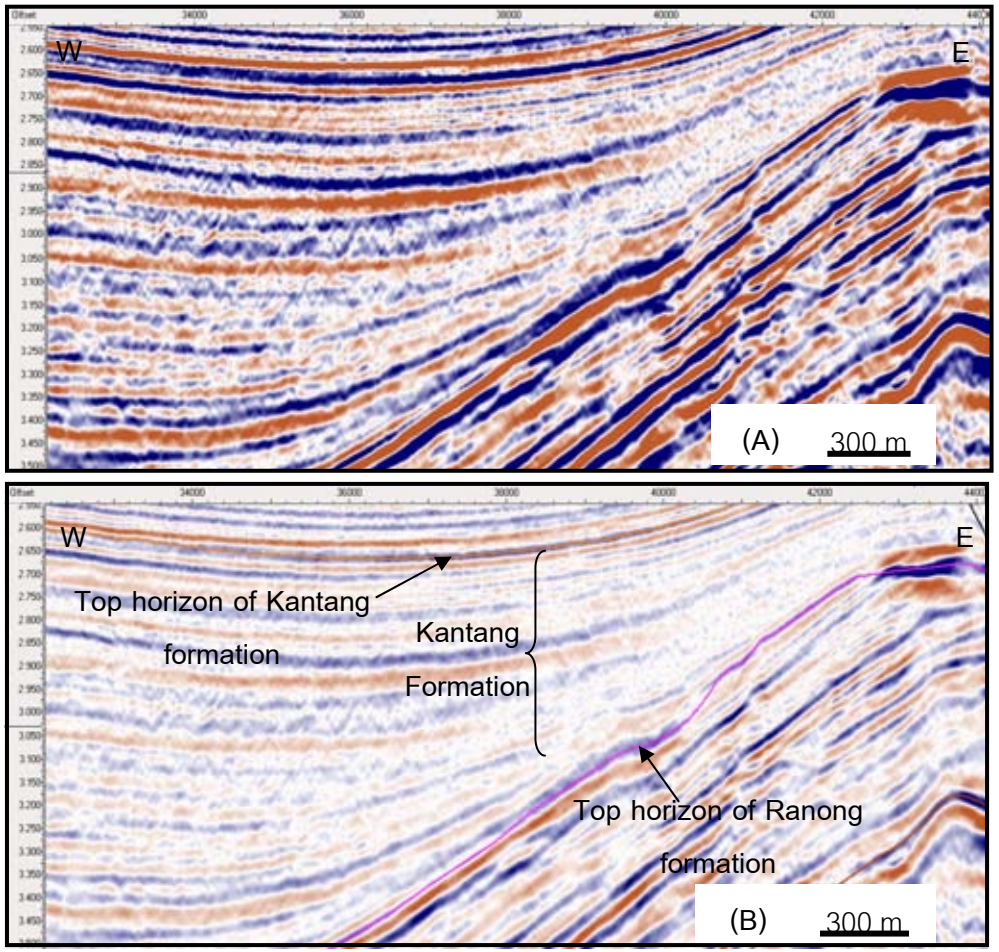

Figure 4.8 Seismic sections displaying the top horizon of the Ranong Formation and Top Kantang Formation. The Kantang Formation is characterized of seismically by a strong amplitudes and moderate to good continuity, as shown from seismic line AD7. (A) Uninterpreted section (B) Interpreted section. and (C) location of the seismic line in the southern Mergui Basin (red box= location of seismic section).

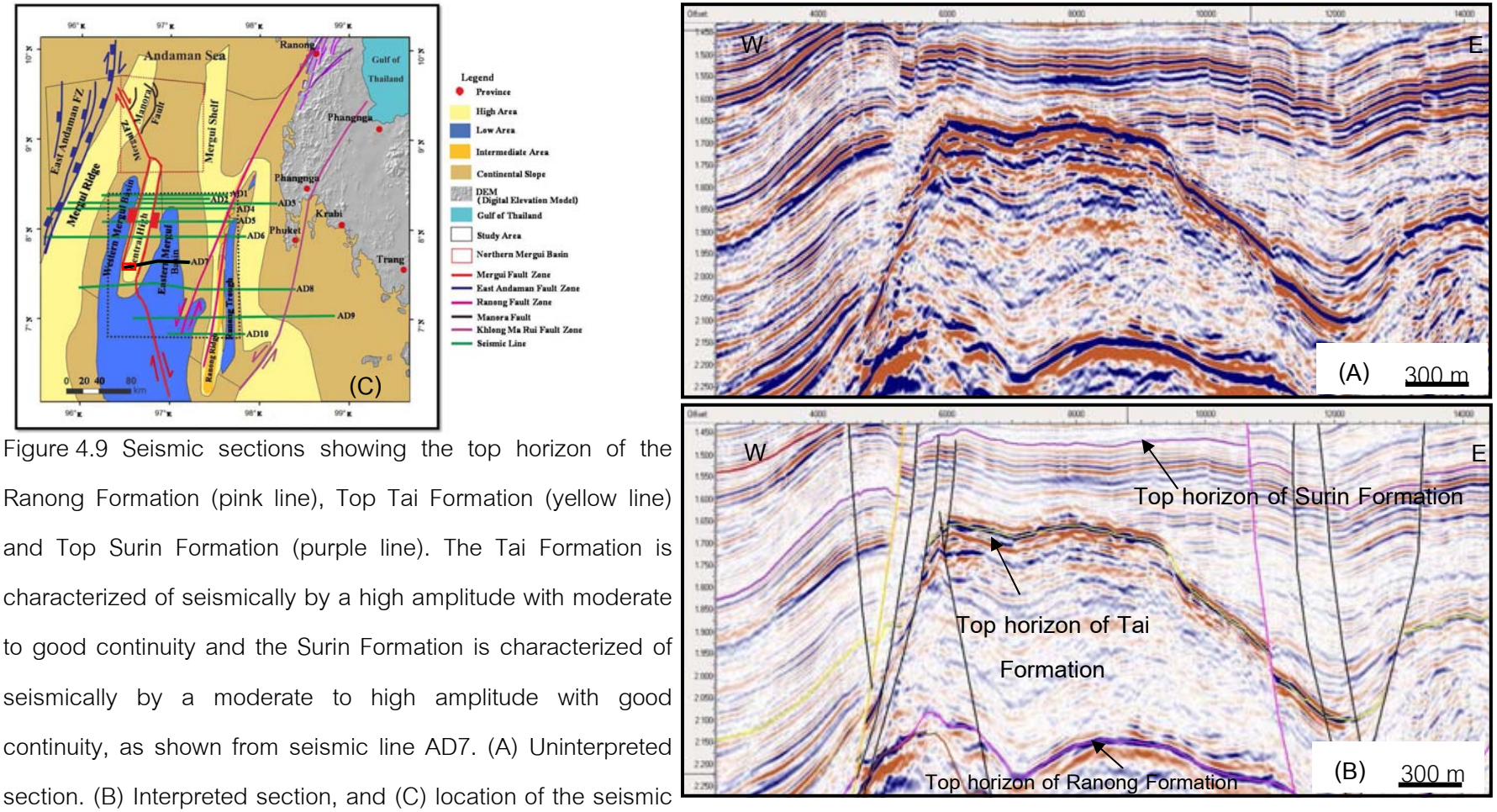

Figure 4.9 Seismic sections showing the top horizon of the Ranong Formation (pink line), Top Tai Formation (yellow line) and Top Surin Formation (purple line). The Tai Formation is characterized of seismically by a high amplitude with moderate to good continuity and the Surin Formation is characterized of seismically by a moderate to high amplitude with good continuity, as shown from seismic line AD7. (A) Uninterpreted section. (B) Interpreted section, and (C) location of the seismic line in the southern Mergui Basin (red box= location of seismic section).

The UMU is located on upper Miocene sediment in the southern area and is depicted by very high amplitndes with good continuity.

4.2.1.9 Thalang Formation

Top horizon of the Thalang Formation is shown in light green and is terminated as onlap surface, which consists of sub-parallel reflections with high amplitudes and moderate to good continuity. Log data reveal that Thalang Formation consisted silty shale and some fine-grained sandstone. Seismic signatures show that horizons of the Thalang Formations have quit uniform thickness. Beside several layers, this formation has an average thickness of 200 meters.

4.2.1.10 Takua Pa Formation

Top horizon of the Takua Pa Formation is overlain by the seabed (turquoise color line in Figure 4.9). This formation is characterized by sub-parallel reflections of clinoform configurations at eastern edges of the basin at the southern part of the basin, suggesting deposition onto the continental slope with the thicker more than in the north (Figure 4.11). The average thickness of the Takua Pa Formation is about 200 meter. The seafloor is characterized by high amplitude with very good continuity (Figure 4.9)

Stratigraphic correlation chart showing in Figures 4.12, displays variation in formation thickness for each of the seismic section, Northt-South cross section in the Southern Mergui Basin and displays composite stratigraphy in Figures 4.13 by determined from interpreted seismic section

In summary, on the basic of the stratigraphic relationships in this study (Figure 4.12), it is suggested that the Ranong Formation and subsequent Yala Formation unconformably underlain by Pre-tertiary basement and is unconformably overlain by the Payang Formation in seismic lines AD1 and AD2 together with studied well data. The Yala Formation in seismic lines AD8-10 conformably overlies the Ranong Formation and is unconformably overlain by the Kantang Formation. The Payang Formation sediment unconformably overlies by shales of Kantang Formation in seismic lines AD3-7 and by correlating with W9A-1, W9B-1 and W9C-1 wells data. The unconformity is marked by

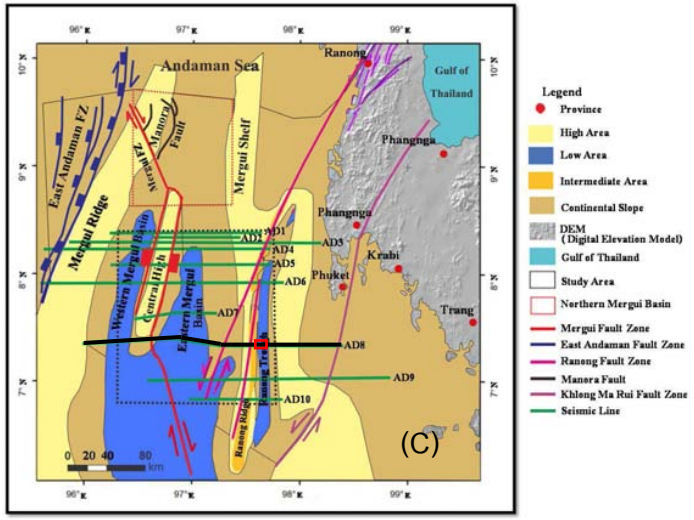

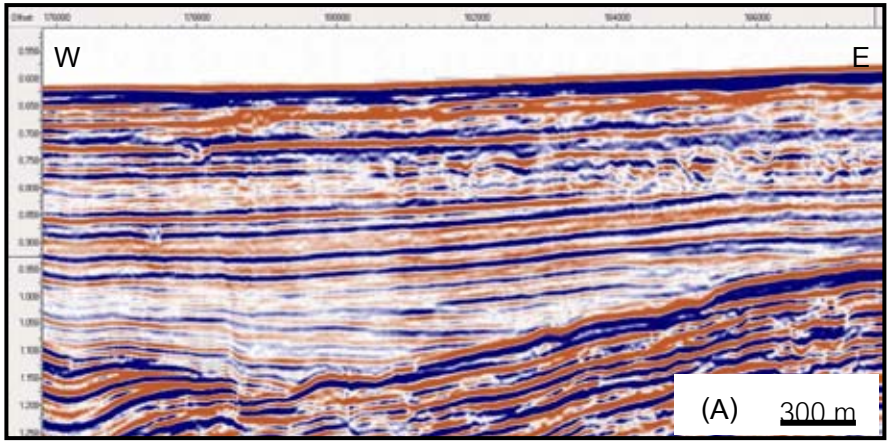

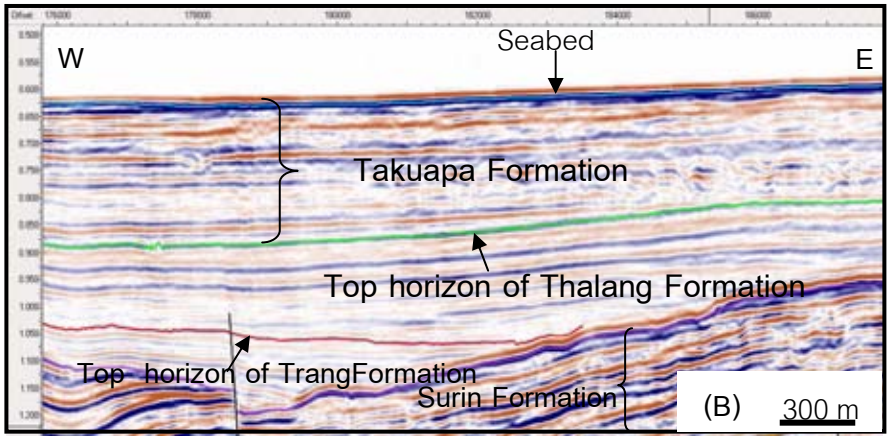

Figure 4.10 Seismic sections showing the top horizon of the Trang Formation (red line), Top Thalang Formation (light green line) and Seabed (turquoise line). The Trang Formation is characterized seismically by a moderate to high amplitude with moderate continuity. The Thalang Formation is characterized seismically by a high amplitude with moderate to good continuity and Seabed is characterized seismically by a high amplitude with very good continuity, as shown from seismic line AD8. (A) Uninterpreted section. (B) Interpreted section, and (C) location of the seismic line in the southern Mergui Basin (red box= location of seismic section).

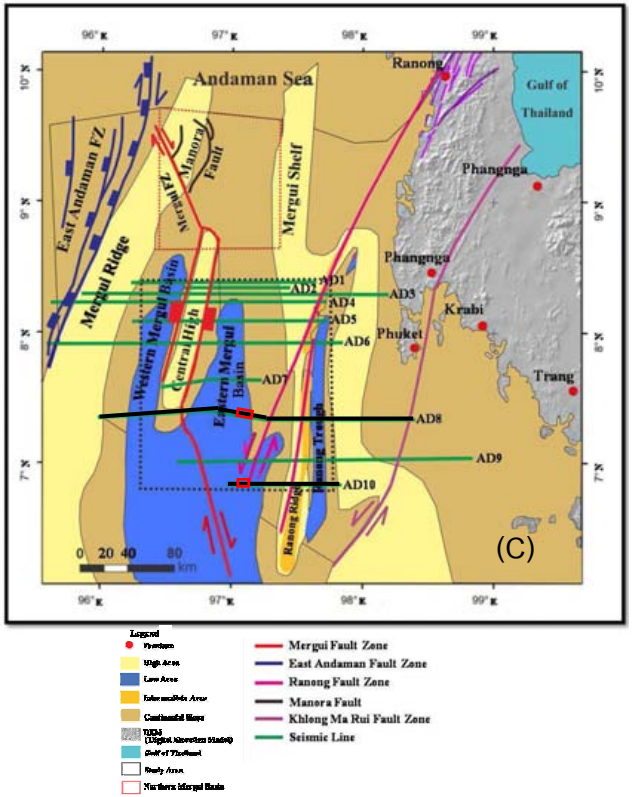

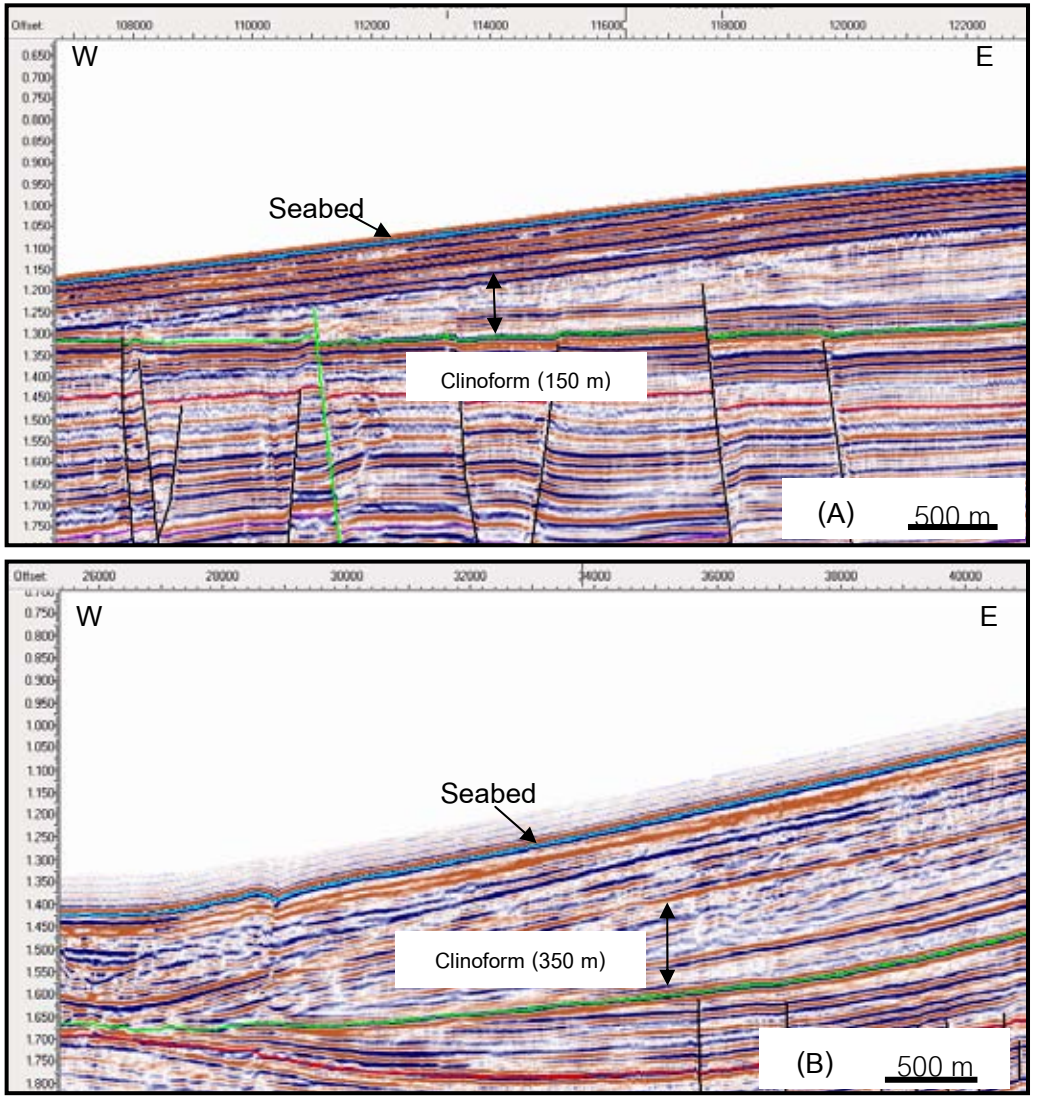

Figure 4.11 Seismic sections showing the southward increase in thickness of clinoform of the Takua Pa Formation (A) Seismic line AD8 and (B) Seismic line AD10, and (C) location of the seismic line in the southern Mergui Basin (red box= location of seismic section).

sharp change from sands to shales. The Payang Formation unconformably overlies the Ranong Formation and is unconformably overlain by the Tai Formation. The Payang Formation was deposited simultaneously with the Tai Formation and Kantang Formation. Seismic lines AD3-10 displays the Kantang Formation unconformably overling the Ranong Formation. The Kantang Formation unconformably overlies the Yala Formation and is unconformably overlain by the Tai and Surin Formations. The Kantang Formation is marked by sharp changes from sands to shales. The Tai Formation is unconformably overlain by the Surin Formation. The Surin Formation unconformably overlies the Tai and Kantang Formations as seen from the enhanced seismic lines. Sediments of the Trang Formation is a facies equivalent of the Surin Formation by deposited simultaneously with the Surin Formation and is unconformably overlain by shale of Thalang Formation by shale of Thalang Formation by correlating with W9A-1, W9B-1 and W9C-1 well data. All seismic lines in this study showing unconformably this study showing unconformably overlies the Trang Formation and is unconformably overlain shales of Takua Pa Formation. In addition, the Takua Pa Formation is unconformably overlain by shales of Thalang Formation, which deposited in shallow marine environments during the Pliocene- Recent.

4.2.2 Seismic stratigraphy

Seismic stratigraphy, terminations, in seismic sections can identify boundaries between formations, they are onlap, toplap, downlap, clinoforms and erosion truncation. In this study, terminology of seismic stratigraphy follows the definition described by Octavian (2002). The Ranong Formation onlaps onto the Top Basement (Figure 4.14) which is hanging wall sides of the normal faults due to extensive rifting activity. Continuation of rifting causes subsidence process, the Payang Formation deposited and onlaps onto the Ranong Formation which this formation have characteristic a wedge shape. In addition, onlaps occur overlying the Trang, Thalang and Takua Pa Formation (Figure 4.15) located at hanging wall of the normal faults in the edge of the Western Mergui Basin which occurs during periods of transgression.

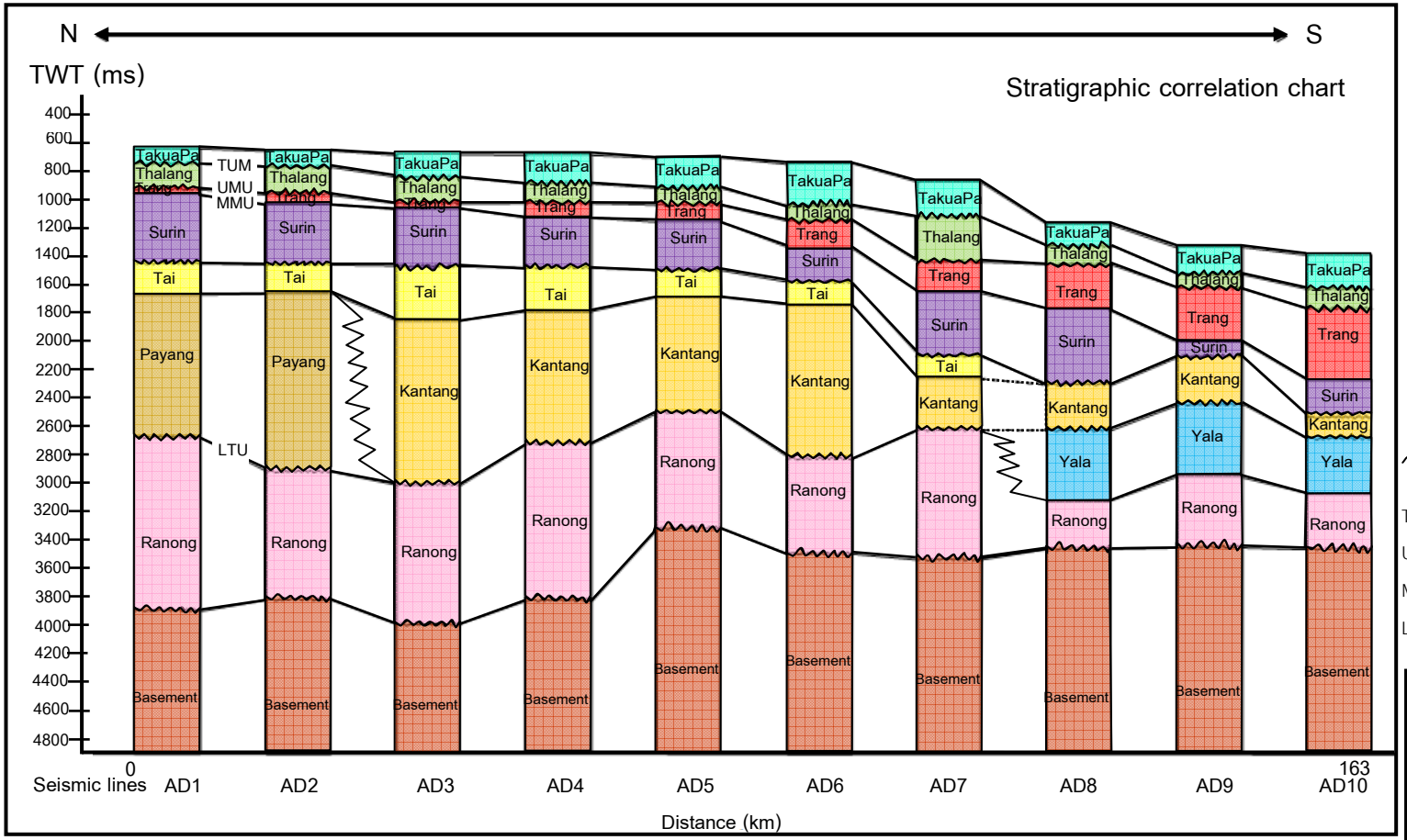

Figure 4.12 Stratigraphic correlation chart showing variation and distribution of all the formations from the enhanced seismic lines in the southern Mergui Basin. (B) Blue line = Northt-South cross section and red box = study area.

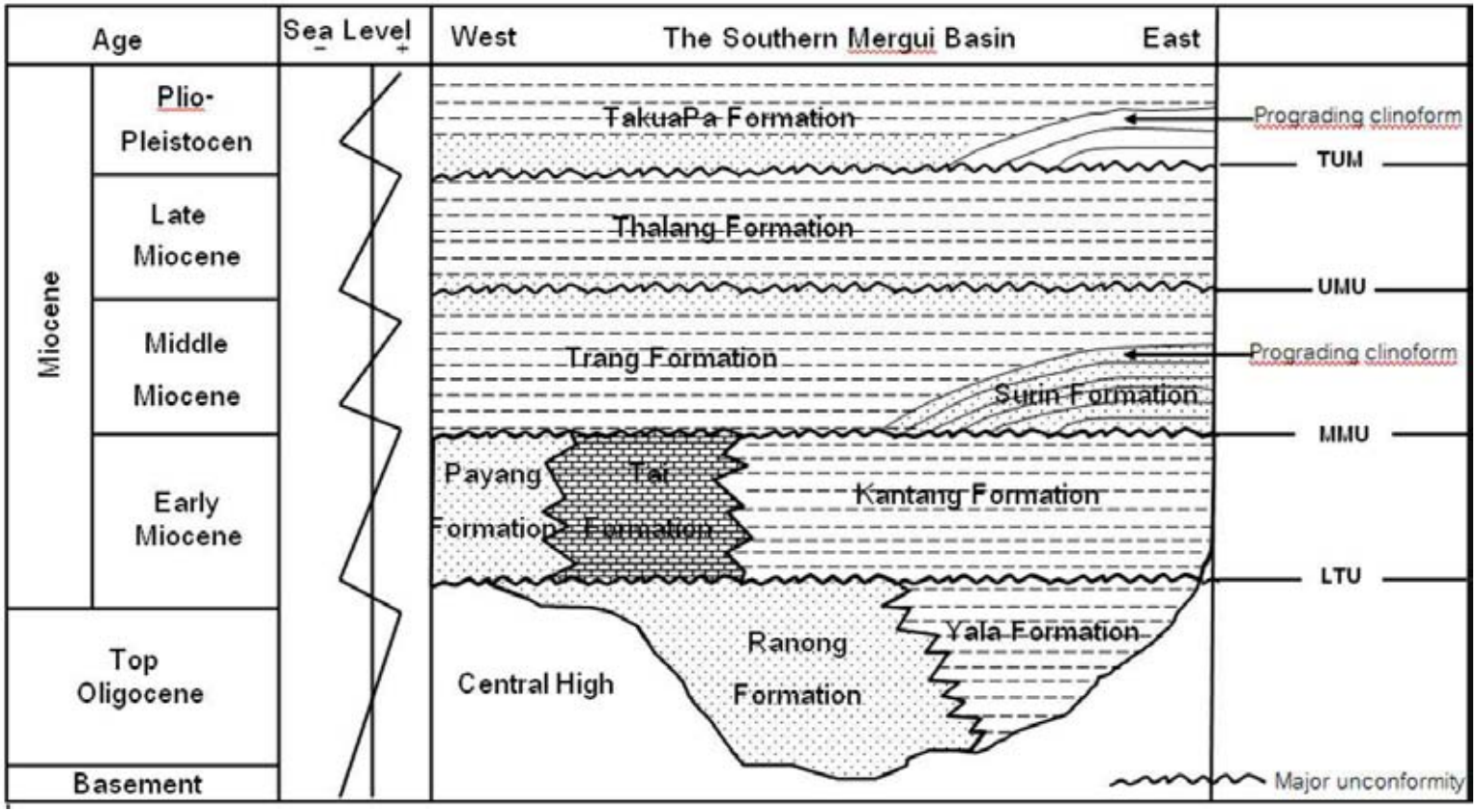

Figure 4.13 Composite stratigraphy determined from interpreted seismic sections (West-East cross section) and wire-line logs of the Eastern Mergui Basin. (modified from Polachan and Racey, 1994). TUM = Top Upper Miocene, UMU = Upper Miocene Unconformity, MMU = Middle Miocene Unconformity, and LTU = Lower Tertiary Unconformity. Note That Clinoform structure an one key index of the Surin Formation.

Toplap and erosion truncation occur of the Kantang Formation onto the Ranong formation located at the edge of basin or the Mergui ridge. In addition, occur erosional surface overlying the Trang Formation by relative with sea level fall and uplift (Figure 4.16) and occur toplap in Thalang Formation (Figures 4.17 and 4.18).

The sediment filling of the basin during a subsidence of Surin Formation, which at the eastern Mergui Basin occur prograding clinoforms in the Surin Formation, which consists of distinct sets of west-dipping clinoforms that downlap (Figure 4.19) onto the Top Payang horizon. There is a truncation surface at certain locations. Prograding clinoforms containing the seismic reflections can be described as high amplitude reflections and high frequency, strong amplitudes. This suggest a typical of progradations process shallow-marine with grain size decreasing away from the shoreline, relative sea level rise, and was believed from source of sediment to be from the Mergui Shelf. In addition, there are prograding clinoforms deposition of the Takua Pa formations at the eastern edges of the basin (Figure 4.20) which suggests a deposition onto the continental slope with the thicker sequences in the southern Mergui Basin than in the northern Mergui Basin (Figure 4.11) and found downlap in this formation (Figure 4.21).

4.3 Structure

Polachan (1988) first recognized the fault system in the Mergui Basin. However not only fault but also folds are recognized following are the detailed description of main structures found in the enhanced seismic section from this study.

4.3.1 Fault

Two systems of faults have been identified from the enhanced seismic data in the southern Mergui Basin, including the strike-slip faults and the dip-slip faults. The dip-slip faults are normal (Figures 4.22 and 4.23) and reverse faults (Figure 4.24). The former are much more common. These dip-slip faults orient in the north-south direction. Both Faults are developed in the basin simultaneously with deposition of the Cenozoic sediments.

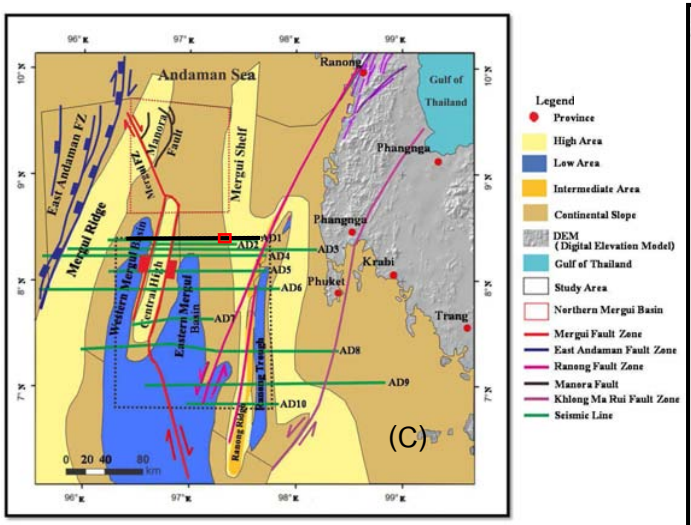

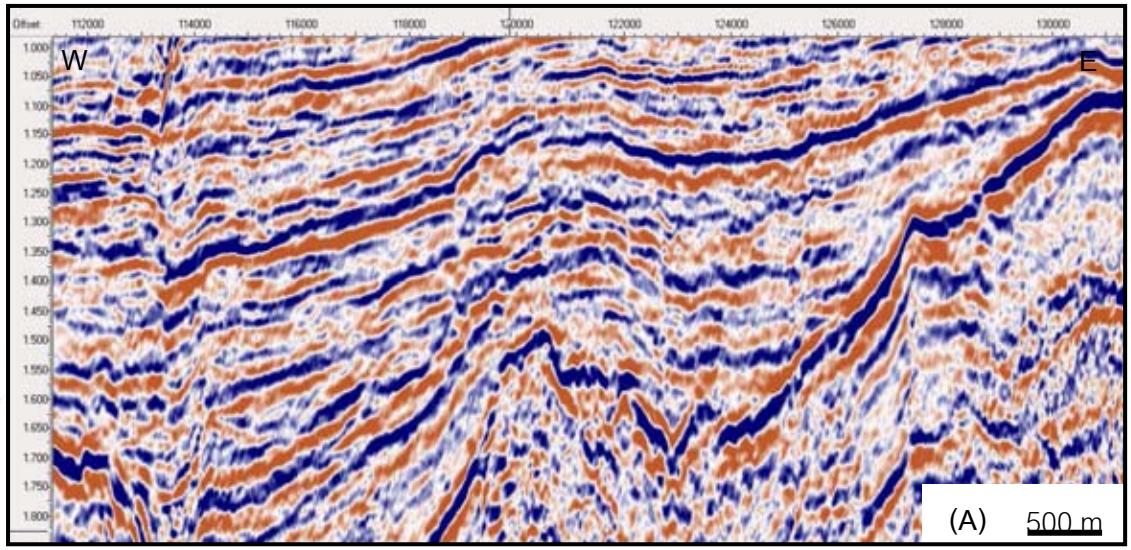

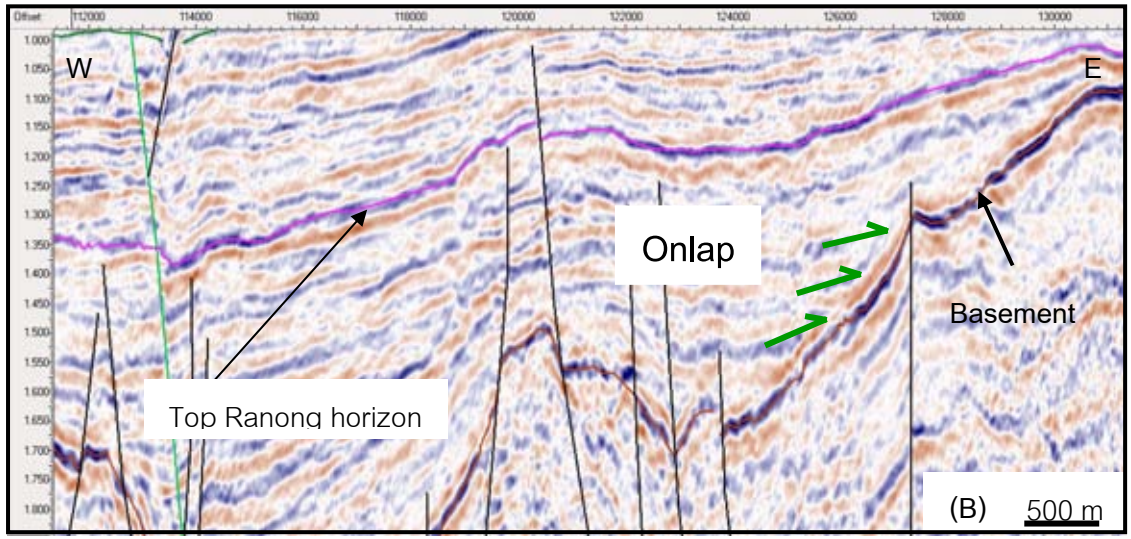

Figure 4.14 Seismic sections showing the top horizon of the Ranong Formation. (A) Uninterpreted seismic line AD1 (B) Interpreted section with indicated onlap (green arrows), and (C) location of the seismic line in the southern Mergui Basin (red box= location of seismic section).

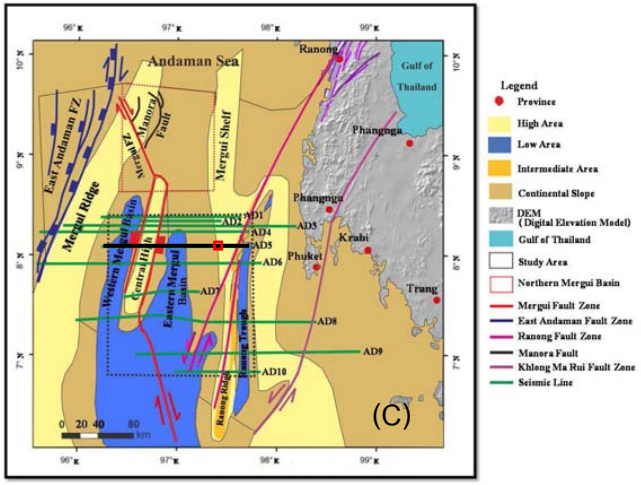

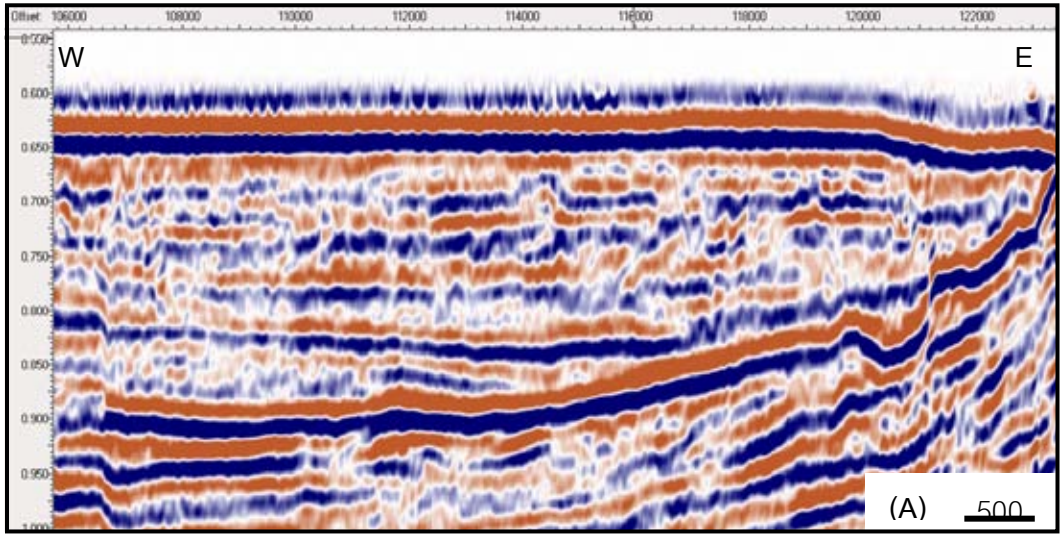

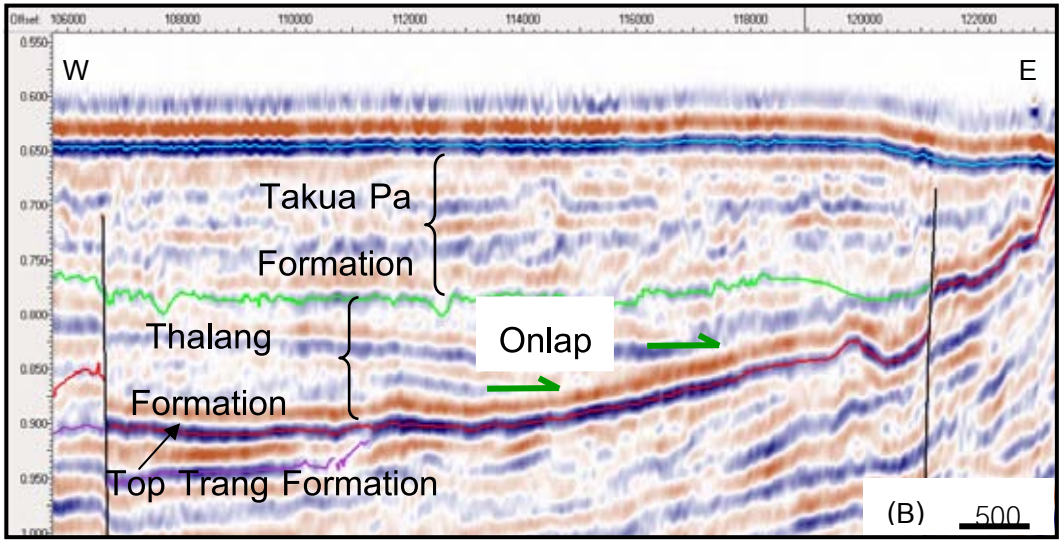

Figure 4.15 Seismic sections showing the onlap overlying the Trang and Thalang Formations. (A) Uninterpreted seismic line AD5 (B) Interpreted section with indicated onlap (green arrows), and (C) location of the seismic line in the southern Mergui Basin (red box= location of seismic section).

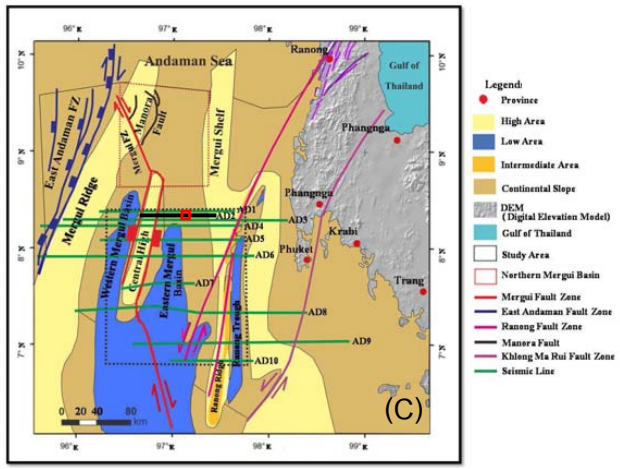

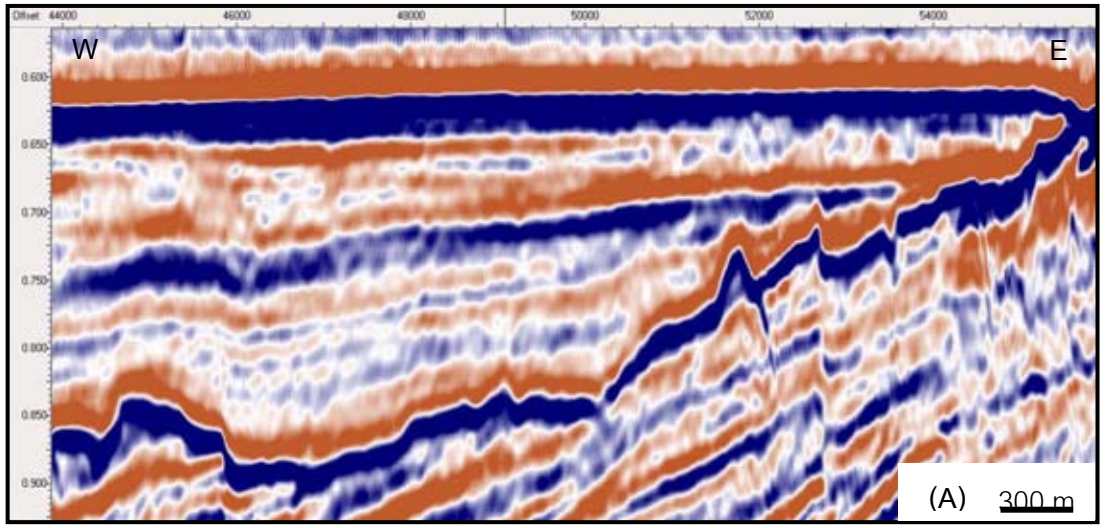

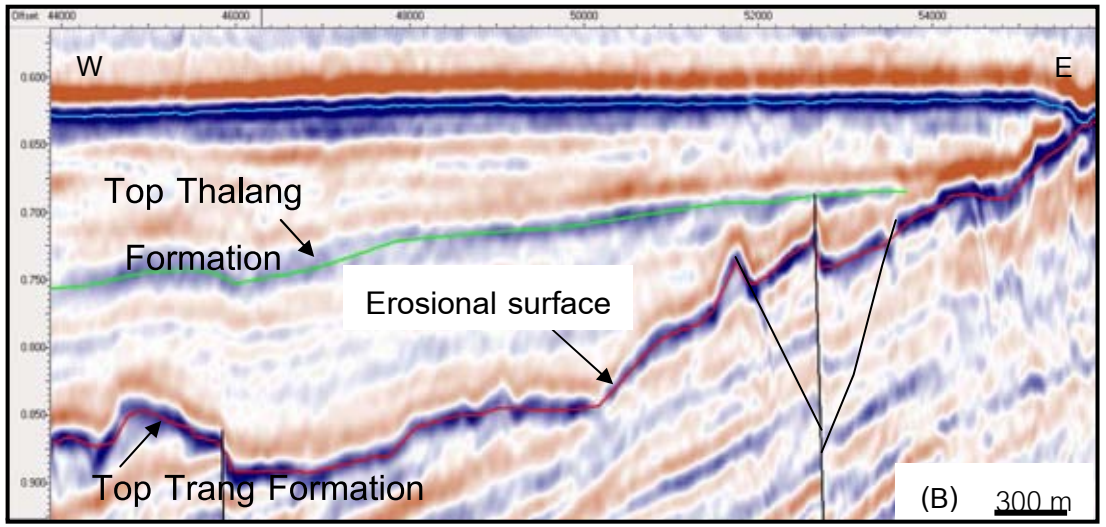

Figure 4.16 Seismic sections showing the erosional surface and associated structure on Trang Formation. (A) Uninterpreted seismic line AD2 (B) Interpreted section, and (C) location of the seismic line in the southern Mergui Basin (red box = location of seismic section).

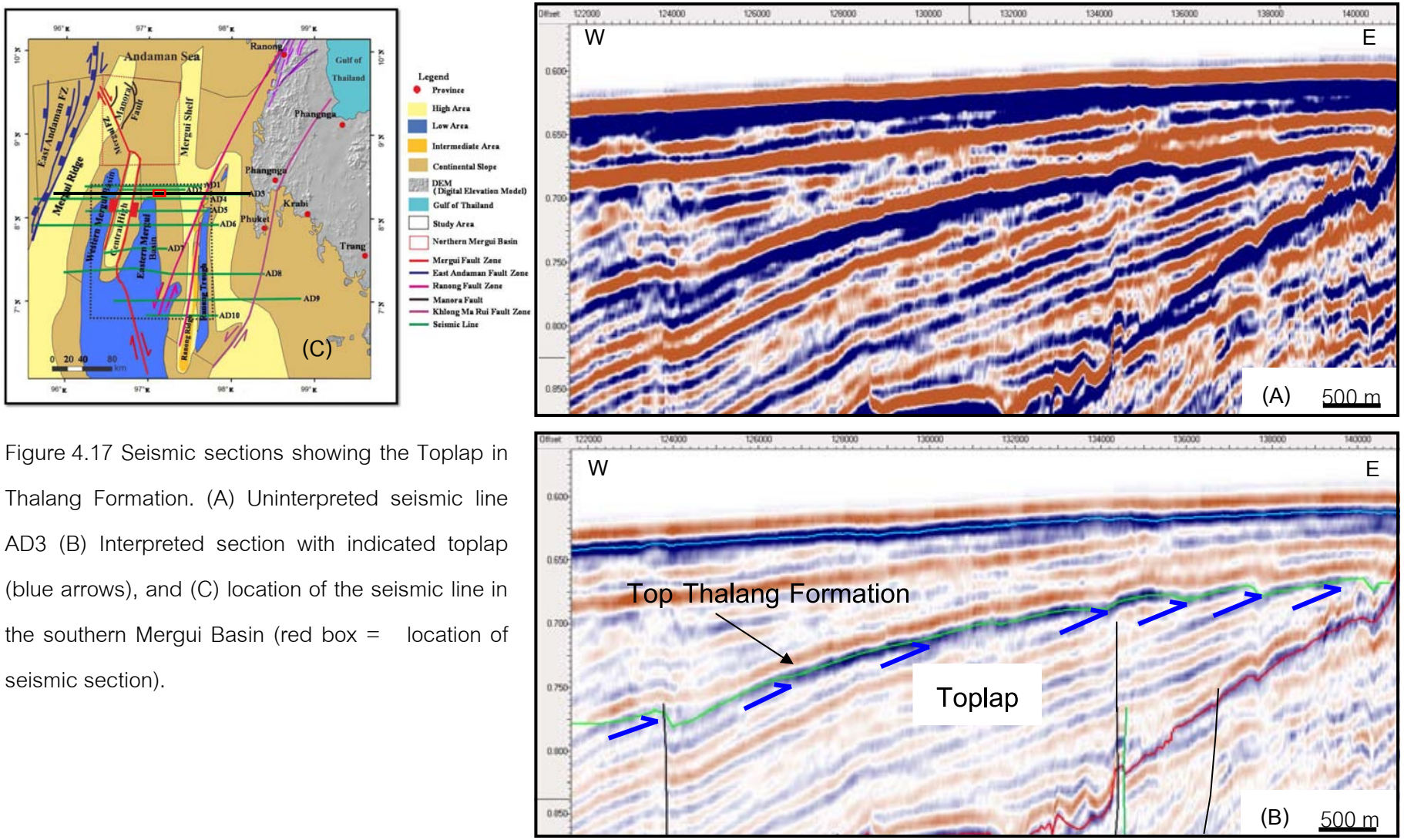

Figure 4.17 Seismic sections showing the Toplap in Thalang Formation. (A) Uninterpreted seismic line AD3 (B) Interpreted section with indicated toplap (blue arrows), and (C) location of the seismic line in the southern Mergui Basin (red box = location of seismic section).

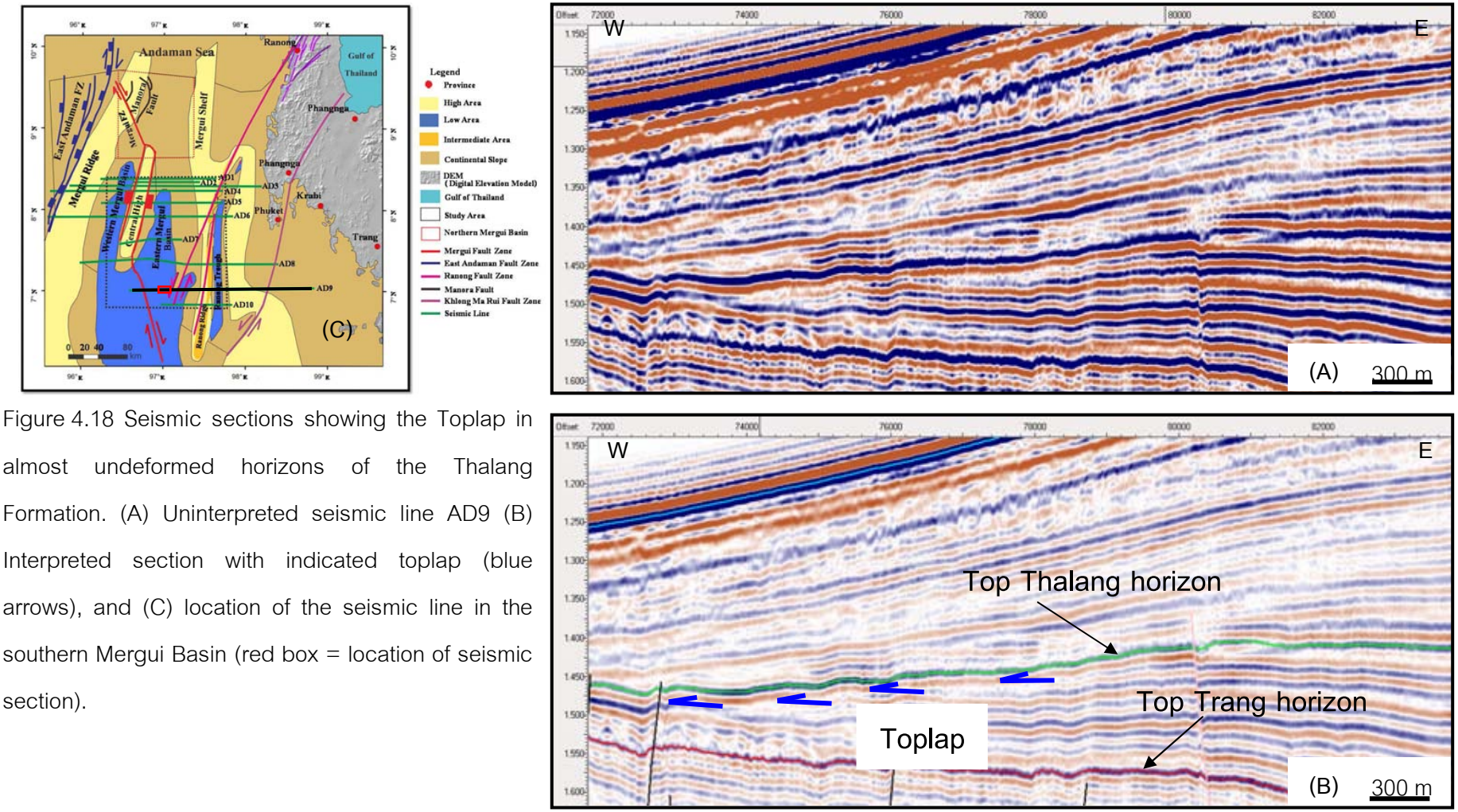

Figure 4.18 Seismic sections showing the Toplap in almost undeformed horizons of the Thalang Formation. (A) Uninterpreted seismic line AD9 (B) Interpreted section with indicated toplap (blue arrows), and (C) location of the seismic line in the southern Mergui Basin (red box = location of seismic section).

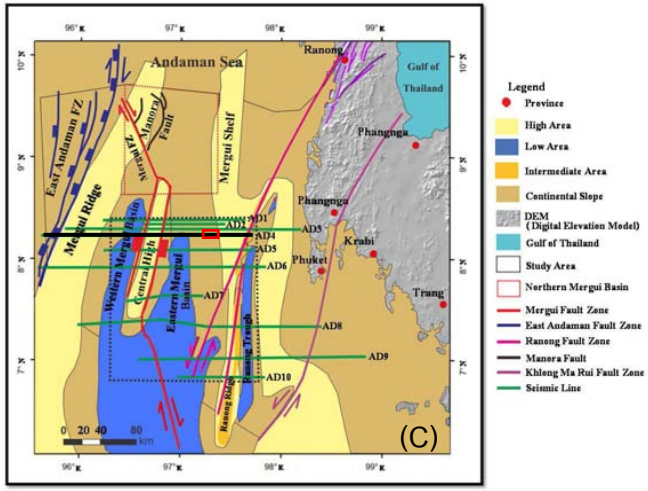

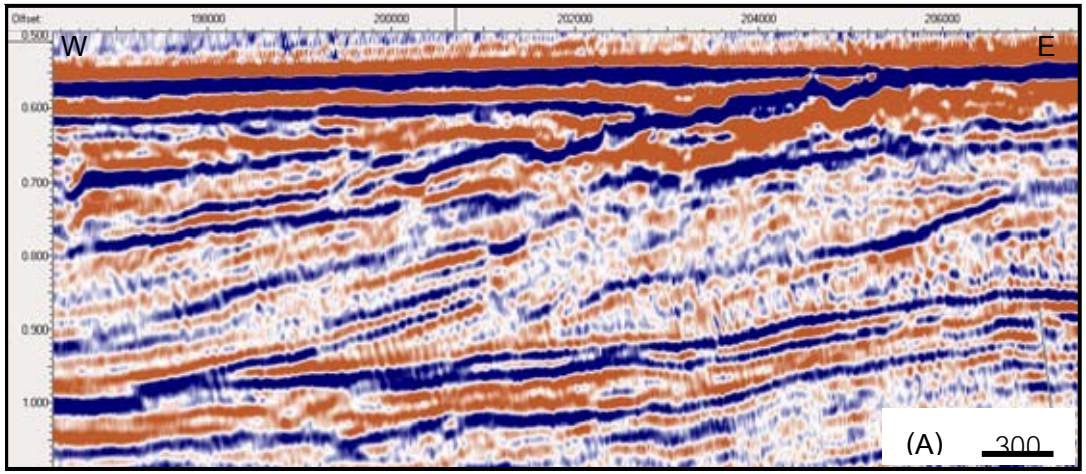

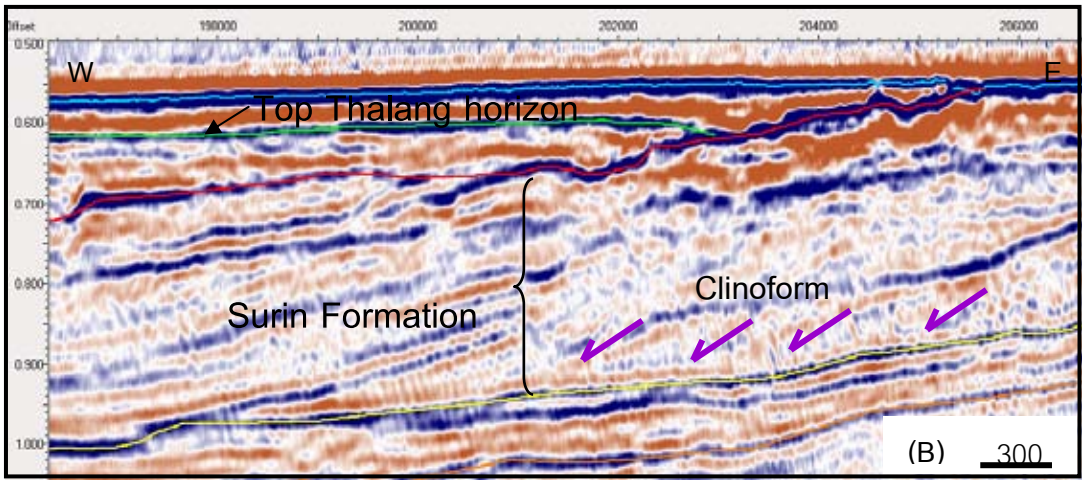

Figure 4.19 Seismic sections showing the clinoform in Surin Formation. (A) Uninterpreted seismic line AD4 (B) Interpreted section with indicated clinoform (purple arrows), and (C) location of the seismic line in the southern Mergui Basin (red box = location of seismic section).

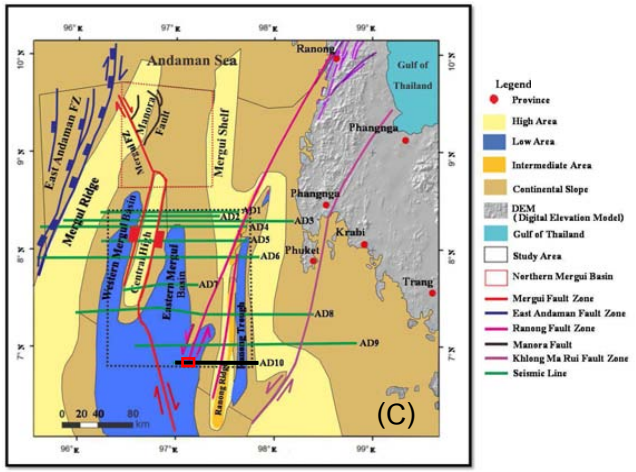

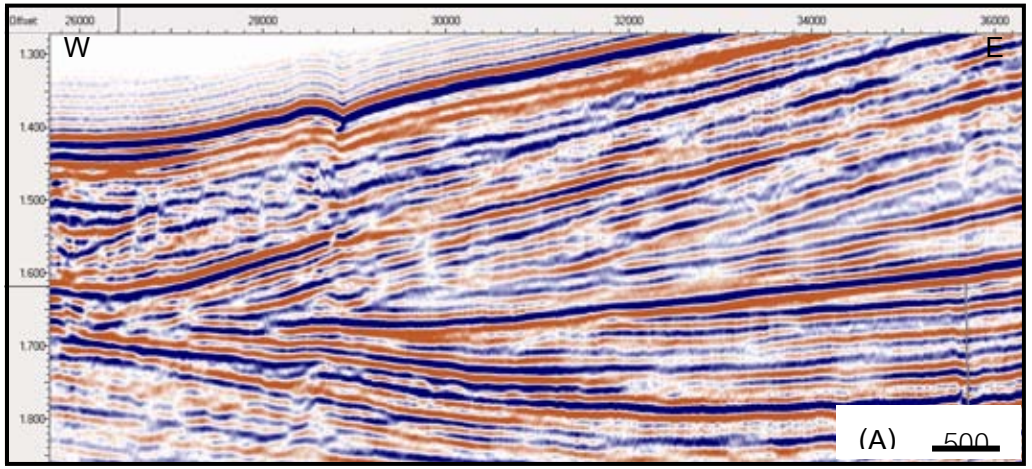

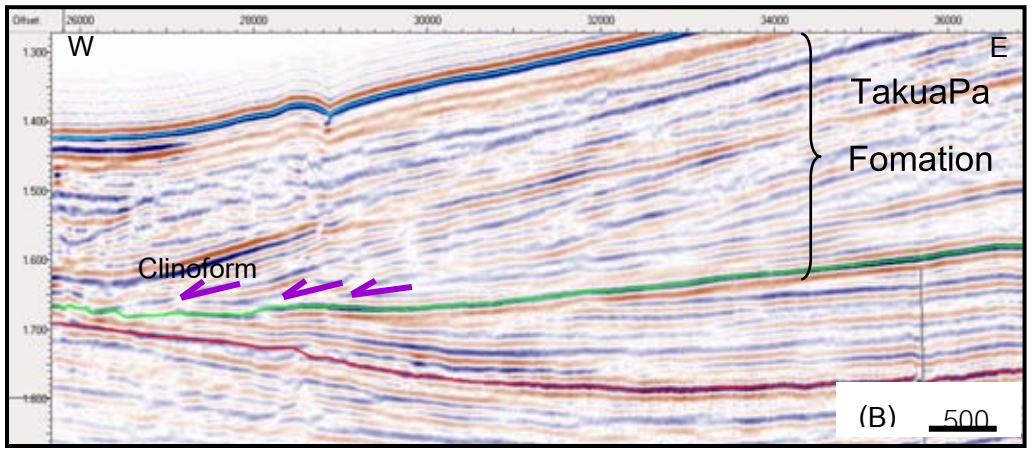

Figure 4.20 Seismic sections showing clinoform structures in TakuaPa Formation. (A) Uninterpreted seismic line AD10, (B) Interpreted section with indicated clinoform (purple arrows), and (C) location of the seismic line in the southern Mergui Basin (red box = location of seismic section). Noted that the horizon show undeformed structure.

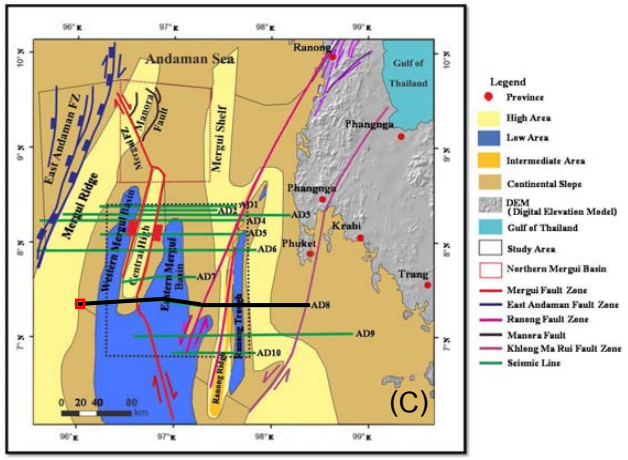

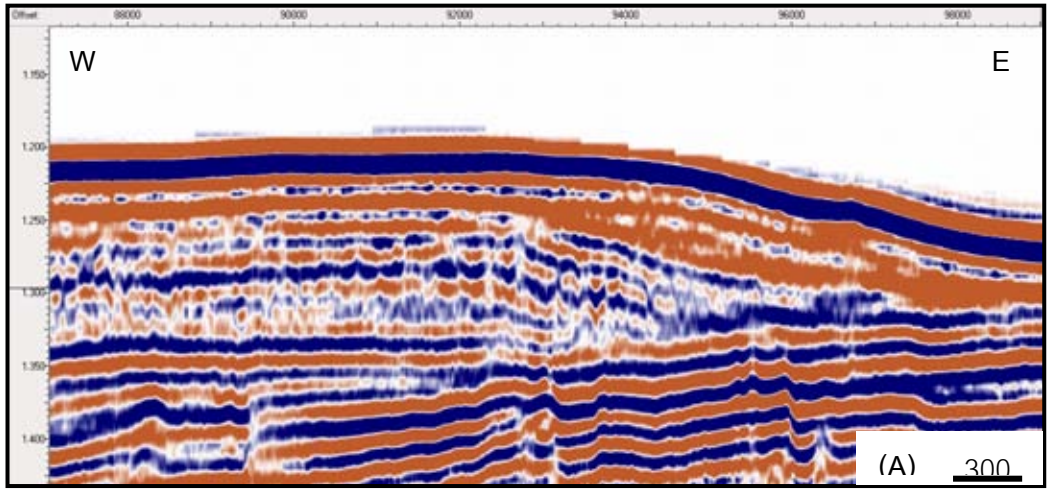

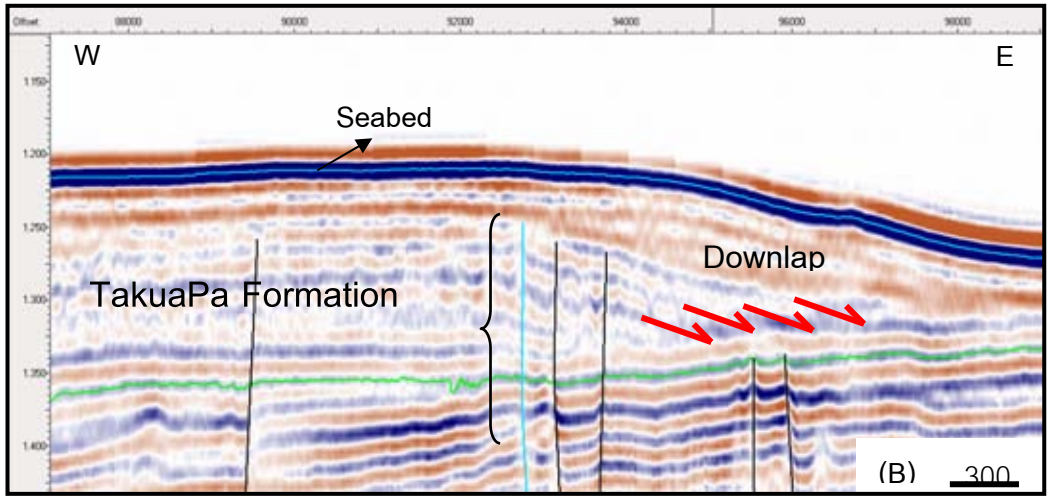

Figure 4.21 Seismic sections showing downlaps in TakuaPa Formation. (A) Uninterpreted seismic line AD9 (B) Interpreted section with indicated downlap (red arrows), and (C) location of the seismic line in the southern Mergui Basin (red box = location of seismic section). Noted that there exists a series of very high-angle normal faults.

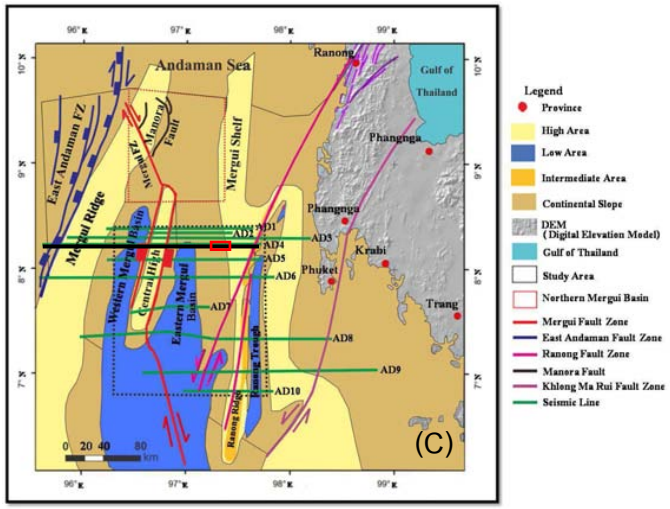

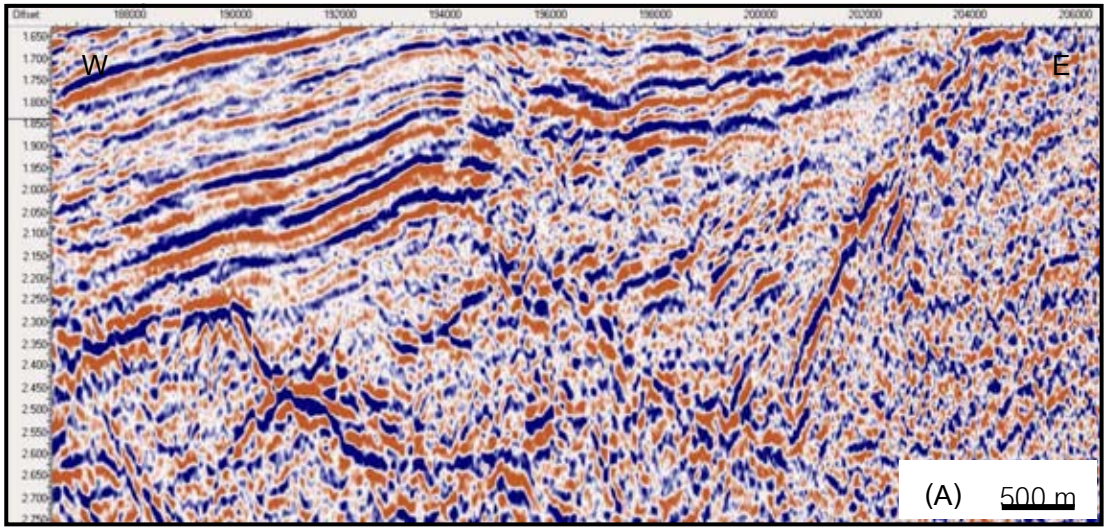

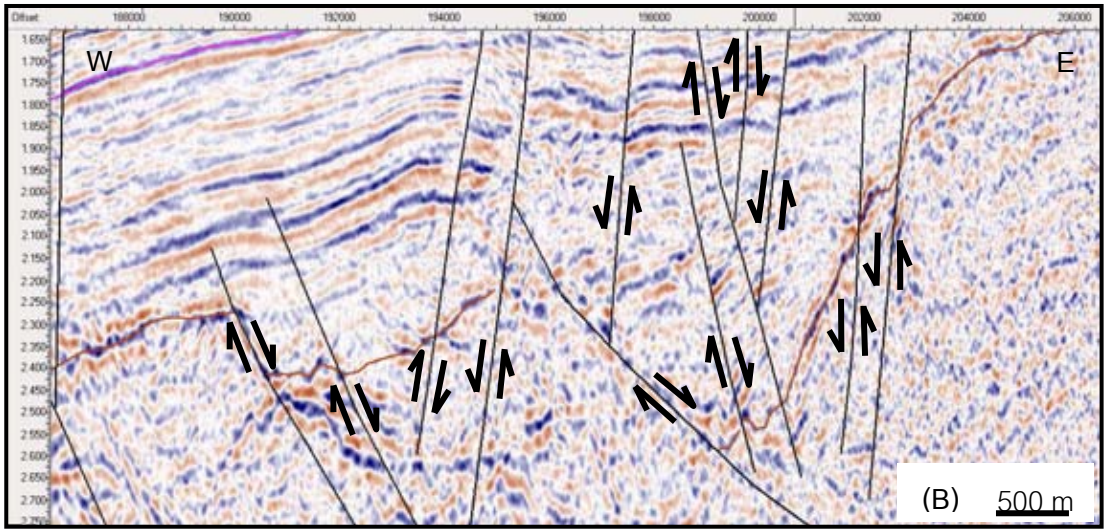

Figure 4.22 Seismic sections showing the normal fault in Ranong Formation. (A) Uninterpreted seismic line AD4 (B) Interpreted section, and (C) location of the seismic line (red box = location of seismic section).

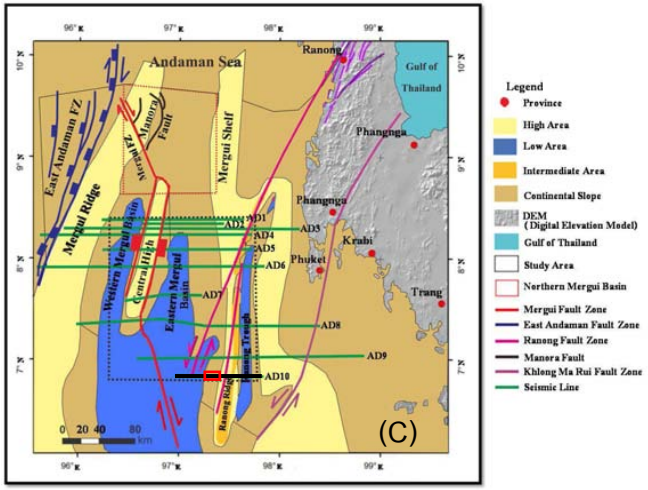

Figure 4.23 Seismic sections showing the high-angle normal faults (F1, F2, F3, and F4) in Basement to Kantang Formations. (A) Uninterpreted seismic line AD10 (B) Interpreted section, and (C) location of the seismic line in the southern Mergui Basin (red box = location of seismic section).

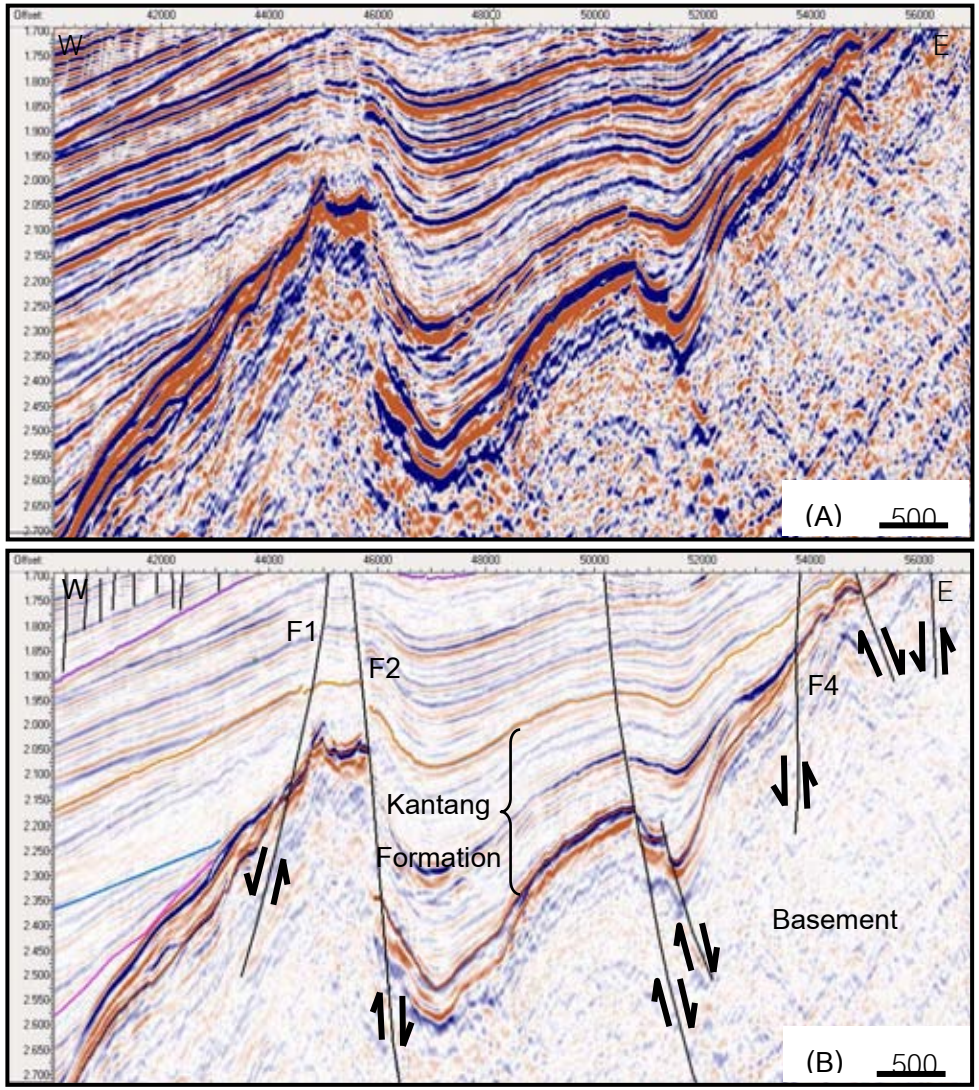

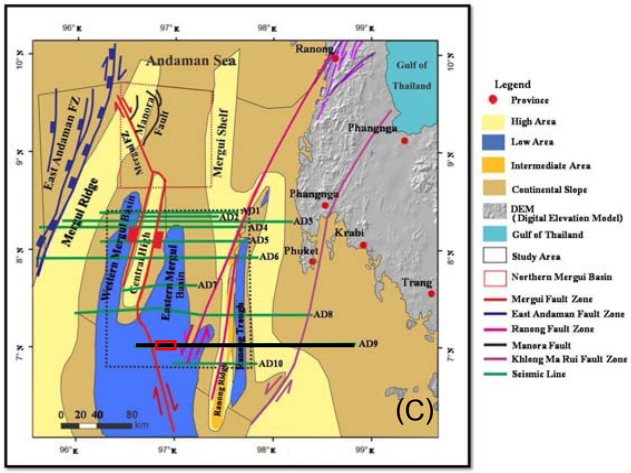

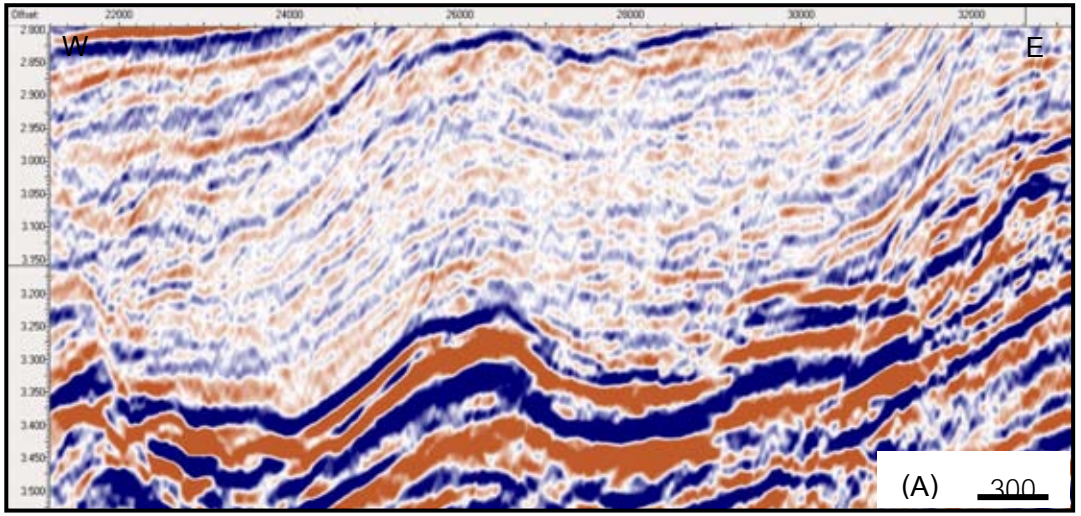

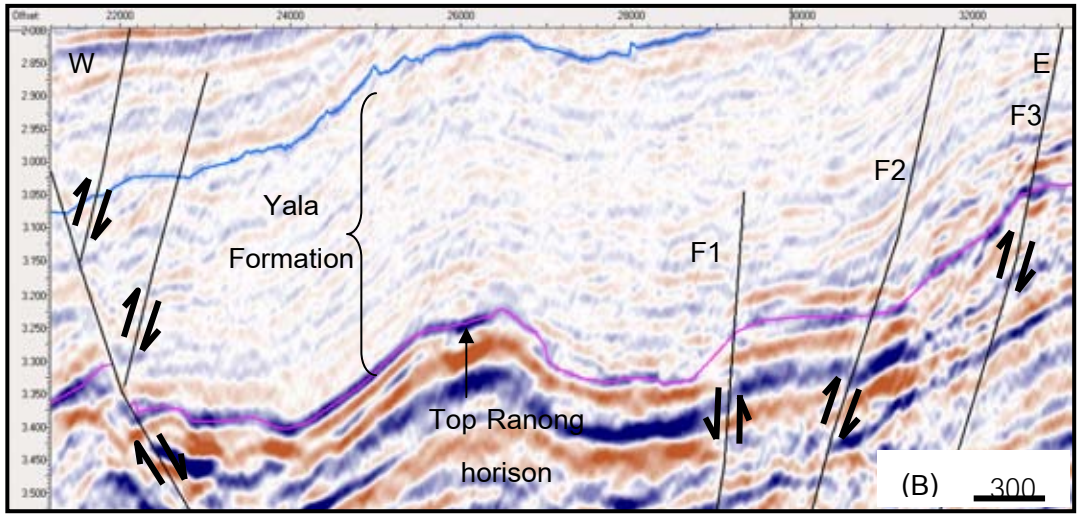

Figure 4.24 Seismic sections showing the reverse faults (F1, F2, and F3) in Ranong to Yala Formations. (A) Uninterpreted seismic line AD9 (B) Interpreted section, and (C) location of the seismic line in the southern Mergui Basin (red box = location of seismic section).

Two major strike-slip faults, observed from these enhanced seismic data, are believed to be the main control of the structural framework in the study area, namely the Mergui fault zone (dextral and NW - SE trending fault) and the Ranong fault zone (sinistral and NE-SW trending fault). Descriptions are shown below.

4.3.1.1 The Mergui Fault is an elongate sigmoidal Z shaped fault (Polachan, 1988) with several negative flower structures (Figure 4.25) developed along the Mergui Fault Zone. The negative flower structures found in this study is as wide as 15 kilometer. The obliquely normal fault with the NNE-SSW trend developed along side of the Mergui Fault Zone. The Mergui Fault exhibits a changes in its direction and orientation. In the northern Mergui basin, this fault displays predominantly NNW-SSE and NE-SW trending (Srisuriyon, 2008). Connecting to the faults of the southern Mergui Basin have to N-S trending normal fault at the Central High. In the Central High area this fault comprises a series of N-S trending normal fault, and the high is bounded by these faults to the east and to the west (Polachan, 1988). Faults observed in the southern Mergui Basin are series of the east-dipping faults that continue from the southern area to the eastern Mergui Basin, and they are series of the west-dipping faults on the Western Mergui Basin. The reactivation of faults (Figure 4.26) and uplift occurred periodically through time, and are believed to be related to the movement of the Mergui Fault zone, which may be the consequence of the Indian plates continued movement further northward into the Eurasian plate.

4.3.1.2 The Ranong Fault appears in the west of the southern Mergui Basin, which is the major strike-slipe fault in the NE-SW direction and dips eastward at steep angles. Judging from the present study, the Ranong fault is as long as 100 kilometer long. Parts of the fault are present on land across the Thai peninsula (see Thipyopas, 2012). The Ranong Fault consist of several fault segments and many of them align in the NE-SW direction, following the main tectonic structure. These fault segments are also a strike slip fault, however some show vertical slip movement the Ranong Fault. In general, the Ranong Fault is a significant left-lateral. It is confidence that the movement along this fault system may have been responsible for the narrow push uplift, and inturn developed the Ranong Ridge with the majors displacement commencing

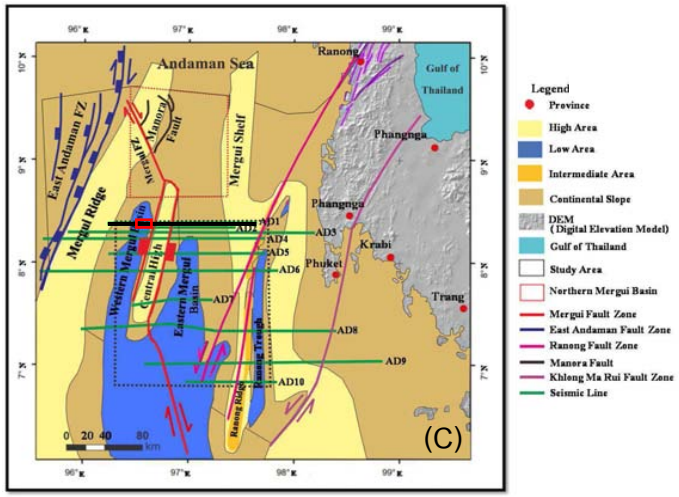

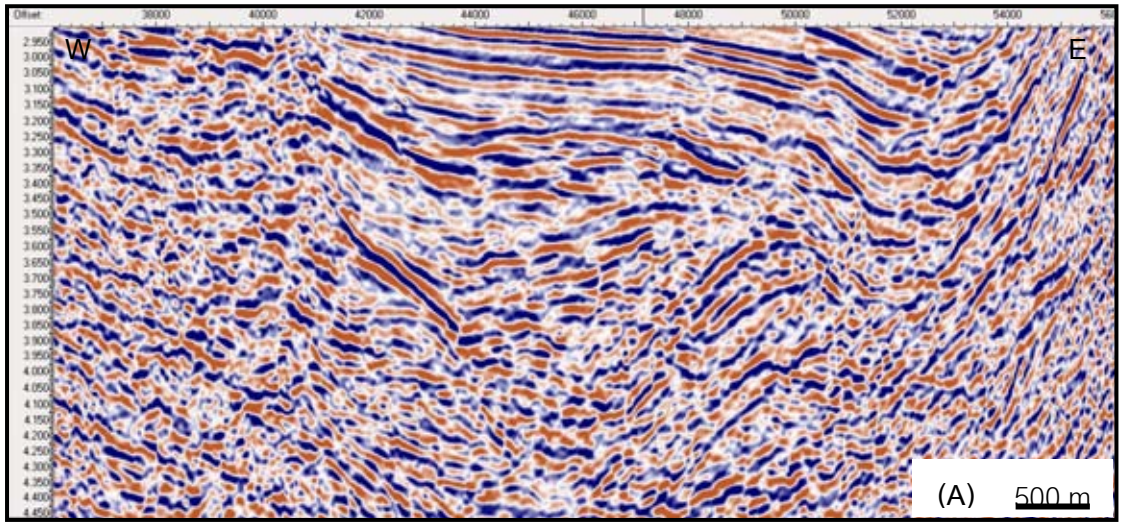

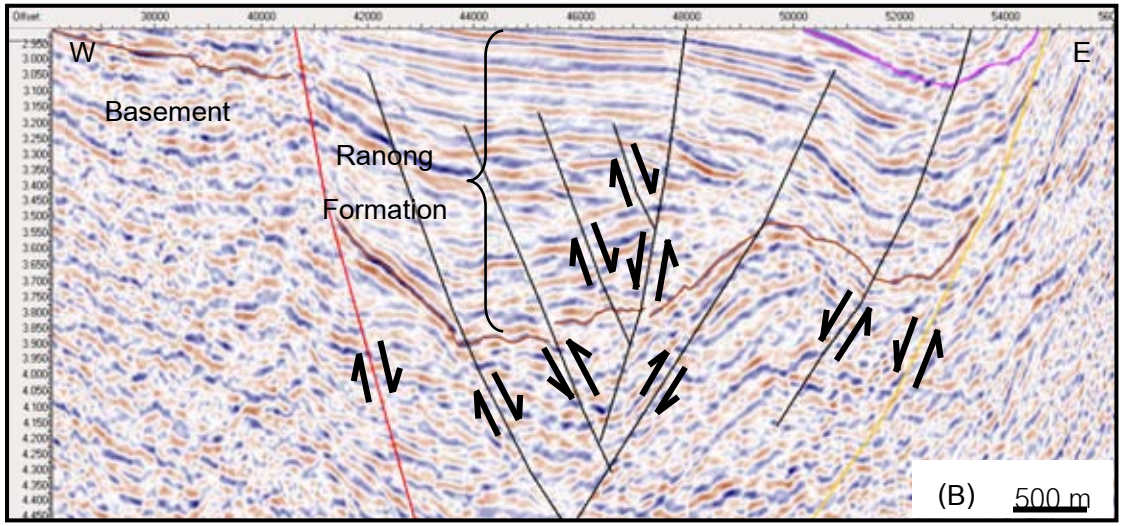

Figure 4.25 Seismic sections showing a negative flower structure in basement to Ranong Formation. (A) Uninterpreted seismic line AD1 (B) Interpreted section, and (C) location of the seismic line in the southern Mergui Basin (red box = location of seismic section).

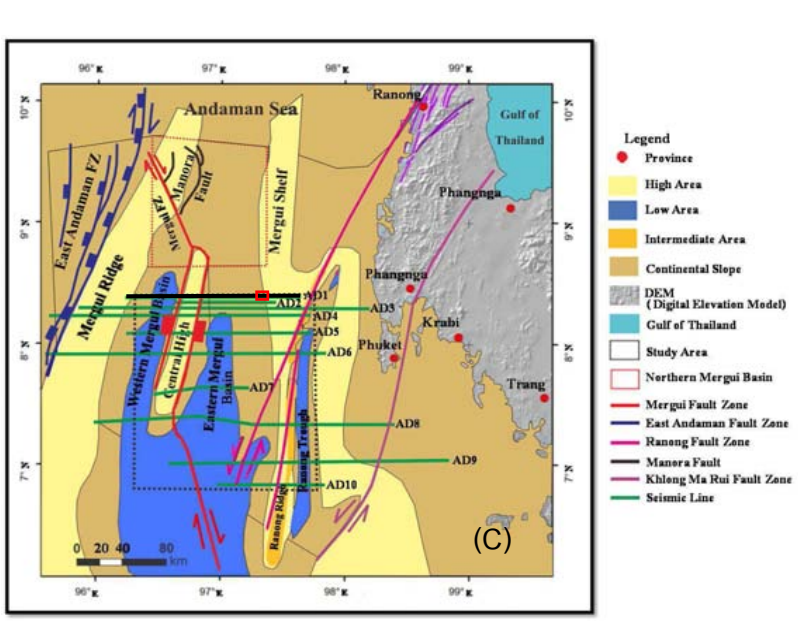

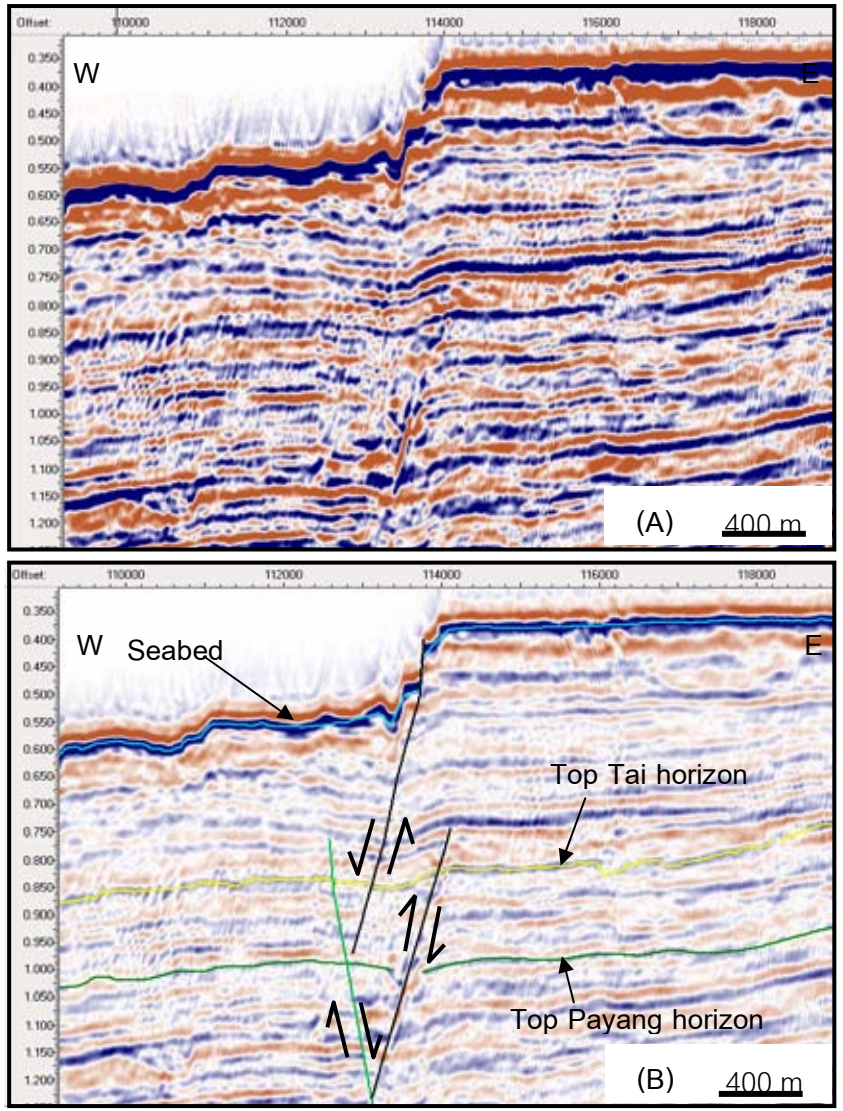

Figure 4.26 Seismic sections showing reactivation of faults along the existing fault fabic in Payang to Tai Formation. (A) Uninterpreted seismic line A1 (B) Interpreted section, and (C) location of the seismic line (red box = location of seismic section).

possibly occurring since the Late Oligocene to Early Miocene. The slip movement associated with present day earthquake has been encountered and continue to develop till present.

4.3.1.3 The normal faults (Figures 4.22 and 4.23) are important in the southern Mergui Basin. The normal faults are dominated by the N-S trending faults with the maximum displacement of about 1,600 ms relating to rifting and uplift and controlling several basement highs. Some of the fault are still active and formed as a series of N-S trending and high-angle east-dipping faults as active boundaries of half graben. The NE-SW antithetic fault trending NE-SW (Figure 4.27) are mainly found in the older Tertiary strata, so they are inferred to have occurred since Oligocene and Early Miocene. The sysnthetic fault (Figure 4.27) are the main control of the extension of the basin. The N-S faults appear to be associated with NNE-SSW splay faults, and their NNE-SSW trend developed mainly along the Mergui fault. However amount of movement along the faults is relatively small (Department of Mineral Fuels, 2006).

4.3.1.4 The NNE-SSW trending faults are usually encountered as the growth faults initiated during sediments deposited in the Oligocene, which developed mainly along the Mergui Fault Zone. Harding (1985) suggested the NNE faults en echelon normal faults associated with divergent dextral shear along the Mergui Fault Zone. Dipslip displacement along these faults is minor compared with the N-S faults. Based on the present interpretation, maximum dip slip is about 3,300 meter. In addition, the NNE-SSW faults cross and join the N-S faults.

4.3.1.5 The reverse fault (Figure 4.24) some of the fault show reverse sense of movement. For example the faults from the seismic line no AD9 exhibit a reverse slip with the displacement of about 500 meter. Additionally, some of the reverse faults are encountered in association with the normal fault and they occur later, causing inversion structures of the basin.

The larger faults that continued upward to the Thalang and Takua Pa Formation were reactivated as various types of faults (Figure 4.26). Most fault continue as normal faults. Some were inverted with anticlines in the hangingwalls, especially in areas near

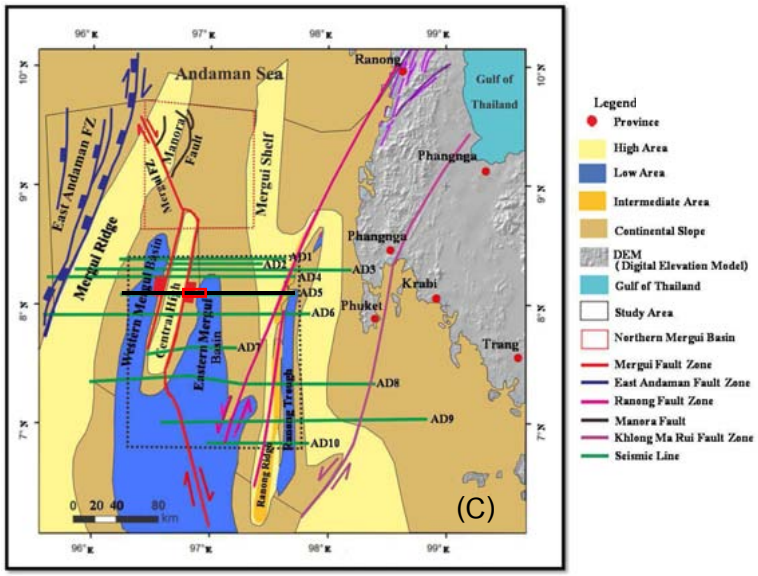

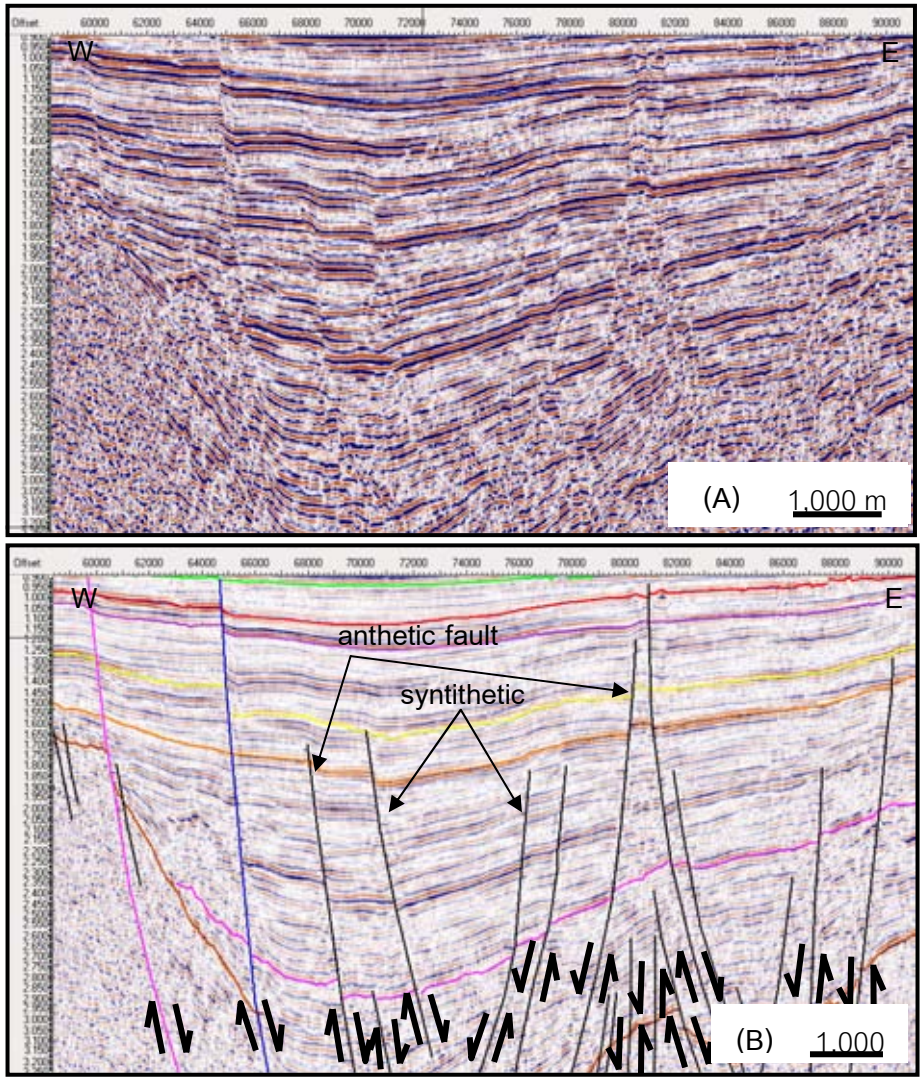

Figure 4.27 Seismic sections showing antithetic and sysnthetic faults. (A) Uninterpreted seismic line A5 (B) Interpreted section, and (C) location of the seismic line of the southern Mergui Basin (red box = location of seismic section).

the eastern basin margin. Inversion of these normal faults (Figure 4.28) may be the manifestation of strike-slip movements related to the Ranong Fault Zone. The wedge shape of the seismic is result of growth faulting. In addition, seismic line AD10 showing a growth fault occur in Trang Formation.

Foldings are observed from the study area are both anticlines and synclines (Figures 4.29 and 4.30). They developed obliquely along the Mergui faults, and are formed in the early stages of strike-slip deformation during in Oligocene age.

4.3.2 Structural framework

Polachan (1988) described identified structures, including Mergui Ridge, Western Mergui Basin, Central High, Eastern Mergui Basin, Ranong Ridge, Ranong Trough and Mergui Shelf. The deformation structures conform well with these described by Srisuriyon (2008) and Mahattanachai (2004). However, by using the enhanced seismic data, these structures are also recogrized in more detailed description than previous reports. The E-W profile across the Mergui Basin is shown in Figure 4.31.

4.3.2.1 The Mergui Ridge is a N-S trending structural high that is flanked by N-S trending westward steeply dipping fault (East Andaman Fault Zone) along the western wedge of the basin and N-S trending, eastward dipping fault (Mergui Fault Zone) along the east of the basin. The Mergui Ridge is a part of the outer shelf slope off the Thai-Malay Peninsula and forms the eastern boundary of the East Andaman Basin. The Ridge is approximately 35 km width from the edge of the Western Mergui Basin to the ridge and 200 km long by separating the Mergui Basin from the Andaman Sea. Structural features include faulting of the older slope sediments at the transition from Mergui Ridge to East Andaman Basin. Sediments deposited on the ridge are thin towards the edge of the ridge where a zone of non-sedimentation of Plio-Pleistocene age. According to Curray et al. (1979), Mergui Ridge represents the western edge of the Sunda Craton.

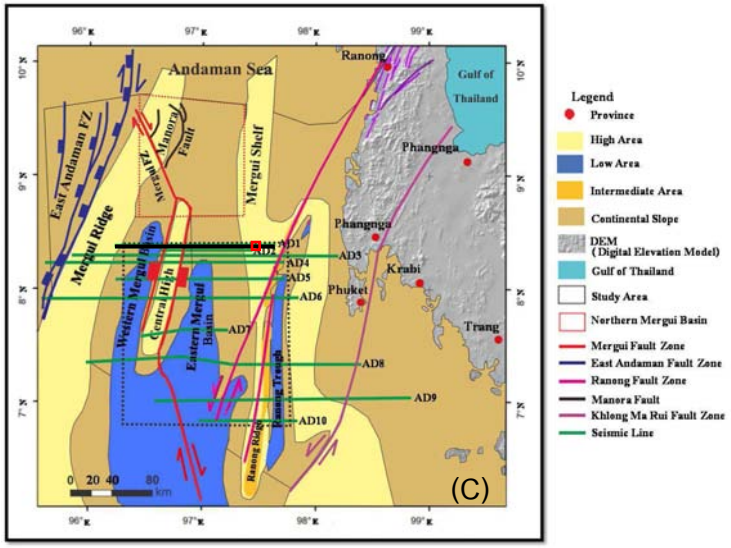

Figure 4.28 Seismic sections showing an inversion of these normal faults in Ranong Formation. (A) Uninterpreted seismic line A1 (B) Interpreted section, and (C) location of the seismic line in the southern Mergui Basin (red box= location of seismic section).

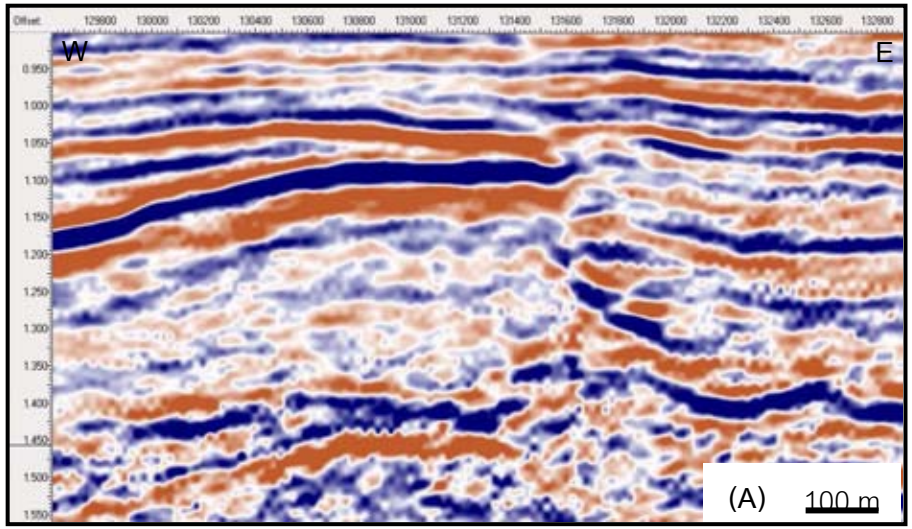

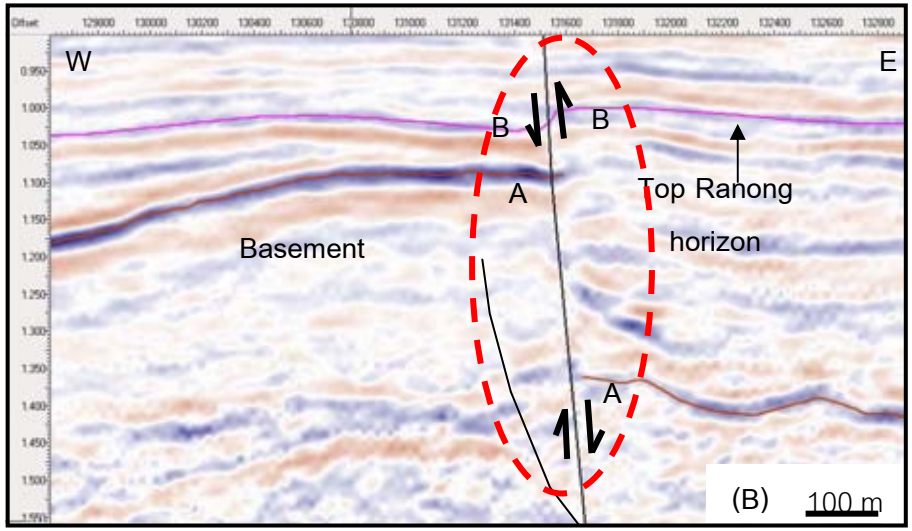

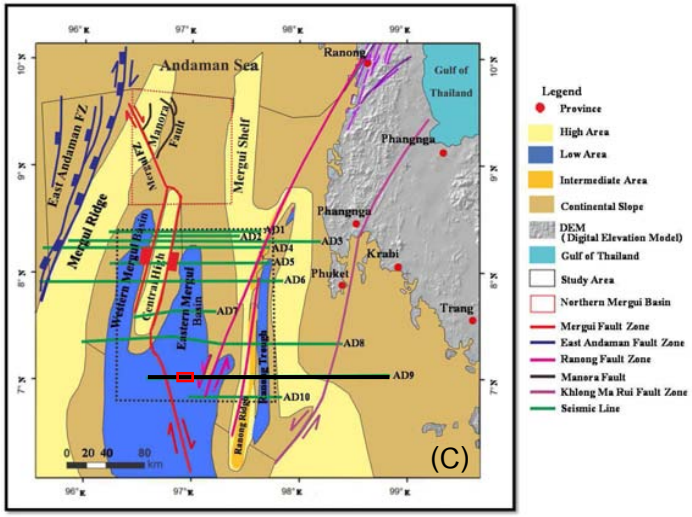

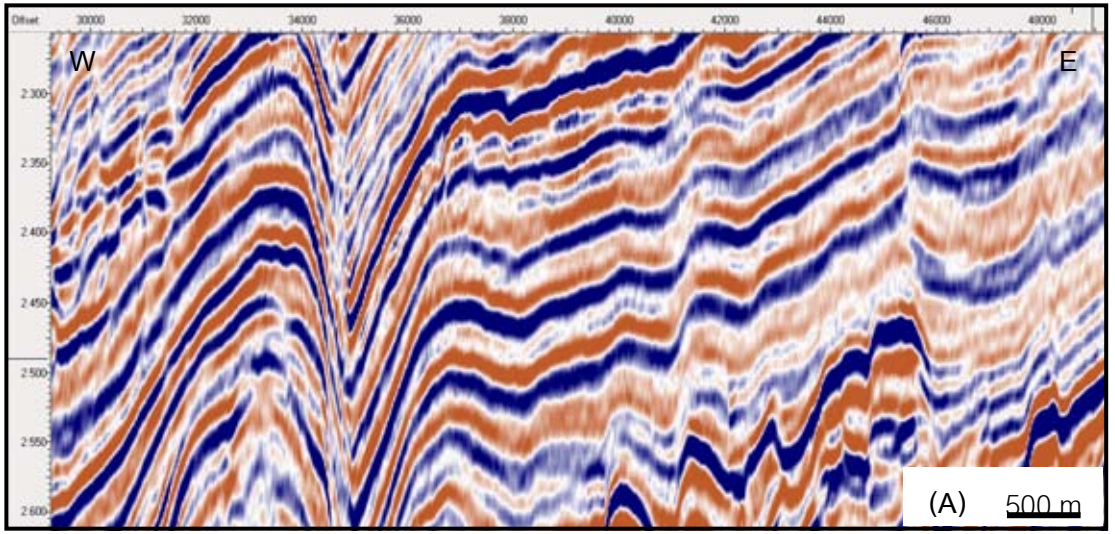

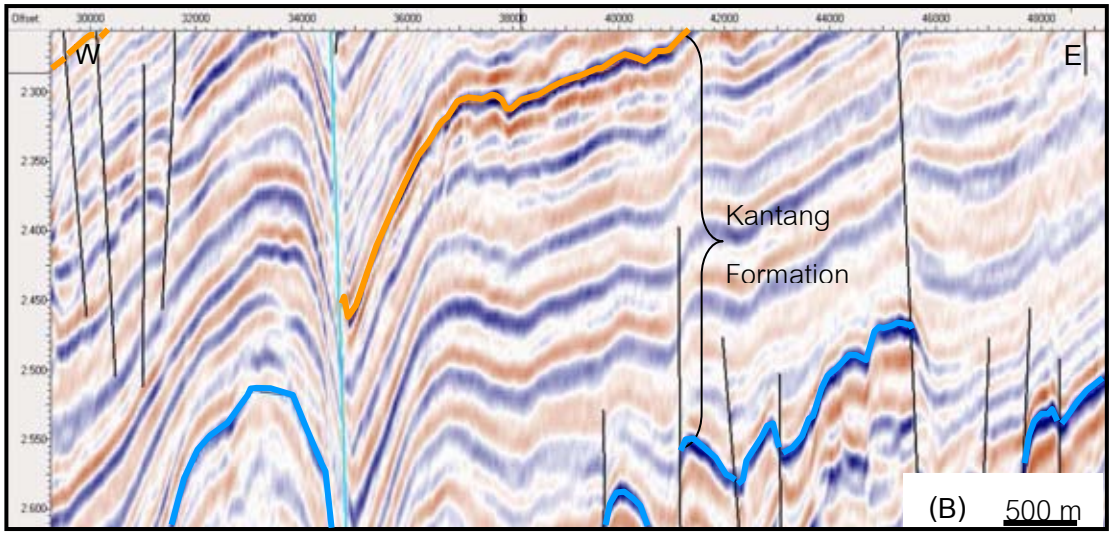

Figure 4.29 Seismic sections showing an anticlinal fold associated with faults developed in the Central High. (A) Uninterpreted seismic line A9, (B) Interpreted section, and (C) location of the seismic line in the southern Mergui Basin (red box= location of seismic section).

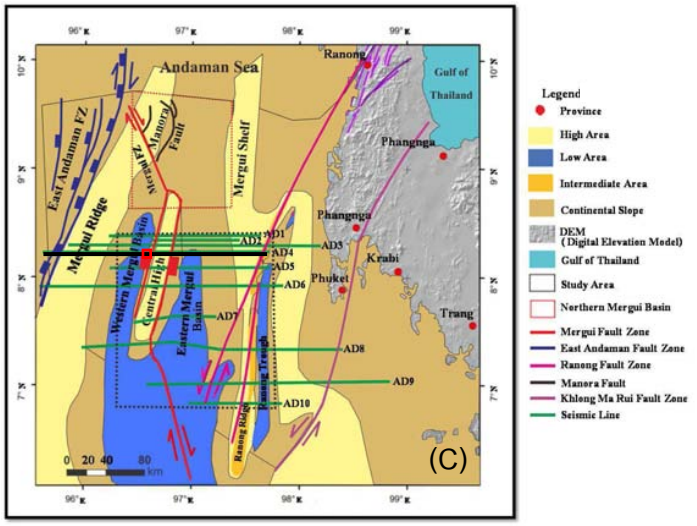

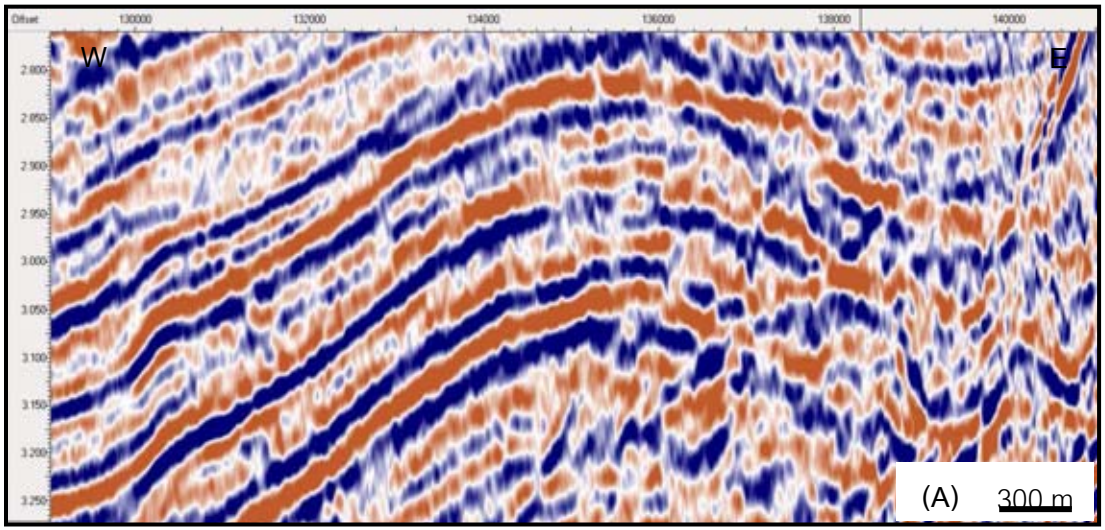

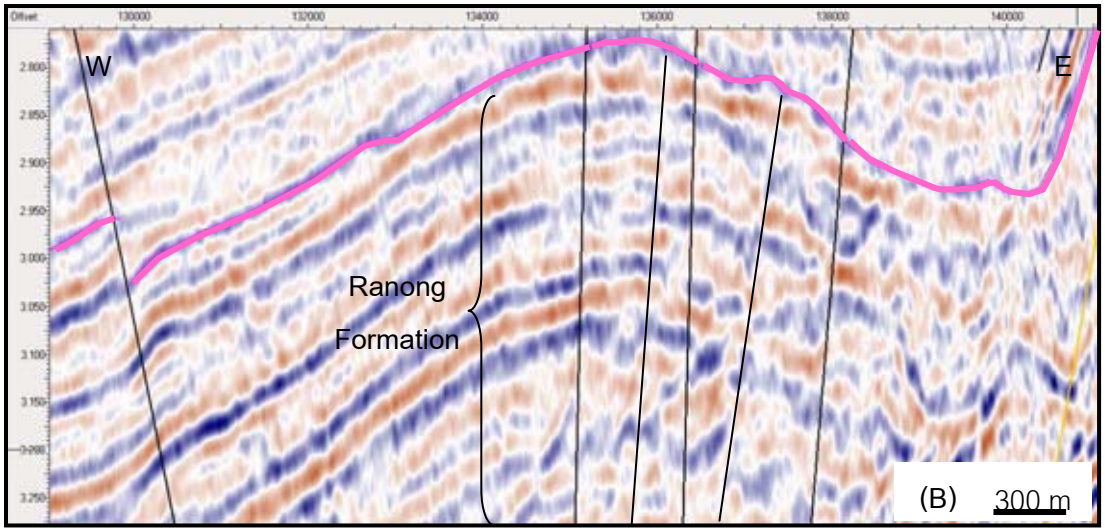

Figure 4.30 Seismic sections showing an anticlinal fold associated with faults developed in the Central High. (A) Uninterpreted seismic line A4 (B) Interpreted section, and (C) location of the seismic line line in the southern Mergui Basin (red box= location of seismic section).

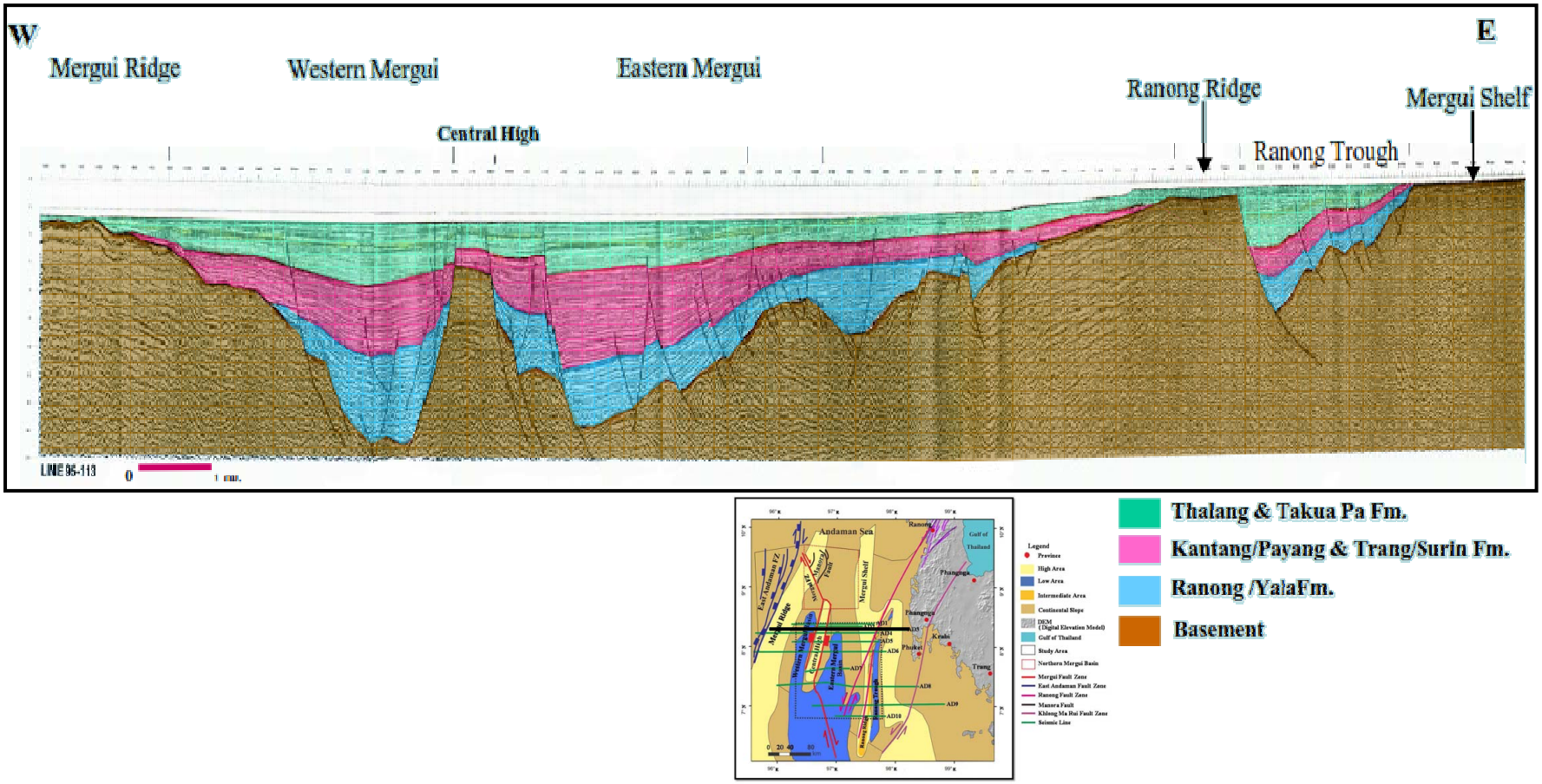

Figure 4.31 Seismic section of the Andaman Sea across the southern Mergui Basin (Srigulwong, 2005).

4.3.2.2 The Western Mergui Basin is N-S trending half-graben, which lies between the Mergui Ridge and Central High. The basin is bounded to the east by the steep westward dipping Mergui Fault Zone. Over 2,740 meter of sediment were penetrated by the Trang and Mergui wells. Sediments in this sub-basin thicken eastwards. The Mergui Fault zone occurs the west-dip Mergui Fault generated and bound the western Mergui half-graben and the half-graben is pinch out to the Mergui ridge.

4.3.2.3 The Central High is a complex NNE-SSW horst block extending along the Mergui Fault Zone. This ridge is bounded to the east and west by easterly and westerly dipping normal faults, respectively. This controlled the nature and extent of the depositional systems which developed as the rifting period. The Central High appeared to rise in the Late Oligocene and stop during the Early Miocene time, which allowed mainly Early Miocene reefal and carbonate rocks in the Mergui Basin deposited on this ridge.

4.3.2.4 The Eastern Mergui Basin lies between the Central High to the west and the Mergui Shelf to the northeast or the Ranong Fault Zone to the southeast. The geological structures within this sub-basin comprise a series of westward tilting N-S trending half-grabens separated by a series of east-dipping N-S trending normal faults. This basin contains several minor faults which are controlled by the basement faults. Sediments in this basin thicken westwards and southwards. The East-dipping Mergui Fault bounds the Eastern Mergui basin, the basin is pinched out to the Mergui Shelf.

4.3.2.5 The Ranong Ridge is a westward tilting N -S trending basement high, bounded to the east by a steeply eastward-dipping N-S trending normal fault. This ridge has been offset left-laterally by the NE-SW trending Ranong Fault Zone. Sediments deposited on this ridge are generally thin and mainly of Plio-Pleistocene age.

4.3.2.6 The Ranong Trough can be described as a half-graben, which formed a deep narrow shape NE-SW trending along the Ranong Fault Zone. The Ranong Trough lies between the Ranong Ridge and the Mergui-Malacca Shelf. Sediments are thickening southward and westward toward the Ranong Fault Zone. From

the seismic data, it is estimated that up to 8,000 metres of sediment lie in the southern portion of this trough. No wells have been drilled in this area.

4.3.2.7 The Mergui Shelf, Basement lithology of the Mergui Shelf is similar to Peninsular Thailand, which is part of the Shan-Thai block of the Sunda Craton. It consists of folded Paleozoic and Mesozoic rocks, overlying Precambrian granitoids and high-rate metamorphic rocks (Nakapadungrat and Putthapiban, 1992).

4.4 Unconformity

Unconformities occur in the studied seismic sections are Lower Tertiary Unconformity (LTU), Middle Miocene Unconformity (MMU), Upper Miocene Unconformity (UMU) and Top Upper Miocene (TUM).

4.4.1 The Lower Tertiary Unconformity (LTU)

The Lower Tertiary Unconformity observed from the enchanced seismic sections overlying the Ranong Formation and the Kantang Formation comprises sub-parallel reflections with strong to moderate amplitudes and good continuity. The Payang Formation lays unconformably over the Ranong Formation and comprises sub-parallel relfections with strong to moderate amplitndes and good continuity. These reflections onlap onto Ranong Formation. In addition, the Yala Formation is unconformably overlain by shales of the Kantang Formation (Figure 4.32). This unconformity relative with water depth decreased and uplift of the basin. Sediment deposition of during the Late Oligocene-Earliest Miocene

4.4.2 Middle Miocene Unconformity (MMU)

The Middle Miocene Unconformity (MMU) observed the Payang Formation is unconformably overlain by the Surin Formation. The Tai Formation is unconformably overlain by shales of the Trang Formation and The Kantang Formation unconformably overlain by the Trang Formation. These characteristic of reflection comprises sub-parallel reflections with strong to moderate amplitudes and good continuity. These reflections toplap the Top Kantang Formation and erosion surface onto the Top Surin Formation. The basin subsidence during the deposition of sediment during the Middle Miocene. This unconformity relative with water depth decreased and uplift of the basin.

4.4.3 Upper Miocene Unconformity (UMU)

The Upper Miocene Unconformity (UMU) shown in red color (Figures 4.33) is picked on onlap and erosional surface, overlying the Trang Formation and Thalang Formation. This unconformity is characteristic of an angular unconformity located at the edge of the Western Mergui Basin relative sea level fall and uplift of the basin. These characteristic of reflection comprises sub-parallel reflections with strong to moderate amplitudes and good continuity. This unconformity observed during in the Late Miocene.

4.4.4 Top Upper Miocene (TUM)

The Top Upper Miocene (TUM) shown in green color (Figures 4.34) is picked on onlap and erosional truncate of the younger sediment of Thalang Formation. This unconformity is picked at the top of the turbidite unit overlain by the Takua Pa shales formation comprises sub-parallel reflections with strong to moderate amplitudes and good continuity. The basin subsidence and relative sea level fall, which the Top Upper Miocene observed during in the Upper Miocene.

4.5 Fault Displacement

Method of Displacement Measurement is shown in Appendix B. The patterns of displacement discussed above can be seen on the cross-section along the fault plan (Figure 4.35 C). The Mergui fault trends in the NNW-SSE direction and dips to the east (Figure 4.35 A and B), with high angle. The fault displacement is measured by the offset in TWT of each horizons on both side of the fault.

The top horizon of Thalang, Trang and Surin Formations have high displacement (Figures 4.36 A, B and C) in the southern area which value of 1,682, 1,791 and 1,872 ms (TWT) and continu to decrease from central to northern areas (about 771, 867 and 931 ms (TWT), respectively).

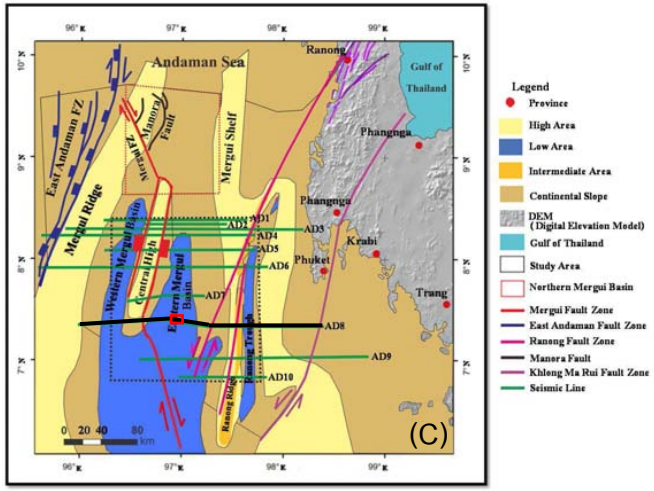

Figure 4.32 Seismic section of line AD8, showing the Lower Tertiary Unconformity (LIU) observed the Yala Formation is unconformably overlain by the Kantang Formation comprises sub-parallel reflections with strong to moderate amplitudes and good continuity. These reflections onlap onto the Kantang Formation and toplap the Yala Formation. (red box = location of seismic section).

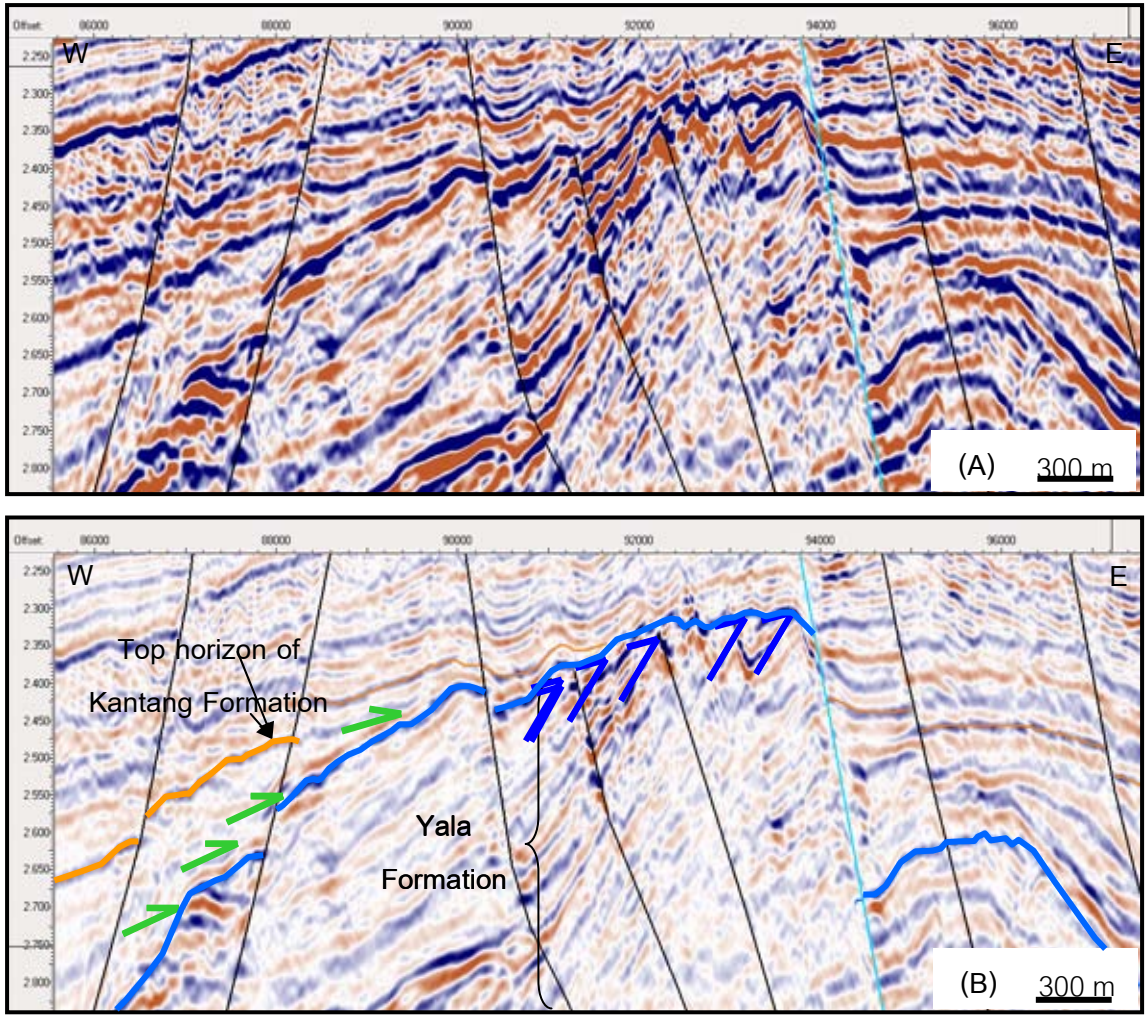

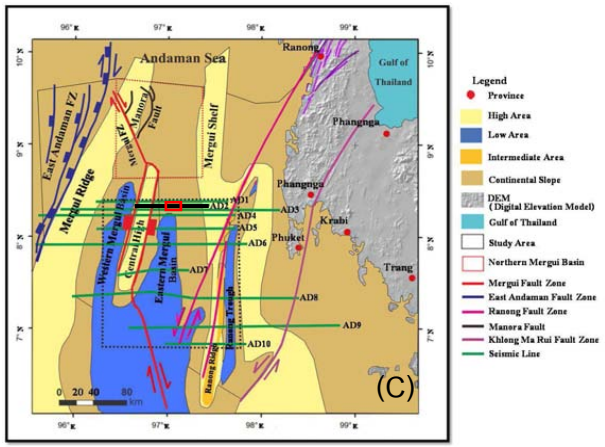

Figure 4.33 Seismic section of line AD2, showing the Upper Miocene Unconformity (UMU) shown in red color is picked on onlap and erosional surface, overlying the Trang Formation by the Thalang Formation. (red box = location of seismic section).

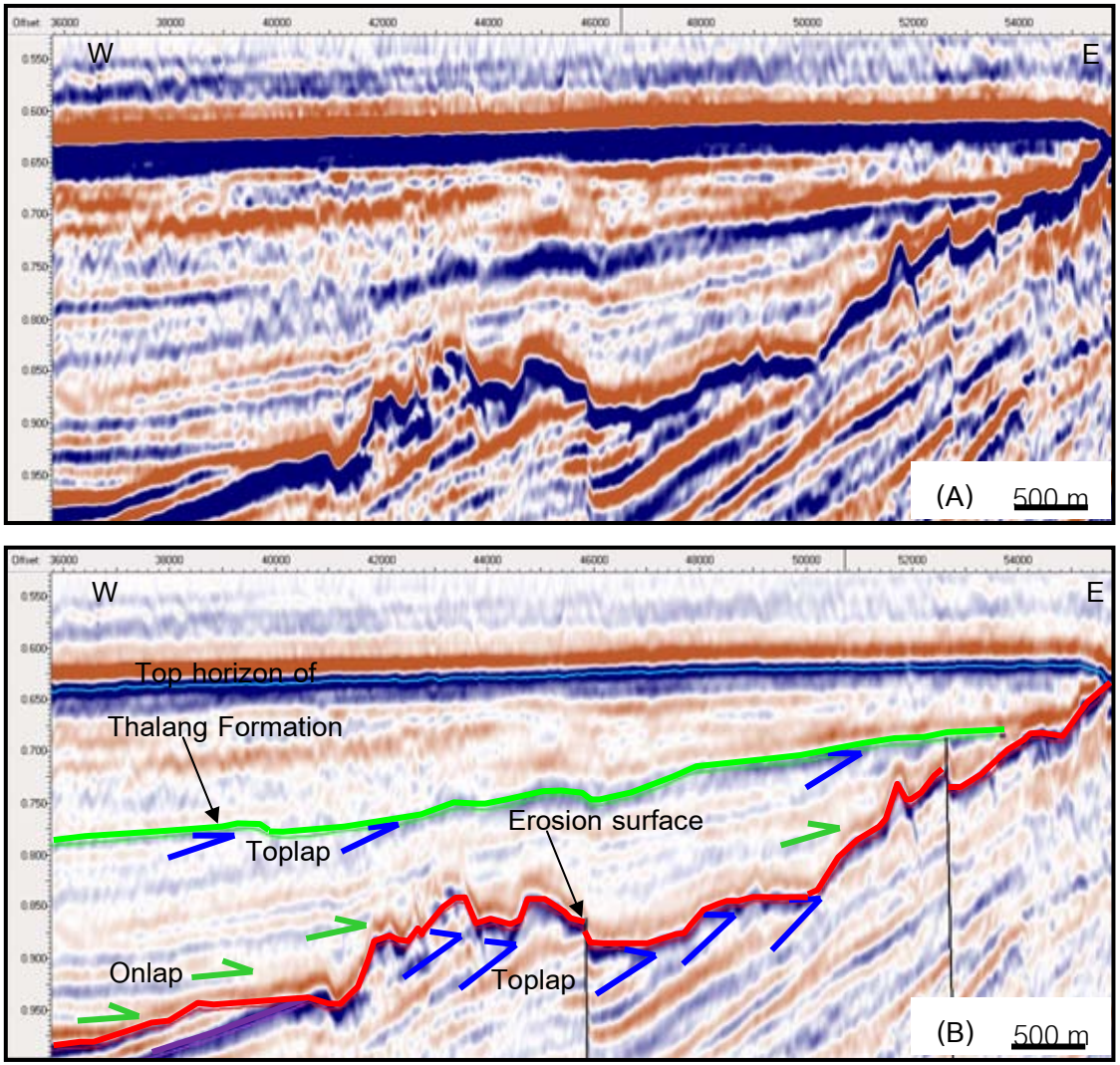

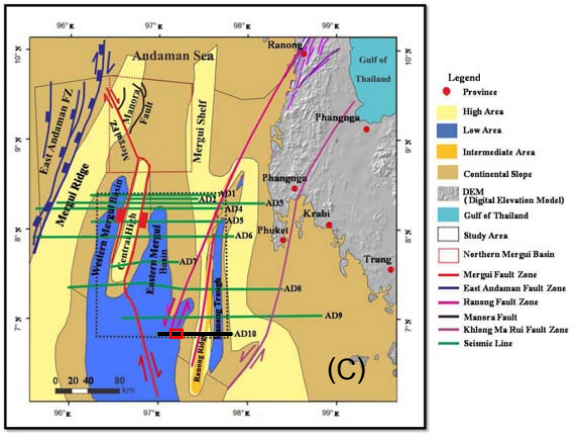

Figure 4.34 Seismic section of line AD10, showing the Top Upper Miocene (TUM) shown in green color is picked on onlap and erosional truncate of the younger sediment of Thalang Formation. (red box = location of seismic section)

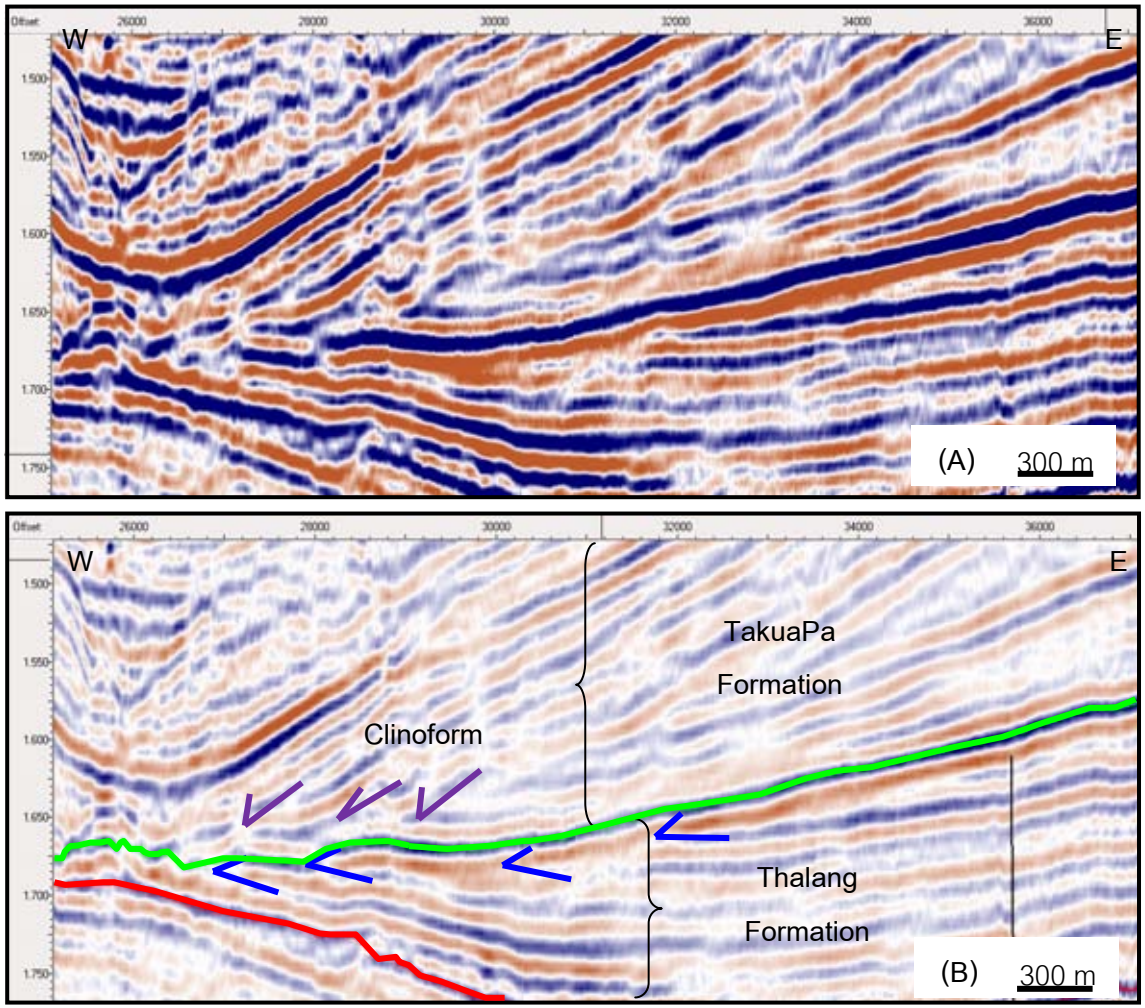

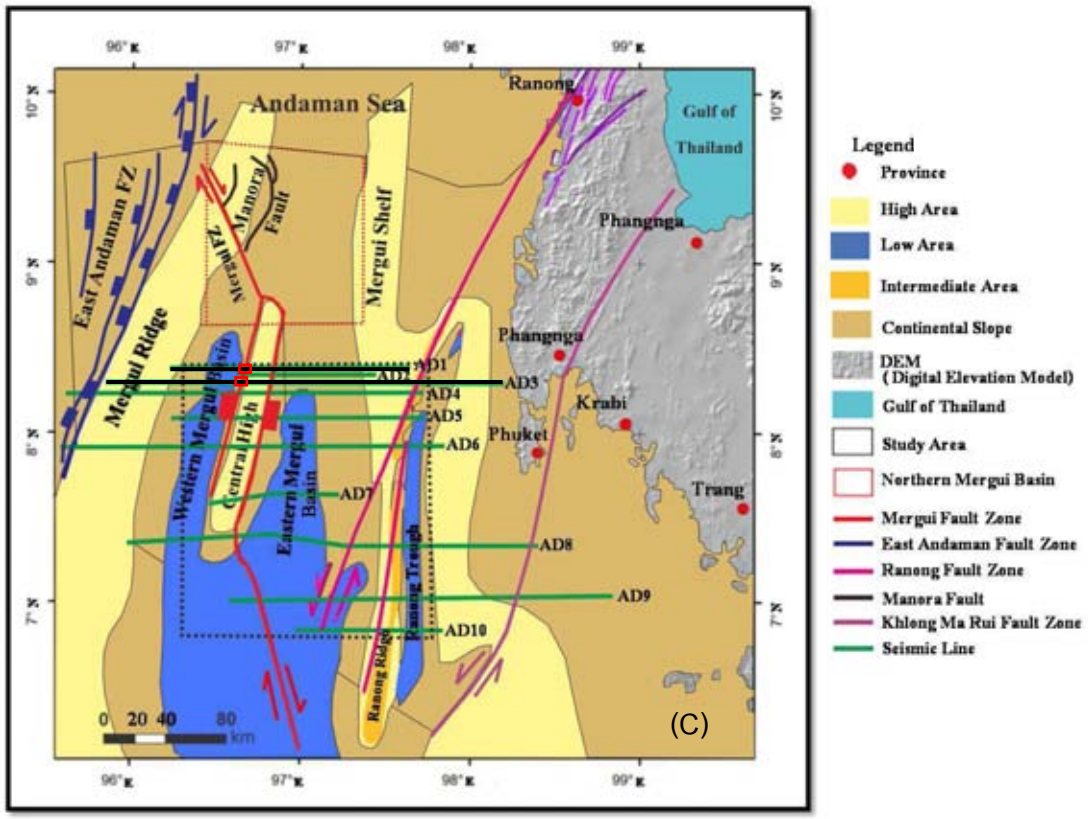

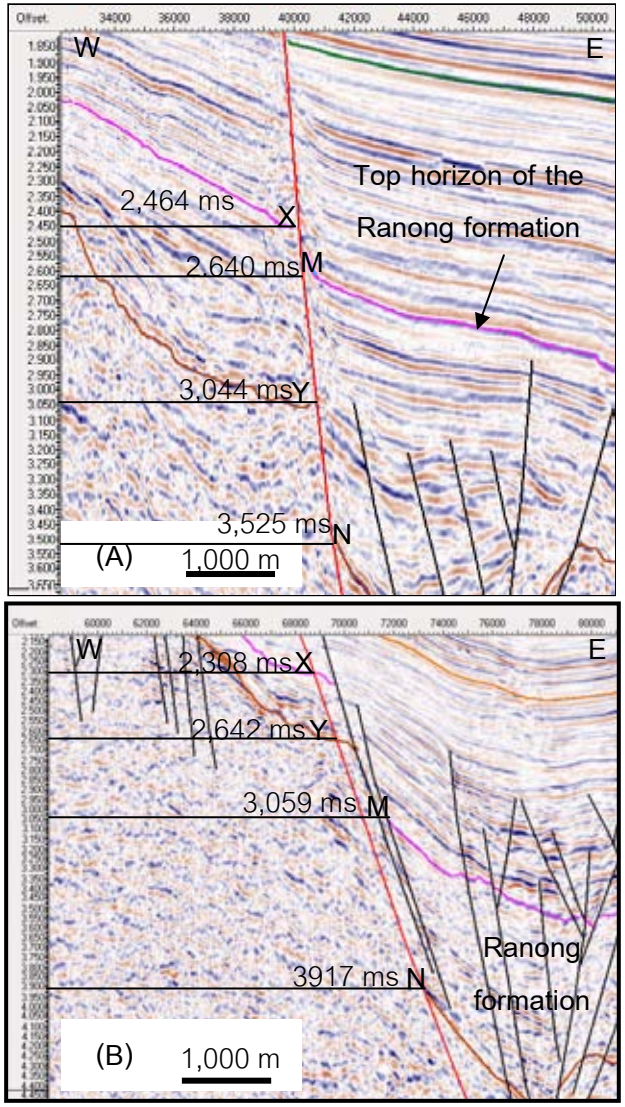

Figure 4.35 The southern Mergui Basin showing an example of fault displacement. The top horizon of Ranong Formation displacement plot of the N-S trending Mergui Fault. (A) Seismic line AD1 and (B) Seismic line AD3, and (C) location of the seismic line in the southern Mergui Basin (red box= location of seismic section).

(A) Top horizon of the Thalang Formation

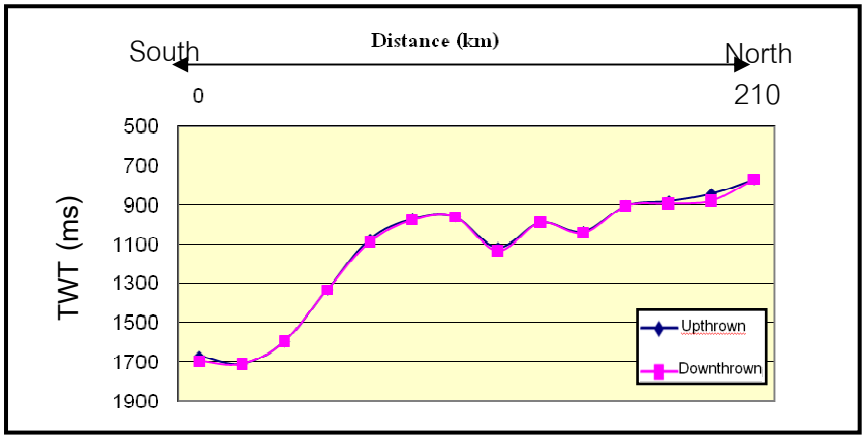

(B) Top horizon of the Trang Formation

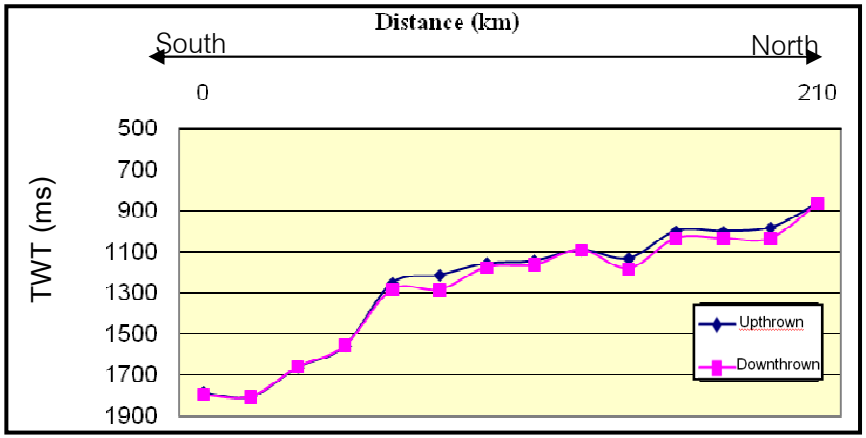

(C) Top horizon of the Surin Formation

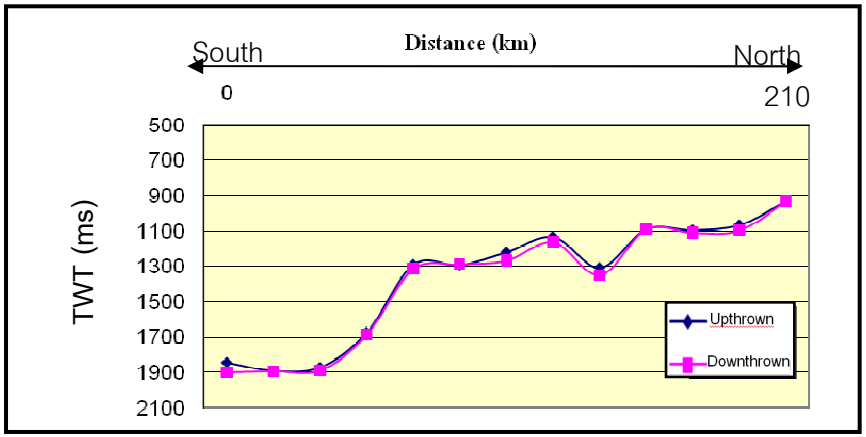

(D) Top horizon of the Tai Formation

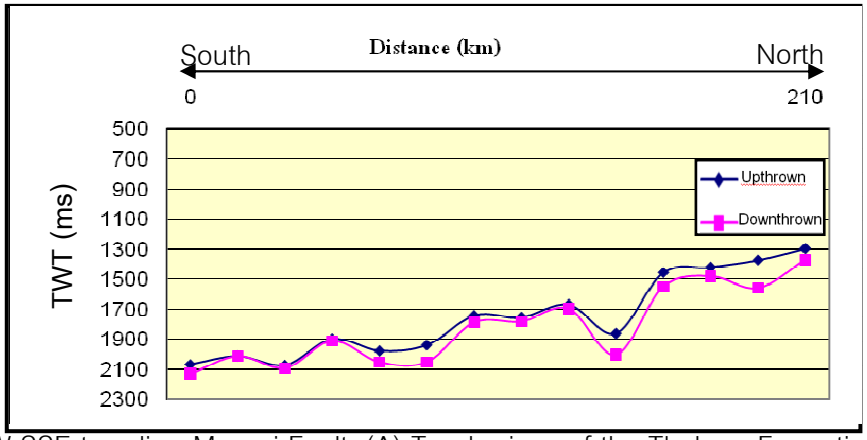

Figure 4.36 The top horizon of formation displacement plot of the NNW-SSE trending Mergui Fault. (A) Top horizon of the Thalang Formation, (B) Top horizon of the Trang Formation, (C) Top horizon of the Surin Formation, and (D) Top horizon of the Tai Formation.

(E) Top horizon of the Payang Formation

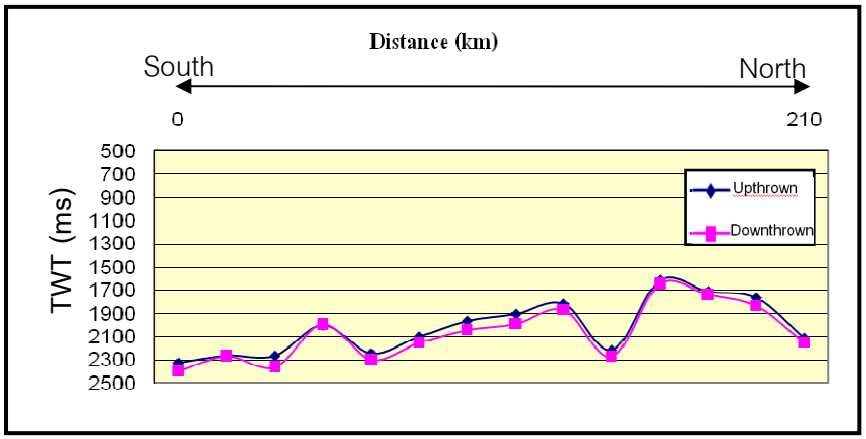

(F) Top horizon of the Kantang Formation

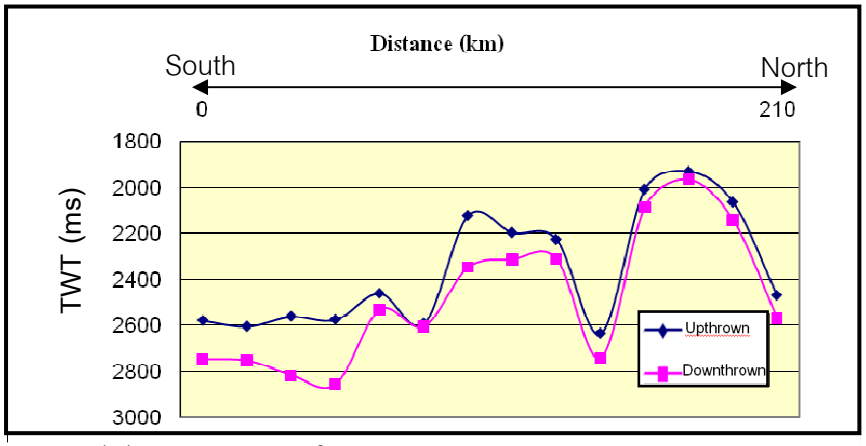

(G) Top horizon of the Ranong Formation

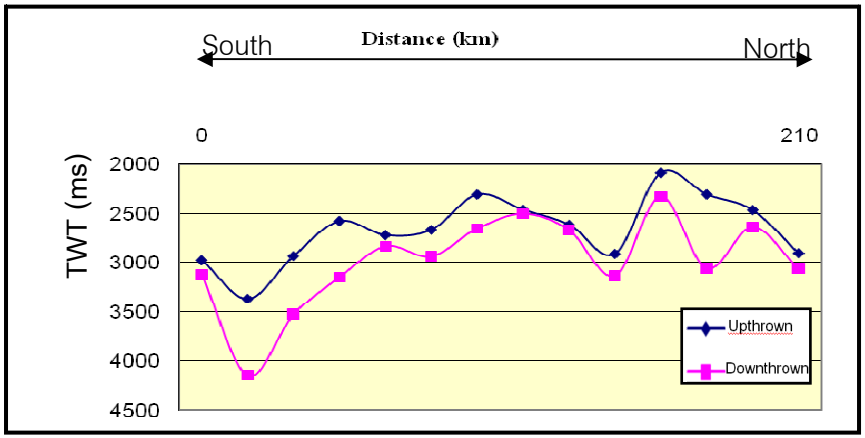

(H) Top horizon of the Basement Formation

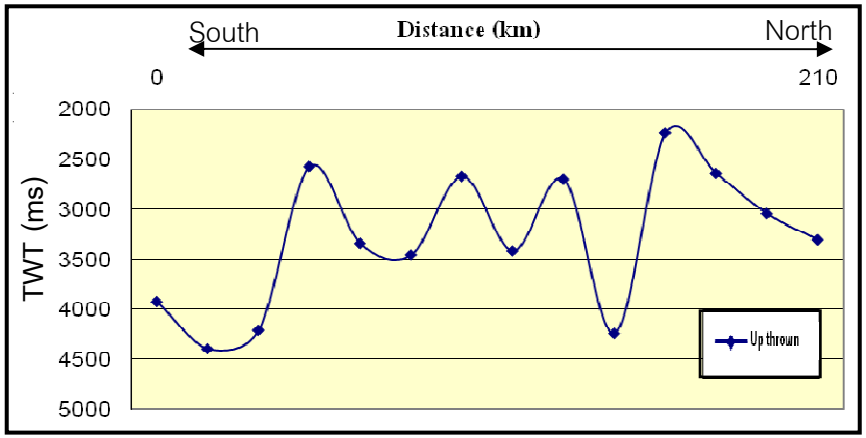

Figure 4.37 The top horizon of Formation displacement plot of the NNW-SSE trending Mergui Fault. (E) Top horizon of the Payang Formation, (F) Top horizon of the Kantang Formation, (G) Top horizon of the Ranong Formation, and (H) Top horizon of the Basement Formation.

The top horizon of the Tai Formation (Figures 4.36 D) shows high displacement in the southern area and decrease to the northern area (from 2,099 to 1,334 ms (TWT), respectively). While, the top horizon of Payang Formation shows high displacement (Figures 4.36 E) in the southern area (2,362 ms (TWT)) and continus to decrease toward the northern areas (2,130 ms (TWT)). Figures 4.37 (F) showing difference between the top horizon of the Kantang Formation from the southern to the central areas, which display move degree of growth fault during deposit of Kantang Formation in the east side of the fault than those in the west side (2,748 and 2,579 ms (TWT), respectively). High displacement of top horizon exists in the southern area and decreases in the central area, and then increases in the north area. In addition, the top horizon of the Ranong Formation shows high displacement (Figures 4.37 G) in the southern area and continue to decrease in the central area, and then increases displacement in the northern area. Differences between the offset of the top horizon of the Ranong Formation shown in Figures 4.36 (G) increases from the southern to the northern areas, which display motion of growth fault during deposit of Ranong Formation in east side of the fault than in west side (2,972 and 3,123 ms (TWT), respectively). Top basement show high displacement (Figures 4.36 H) in the southern area and continued decreases in displacement toward the central area and then increases in displacement toward the northern areas.

The fault displacements of the Ranong to Kantang Formations range from about 0 to 1,600 msec. The total thickness of the basin fills reach a maximum value of about 5,500 msec in the southern Mergui Basin. Most syn-rift normal faults terminate upward near the top of the Ranong Formation, although some faults with large displacements were reactivated and continue upward to the level of the Thalang and Takua Pa formations. The Normal faults was move action during the set up of the sub-basin in the southern Mergui Basin. The horizon displacement plot of the NNW-SSE trending Mergui Fault, which Basement, the Ranong Formation and the Kantang Formation have high displacement (Figures 4.36 and 4.37). Displacement of the Ranong Formation is as high as 780 ms (TWT) in the northern area and decreases of displacement in the central

area, and then increases of displacement in the southern area of 600 ms (TWT). The displacement of the Kantang Formation in the northern and southern areas are as high as 200 and 300 ms (TWT), respectively. The Mergui fault developed from the Basement rock and cut into the Cenozoic section (Figure 4.38), showing high displacement location of the basement rock at an averge depth of 1,400 ms (TWT). The Ranong Formation has been eroded off and Miocene sediments lie unconformably at the Mergui Ridge. Movements of the Mergui fault occured at the same time as in deposits of the Ranong and Kantang Formations.

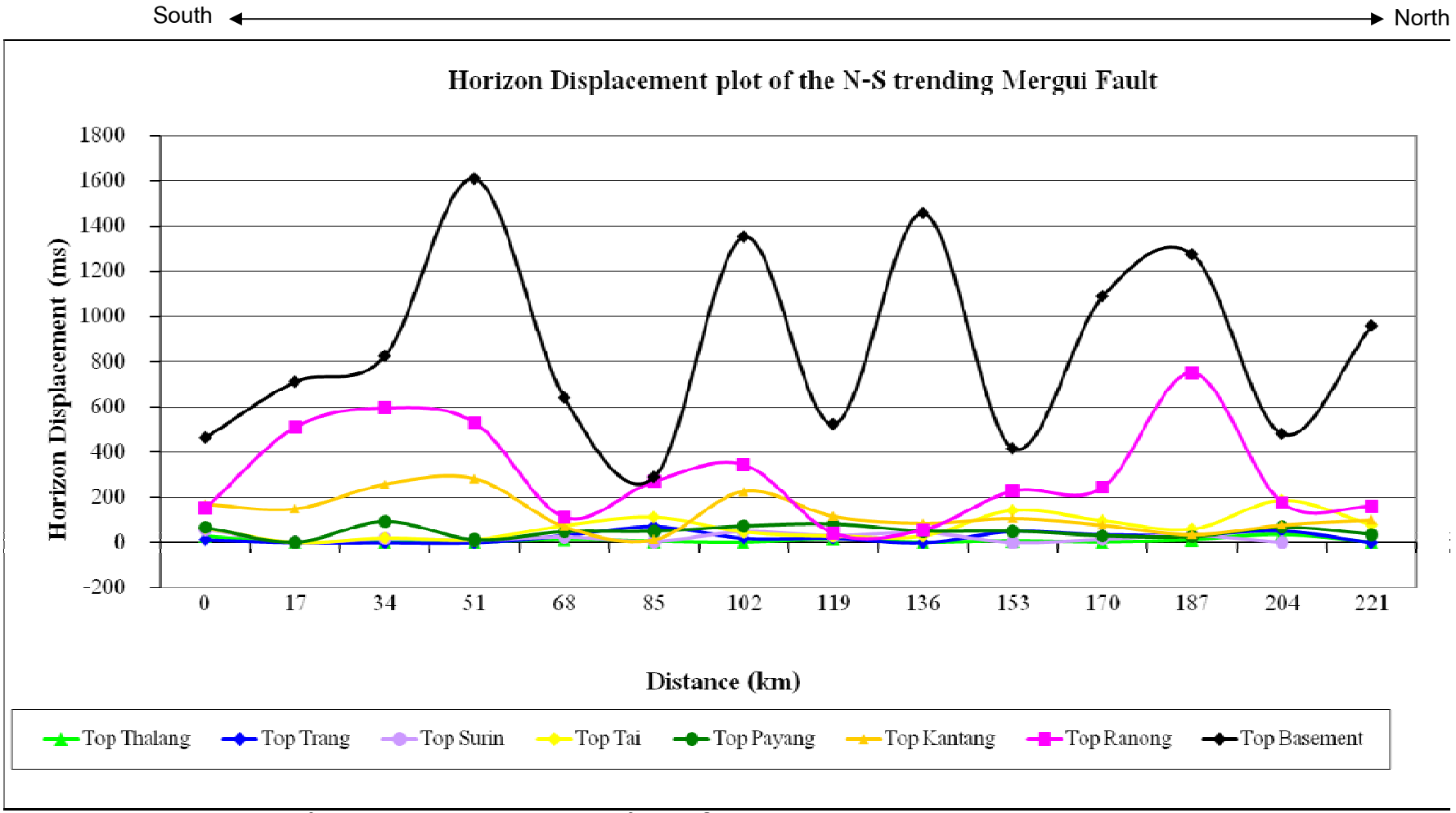

Figure 4.38 The top horizon of Formation displacement plot of the N-S trending Mergui Fault in the southern Mergui Basin.

CHAPTER V
DISCUSSION

This chapter focuses on discussions which can be grouped into 4 major topics, namely (1) stratigraphy compared with those of the other studies, (2) structural displacement, (3) history of Mergui Basin, and (4) active fault analysis.

5.1 Stratigraphic comparison (with earlier works)

5.1.1 Thickness of individual horizons

Stratigraphy in the Mergui basin reported by Polachan (1988) is used in the present study to describe individual rock units. The more sandy sequence of Ranong Formation with thickness varying from 338 meter to about 1,162 meter was closely related to normal fault movements, implying that the sedimentary strata diverge towards fault planes. This suggests that the Ranong Formation was deposited during extensive normal faulting in the rifting phase of basin development. The Ranong Formation is regarded as sediments of rift basins thickening towards syndepositional faults. The sediment supply in the south was probably limited as seen from the present seismic sections that the maximum thickness of the Ranong formation decreases from about 2,641 meter in the east to about 264 meter in the west. This suggests that the Southern basin had greater subsided to the east than to the west. Similar situation was found in the northern basin by Srisuriyon (2008). The thickness of the Ranong Formation in the northern Mergui Basin varies from 140 merter to 1,046 meter from north to south (Srisuriyon, 2008). This scenario indicates that the sourthern basin has thickness of the Ranong Formation more than that of the northern basin. Such scenario indicates that the basin becomes deeper or more subsided in the south than in the north.

The shale-dominated Yala Formation has the thickness varying from 560 to 1,043 meter. The formation with deep-water condition largely occurs in the southern part of the southern Mergui. Such case supports the idea that tectonic subsidence may have formed in the south more commonly than in the north. According to Srisuriyon (2008),

the Yala Formation was not found in the northern Mergui Basin. This leads to the conclusion that provenances (or sources of sediments) are from the north and the east.

The thickness of the Kantang Formation increases from about 100 to 150 meters at both basin margins and above basement highs to about 1,000 meters in the basin centre. Thus the stratigraphic configuration suggests that basin subsidence during the deposition of the Kantang Formation was more uniform than that during the deposition of the Ranong Formation.

The carbonate-enriched horizon of the Tai Formation has the thickness of 485 meter. It largely occurs in the central part of the study basin. Because the Tai Formation consists of reefal carbonate rocks, so the formation occurs mainly in the shallow-water environment. This indicates basin high for the southern Mergui Basin. However some wireline data show the carbonates in the deeper part.

The thickness of the Trang Formation gradually increases from about 100 meter to 500 meter from the northern Mergui Basin to southern Mergui basin. However some seismic section show the formation gradually decreases from about 300 meter in the basin centre to 100 meter towards the basin margins. Exception is the southern part of the basin where sediment supply was relatively limited and the formation has a wedge-shaped geometry.

For the younger and overlying sequences (such as Thalang and Takua Pa Formations) their thickness does not change much from the north to the south and the east to the west (see Figure 5.1). It is interesting, as recognized from this study, that the large clinoform structures in the Surin Formation has been clearly observed from the enhanced seismic sections (line no AD4, see Figure 4.20). This sedimentary structure becomes major stratigraphic characteristic of this formation. Such characteristic and feature has not been reported by Polachan (1988).

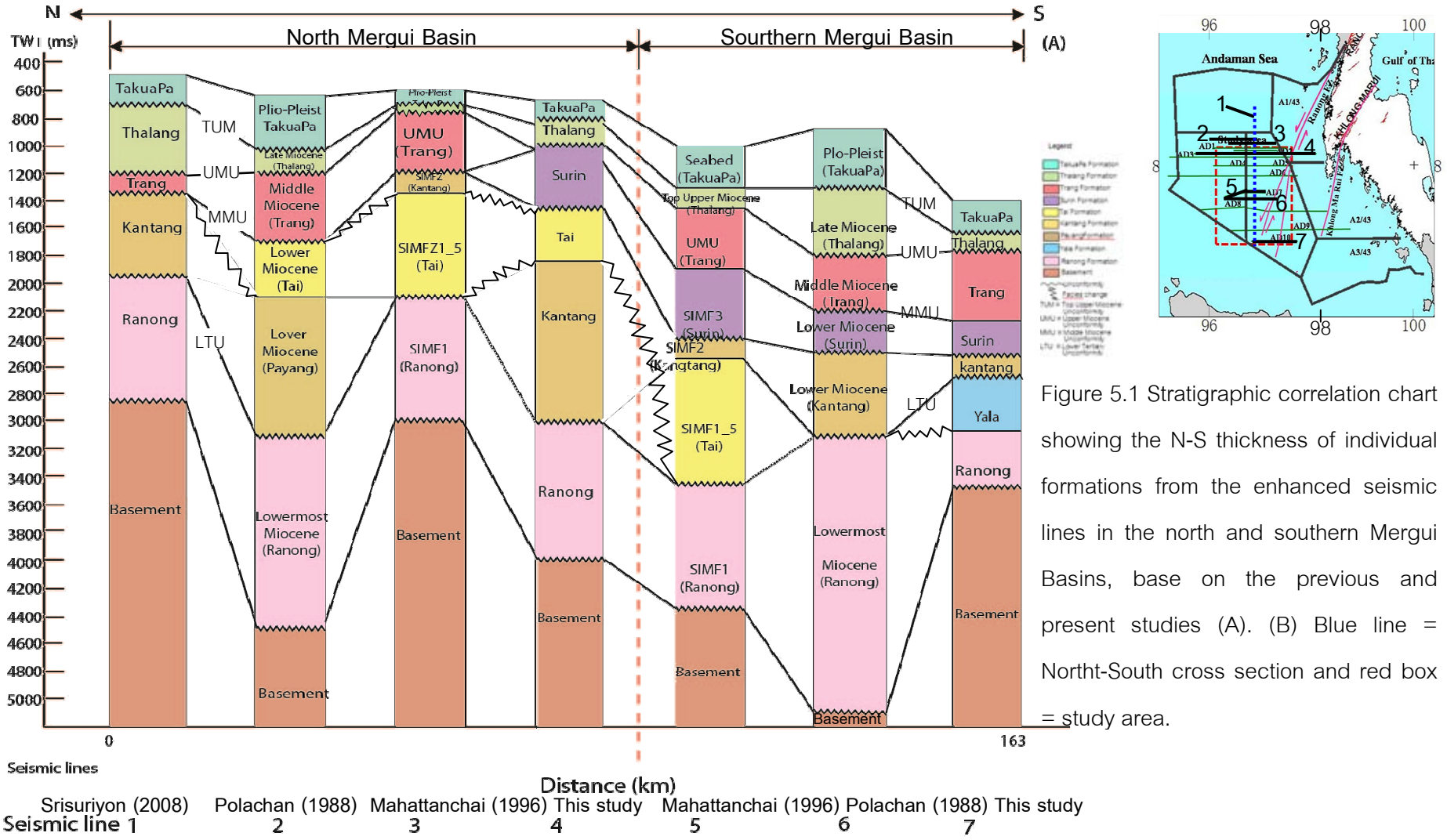

Figure 5.1 Stratigraphic correlation chart showing the N-S thickness of individual formations from the enhanced seismic lines in the north and southern Mergui Basins, base on the previous and present studies (A). (B) Blue line = Northt-South cross section and red box = study area.

5.1.2 Depocenters in the study area.

As displayed in Figure 5.2, it is well observed from the studied seismic sections that there are variable in the thickness of the Ranong, Yala, Payang and Kantang Formations for the southern Mergui Basin (Table 5.1). The results show that depocenters change to be from the west (thinner) to the east (thicker), suggesting the major basin subsidence occuring half grabens in the eastern part of the area. A comparison has been made between those of the sourthern and the northern part of the Mergui Basin, it is found that the southern part is able to serve as a major depocenter, of the Mergui Basin. Figure 5.2, 5.3 and 5.4 show plots of the maximum thickness along individual studied sections.

The result-show that deposition of the Ranong and Yala Formations took place during extrusive subsidence of early rifting, where the normal faulting generate half-graben depocentres. The Ranong Formation thickness markedly towards the depocentres of these subbasins and thins or disappears towards basement highs. After the deposition of the Ranong formation, local inversion of existing normal faults or strike-slip reactivation of faults have been formed in the vicinity of the Ranong Fault occurred. While Kantang and Payang Formations are subsidence in the depocentres of the isolated sub-basins and over structural highs. These processes appear to have ceased prior to the deposition of the Surin Formation.

Table 5.1 Summary of the maximum thickness of combined Ranong and Yala, Payang, Kantang and Tai, Surin and Trang Formations along individual studied sections in the Mergui Basin.

Seismic lines	Ranong and Yala Formations (m)		Payang, Kantang and Tai Formations (m)		Surin and Trang Formations (m)	
	Wastern Mergui Basin	Eastern Mergui Basin	Wastern Mergui Basin	Eastern Mergui Basin	Wastern Mergui Basin	Eastern Mergui Basin
AD1	1,117	1,270	1,132	1,265	639	520
AD2	1,181	1,040	1,116	1,419	502	607

Table 5.1 (Cont).

Seismic lines	Ranong and Yala Formations (m)		Payang, Kantang and Tai Formations (m)		Surin and Trang Formations (m)	
	Wastern Mergui Basin	Eastern Mergui Basin	Wastern Mergui Basin	Eastern Mergui Basin	Wastern Mergui Basin	Eastern Mergui Basin
AD3	1,075	1,165	1,766	1,639	627	538
AD4	1,710	1,605	1,196	1,402	685	544
AD5	1,628	1,200	1,675	1,066	702	519
AD6	828	1,217	1,393	1,252	784	586
AD7	264	2,641	389	1,310	610	1,200
AD8	1,532	2,211	871	818	541	1,116
AD9	-	1,914	-	770	-	761
AD10	-	1,981	-	574	-	462

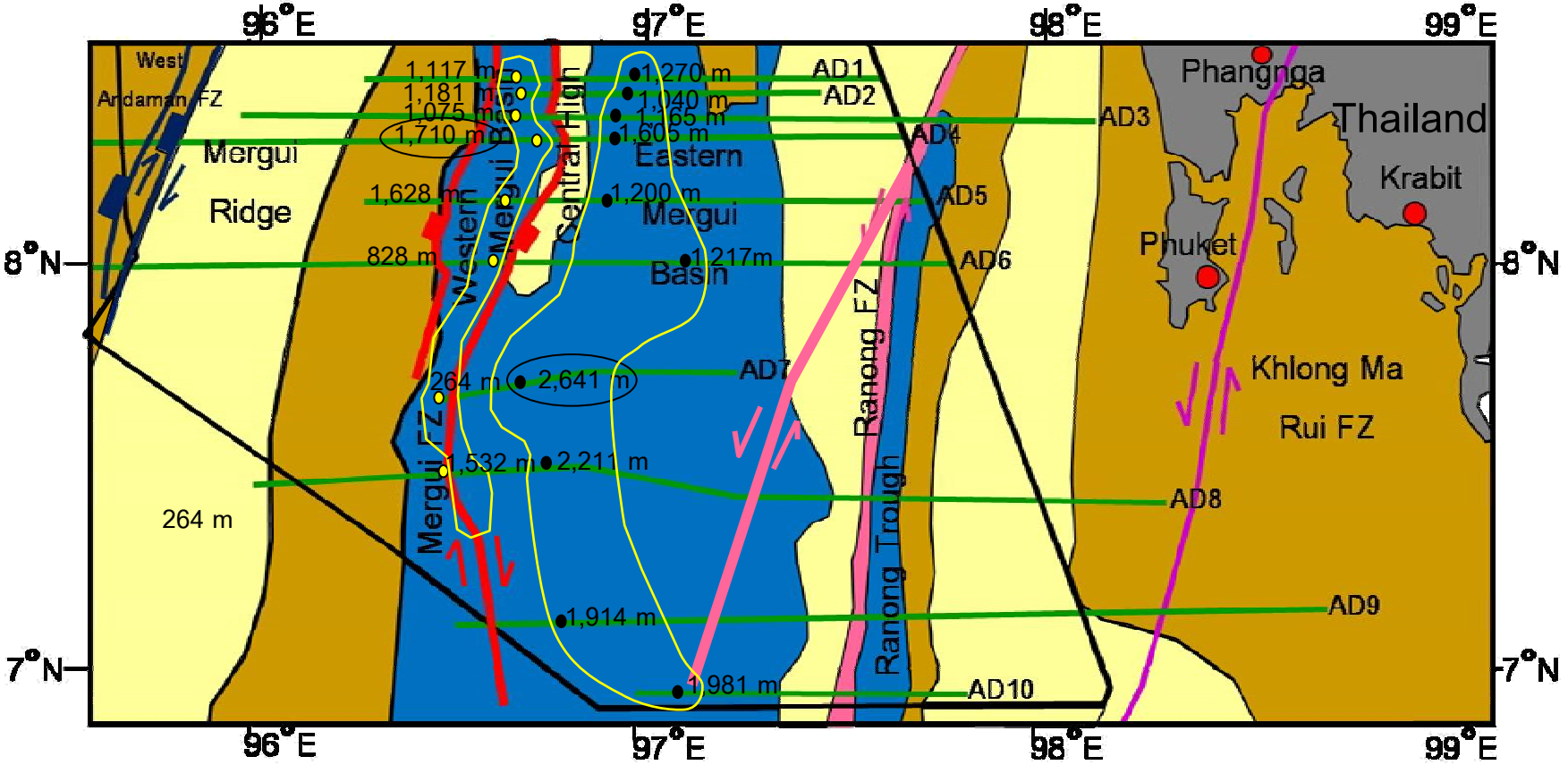

Figures 5.2 Map of major structure of the southern Mergui Basin showing the studied seismic lines and locations of maximum thickness of combined Ranong and Yala Formations (modified from Polachan, 1988, Mahatanachai,1996, Srikulwong, 2005 and Thipyopass, 2010).

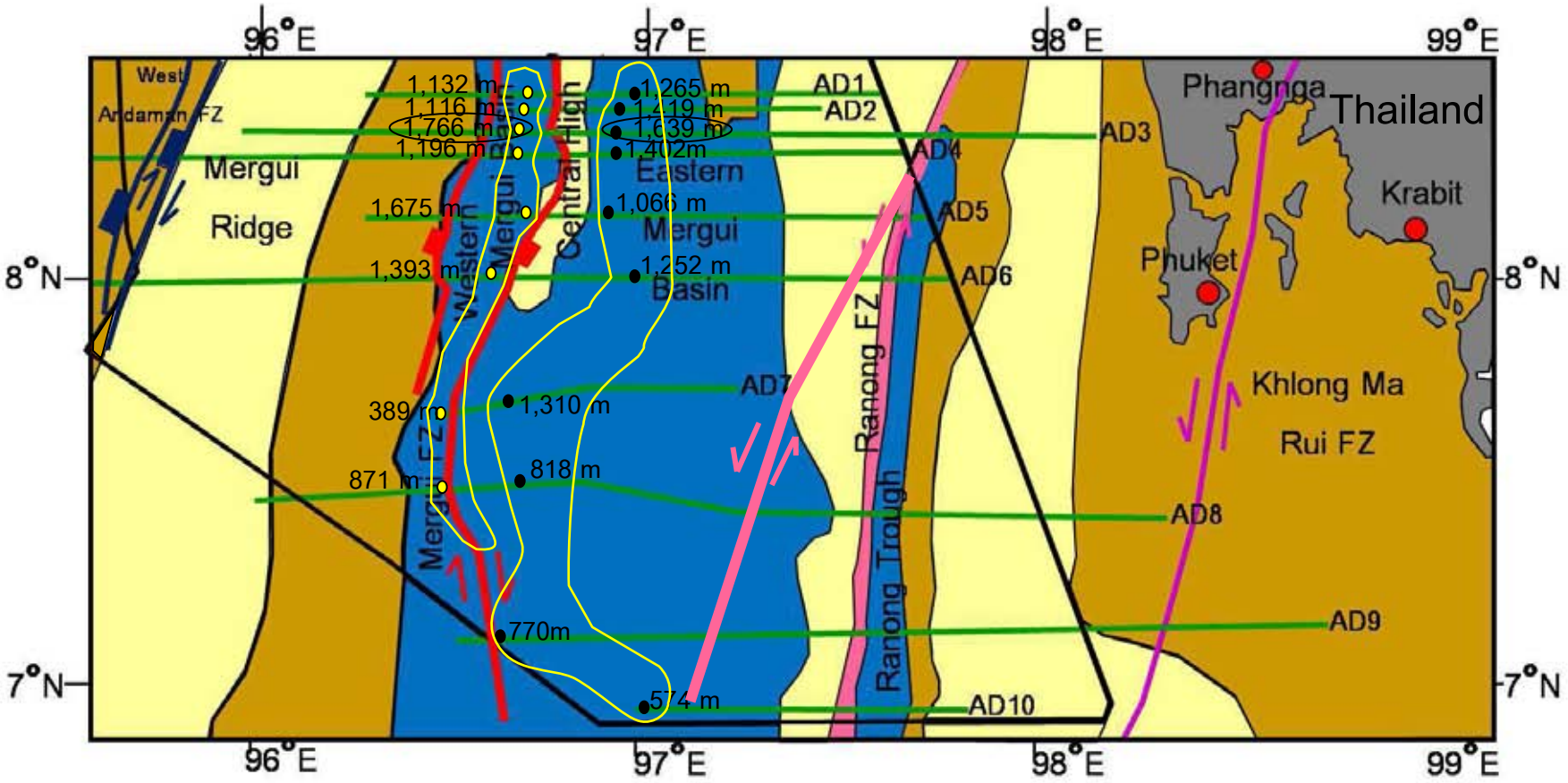

Figures 5.3 Map of major structure of the southern Mergui Basin showing of the studied seismic lines and locations of maximum thickness of combined Payang, Kantang and Tai Formations (modified from Polachan, 1988, Mahatanachai,1996, Srikulwong, 2005 and Thipyopass, 2010).

104

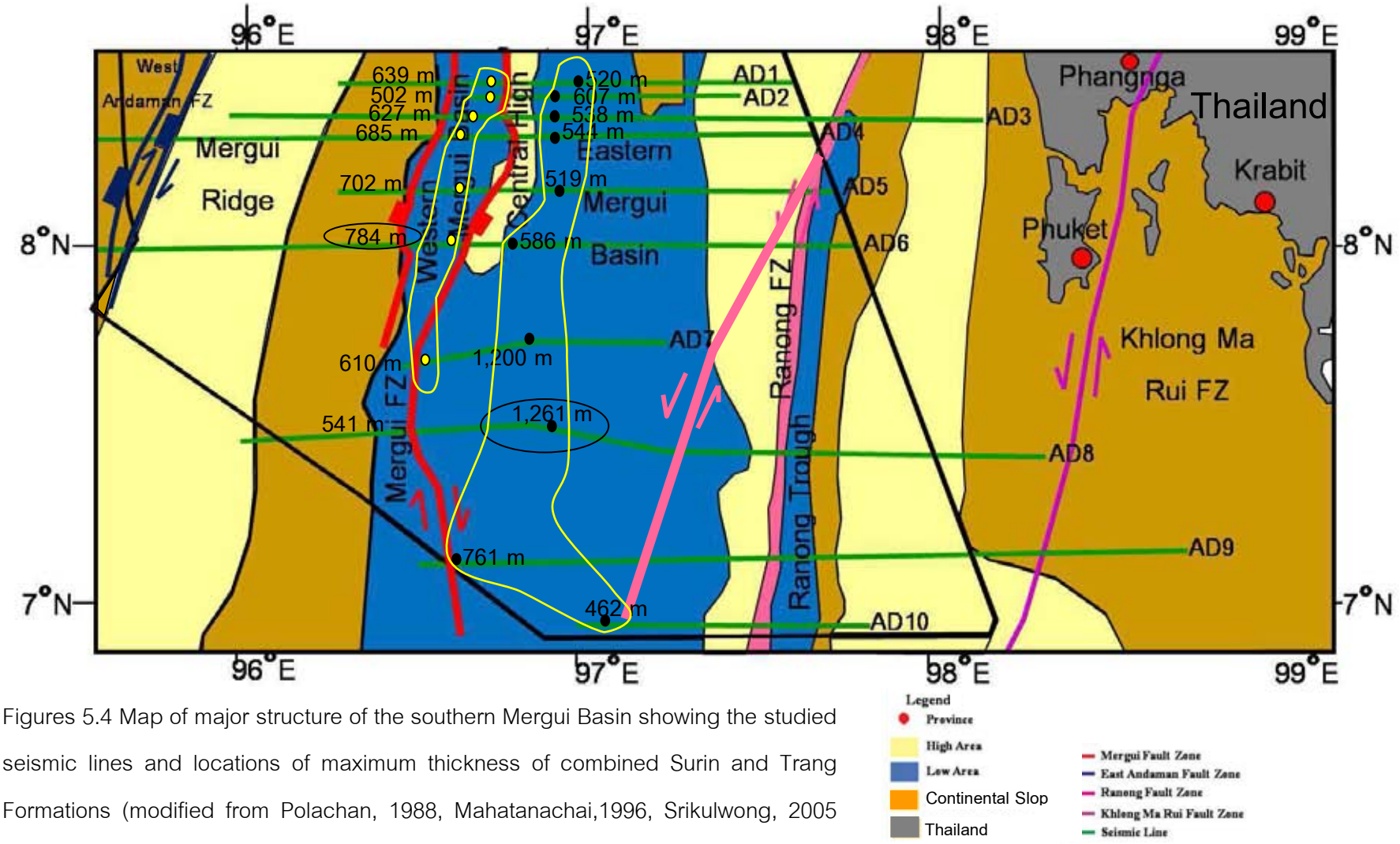

Figures 5.4 Map of major structure of the southern Mergui Basin showing the studied seismic lines and locations of maximum thickness of combined Surin and Trang Formations (modified from Polachan, 1988, Mahatanachai,1996, Srikulwong, 2005 and Thipyopass, 2010).

5.1.3 Sedimentary Structures

Sedimentary structures are important for stratigraphic analyses, particularly when sections are used. Such structures are spatially and temporally controlled by faultings, tectonic settings and sea-water changes. The Ranong Formation onlaps onto the Top Basement horizon, especially where the basement is shallow – such as footwalls of normal faults during periods of extensive rifting activity. However, sediment of the Payang Formation deposit and onlap onto the Ranong Formation by relative with continuation of rifting. In addition, onlaps occurs overlying the Trang, Thalang and Takua Pa Formations located at edge of the Western Mergui Basin during periods of transgression. The Kantang Formation occurs erosional surface onto the Ranong formation at the edge of basin (or the Mergui ridge) and overlying the Trang Formation, in response for relative sea level fall and uplift.

Prograding clinoforms have been encountered at eastern edges of Surin Formation, the Trang and Takua Pa Formations of the studied southern Mergui Basin. This suggests that deposition occurred onto the continental slope, which prograded wesrward from the eastern Mergui Basin to western Mergui Basin as shown by the thicker sequences in the southern Mergui Basin more than in the north Mergui Basin.

The prograding clinoforms in the southern Mergui Basin seems to occur during Pliocene as a result of uplift at the Ranong Ridge. As shown in almost all interpreted enhanced seismic sections and the complied wire-line log data, it is visualized that unconformities have been observed clearly in comparision with those reported in the previous works.

5.1.4 Unconformity

The regional unconformities which are identified by these enhanced seismic horizons correspond to the following major tectonic events. Unconformities occur in the present seismic sections are Lower Tertiary Unconformity (LTU), Middle Miocene Unconformity (MMU), Upper Miocene Unconformity (UMU) and Top Upper Miocene (TUM). Apart from the MMU, most of the unconformities are characteristic of an angular unconformity and comprise sub-parallel reflections with strong to moderate amplitudes

and good continuity. Top horizon of the Ranong Formation, seismic surface represents the Late Oligocene to Early Miocene Unconformity. Top horizon of the Kantang Formation, seismic horizon corresponds well to an unconformity occurring at the end of Early Miocene. Top horizon of the Trang Formation corresponds to an unconformity that occurred during the Upper Miocene and Top horizon of the Thalang Formation.

Based on the result presented above, it is visualized that the first episode of sedimentation began in the southern Mergui Basin during the Oligocene, similar to that observed by Srisuriyon (2008) in the north. Each episode of sedimentation was periodically terminated by major tectonic events as supported by unconformable surfaces occasionally occurred through times. In consequence to the major fault movements, sedimentary fills of the southern Mergui Basin were complicated and difficult to correlate due to the presence of associated of faults, tectonic uplift, and rapid subsidence that may have caused the changes of seismic facies within the same seismic package.

5.1.5 Paleo-environments and tectonic settings

Based on the seismic stratigraphy, biostratigraphy and lithology by wire-line loggings, the paleo-environments can be broadly subdivided into subdivided into 5 epochs, i.e. (1) Late Oligocence- Earliest Miocene, (2) Earliest Miocene-end Early Miocene, (3) Middle Miocene, (4) Late Miocene and (5) Pliocene- Recent.

After, the Mergui basins had been rifted tectonically and subsequently subjected to continuous subsidence, large amount of sediments were deposited continuously in an alluvial plain environment. Later the deposition was changed in response to invasion of sea water to the whole sedimentary basin. Such marine deposition occurred in the Later Oligocene time. The epochs are represented by the Ranong Formation, which could be interpreted as fluvial channel or deltaic sandstone developed within mud-dominated flood-plain or lacustrine strata. The Yala Formation is considered to be deposited in deep environment during the late Oligocence- earliest Miocene.

In the earliest Miocene-end of early Miocene, the sea-level has fallen suddenly with accompany of basin uplift, (as evidenced by inversion seen in seismic line no AD9)

causing erosion and unconformity. Sediments of the epochs can be divided, from older to younger, into 2 formations, e.g., Kantang Formation and Tai Formation. These 2 formations (Kantang and Tai) have been interpreted as deep marine and shallow carbonate reefs, respectively.

Similar environments have been reported by Srisuriyon (2008) and Mahattanachai (1996) for the north Mergui Basin. However Payang Formation, which is dominated in the northern Mergui Basin, has not been found in the southern Mergui Basin and is considered to have been deposited in the shallow marine environment.

Subsequent to the rifting and erosional phases continuously in the Middle Miocene. Sedimentation has been dominated by Trang Formation which is herein regarded as deposition in the deep marine (low energy) as shown by occurrence of colloform structures. The same scenario has been encountered for the environment of deposition in the northern Mergui Basin (see Srisuriyon, 2008 and Mahattanachai, 1996). However stratigraphy of the north is also characterized by Surin Formation which has not been observed in the south. This formation has been interpreted by these two workers to have been deposited in the shallow marine environment.

At the marginal part of the basin, the sediments of the lower part were truncated by the younger sediments, but it appears to be a continuous deposition into the basin in the late Miocene, as evidenced by Thalang Formation, which was deposited in deeper marine and turbidite environments. The basin subsequently was again subsided tectonically and the sediments were mainly deposited in deep-sea environment in the Pliocene- Recent time. However the presence of clastic clinoforms in the west-dipping suggests a deposition in shallow marine environments.

5.2 Fault Displacement

The NNW-SSE trending Mergui Fault (Figure 5.5) displayed a displacements at the syn-rift interval range from about 0 to 1,600 msec. The methodology of displacement calculation is shown in detail in the Appendix B. The total thickness of the basin fills reach a maximum of about 5,500 msec in the southern Mergui Basin. Most syn-rift

normal faults terminate upward near the top of the Ranong and Yala Formations, although some associated faults with large displacements were reactivated and continue upward to the level of the Thalang and Takua Pa Formations. Normal faults with small displacements (10 msec) were interpreted to have occurred within the post-rift interval. The NNW-SSE trending Mergui Fault has a maximum displacement of about 1,600 ms relating to rifting and uplift and controlling several basement highs.

The Horizon Displacement plots of the Mergui Fault of the Southern Mergui basin are shown in Figure 5.5. Comparison is made for such displacement to the Northern Mergui Basin (Srisuriyon, 2008). The pattern of the NNW-SSE trending Mergui Fault in the Southern Mergui Basin or the Mergui fault in the North Mergui Basin, displacement can be seen on the cross section along the fault plan. The Mergui fault displacement in the North Mergui Basin shows 3 high displacement locations of the basement rock at an average depth of 1,200 ms (Srisuriyon, 2008), which different with the NE-SW trending Mergui Fault in the Southern Mergui Basin shows variations of high displacement locations of the basement rock at an average depth of 1,427 ms. In addition, the Southern Mergui Basin shows high displacement location of the Ranong and Kantang Formations at an average depth of 590 ms and 220 ms, respectively. Movement along the NNW-SSE trending strike slip Mergui Fault in the Northern Mergui Basin may have caused thicker of sedimentary strata in the west of the fault plane than in the east (Srisuriyon, 2008), whereas in the southern Mergui Basin, this situation become vise versa.

5.3 History of Mergui Basin

The tectonic events that occurred within the area under study, the majority of events result from strike-slip movement on the Mergui Fault Zone and the Ranong Fault Zone which also caused extension in E-W direction. The Mergui Basin started to develop from the south where the Mergui Shelf began to split apart from the Mergui Ridge. Subsequently, the Oligocene basin occurred as the isolated half graben across the

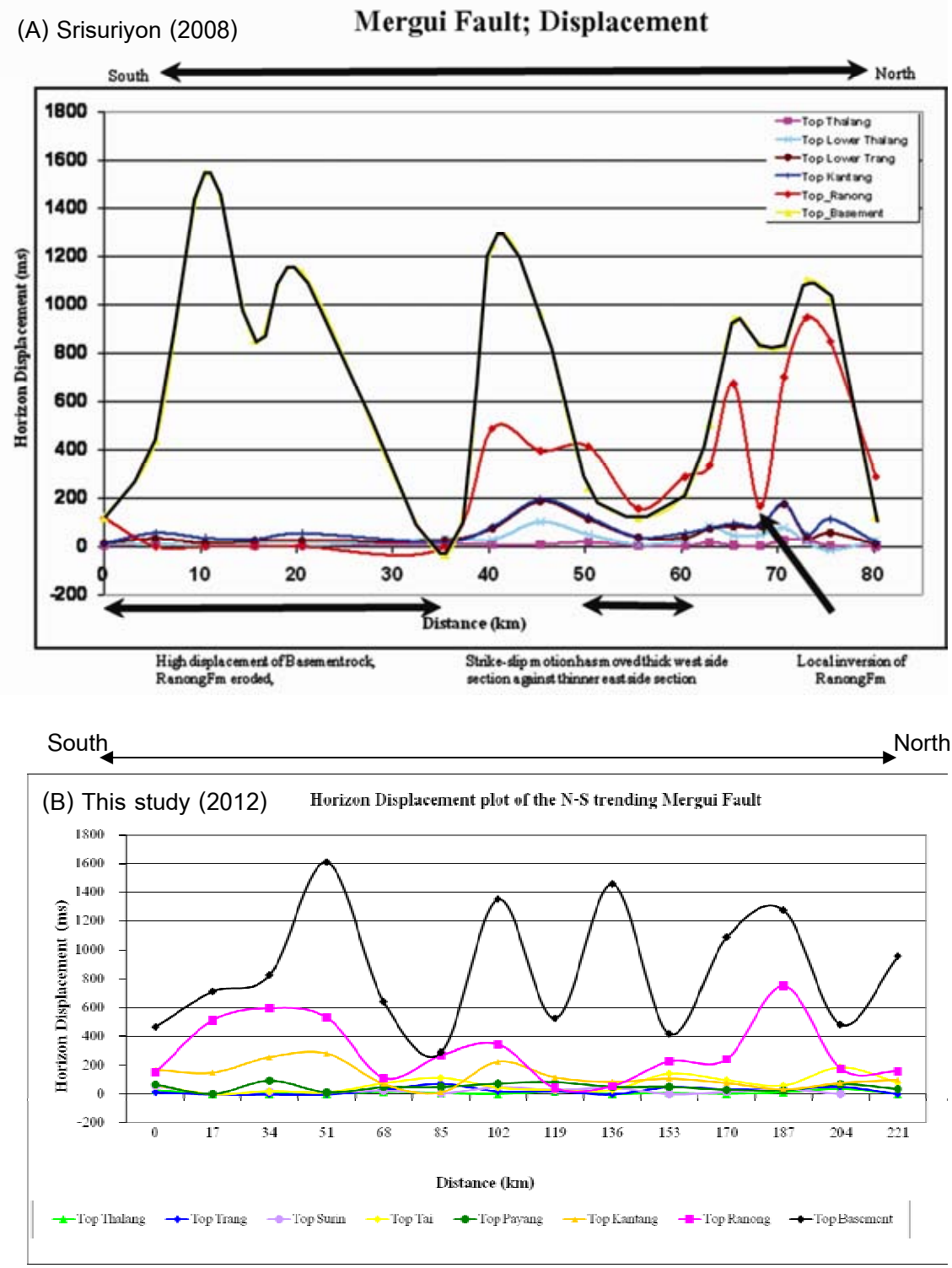

Figure 5.5 The comparison Horizon Displacement plot of the Mergui Fault between the Northern Mergui basin (Srisuriyon, 2008) and The Southern Mergui basin (This study, 2012).

study area (Figure 5.6). In Late Oligocene- earliest Miocene time was the main extensional phase. Displacement and development of structures associated with the Mergui and Ranong Faults extend high into the section, which the fault growth continued into the Middle Miocene.

During end stage of the Early Miocene, deep marine shale were deposited in the basin while reefs were built up on the Central High. The basin appears to have extended along dominant of N-S trending half grabens in all part of the basin. The N-S normal fault related to the dextral movement of the Sumatra Fault system. In the Middle Miocene, the Mergui basin continued to subside, and the depocenter was located along the Mergui Fault Zone, which thin sediments of shallow marine were deposited in the eastern part of the basin. Unconformity appears to be a regional compressional event.

Pull apart and initial transtensional synrifting event (~55-35 Ma) may have commenced, and as a result rift sediments may have been deposited by continental extension and mantle plume. This may have happened due to a change from a passive continental margin to subduction in response to the interaction of India and Asia. This episode may have been terminated as evidenced by the presence of Middle Tertiary Unconformity (MTU), as clearly shown in the seismic data.

5.4 Active Fault

In this study, there are two major strike-slip faults observed from seismic data that are considered as the main control on the structural framework in the southern Mergui study area. They are the dextral NW - SE trending Mergui fault zone (MFZ) and the sinistral NE-SW trending Ranong fault zone (RFZ).

As shown in earlier section, movements along the faults were related to the opening of the Mergui Basin in the central part of this study area and the Andaman Basin to the northwest. The NNW-SSE trending Mergui Fault is located in the center of Mergui Basin. The NNE-SSW trending Eastern Andaman Faull zone is located northwest of the survey limit and formed the eastern boundary of the Andaman Basin. Evidence for faulting at the seafloor was observed along these major faults. There are also several

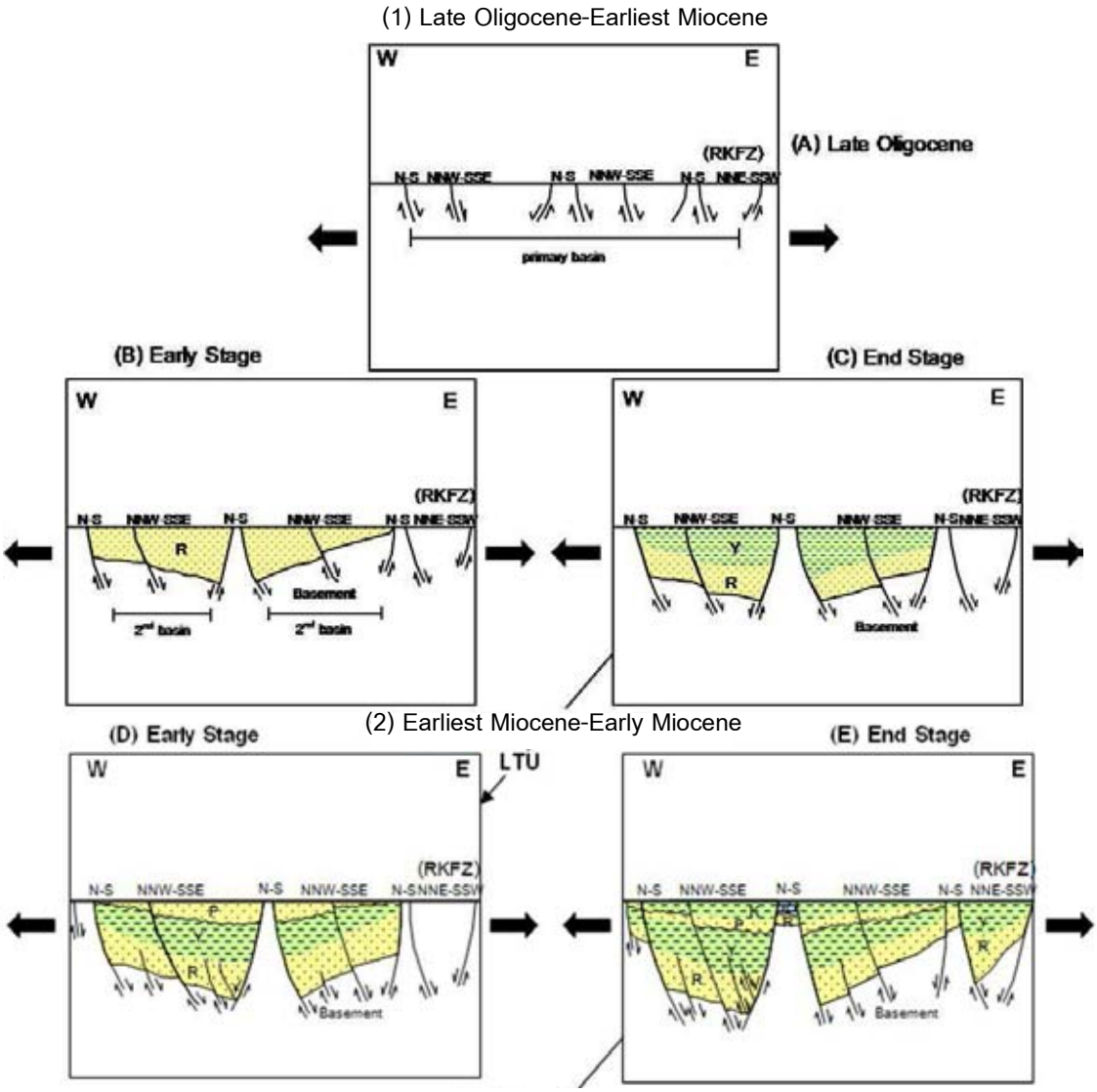

Figure 5.6 Structure evolution of the southern Mergui Basin consists of 5 stage, namely (1) Late Oligocene – Earliest Miocene (2) Earliest Miocene-Early Miocene (3) Middle Miocene (4) Westward progradation of the Surin and Trang Formations due to extensive opening of the Andaman Sea during Late Miocene and (5) Deposition of the Plio-Pleistocene Thalang and Takua Pa Formations.

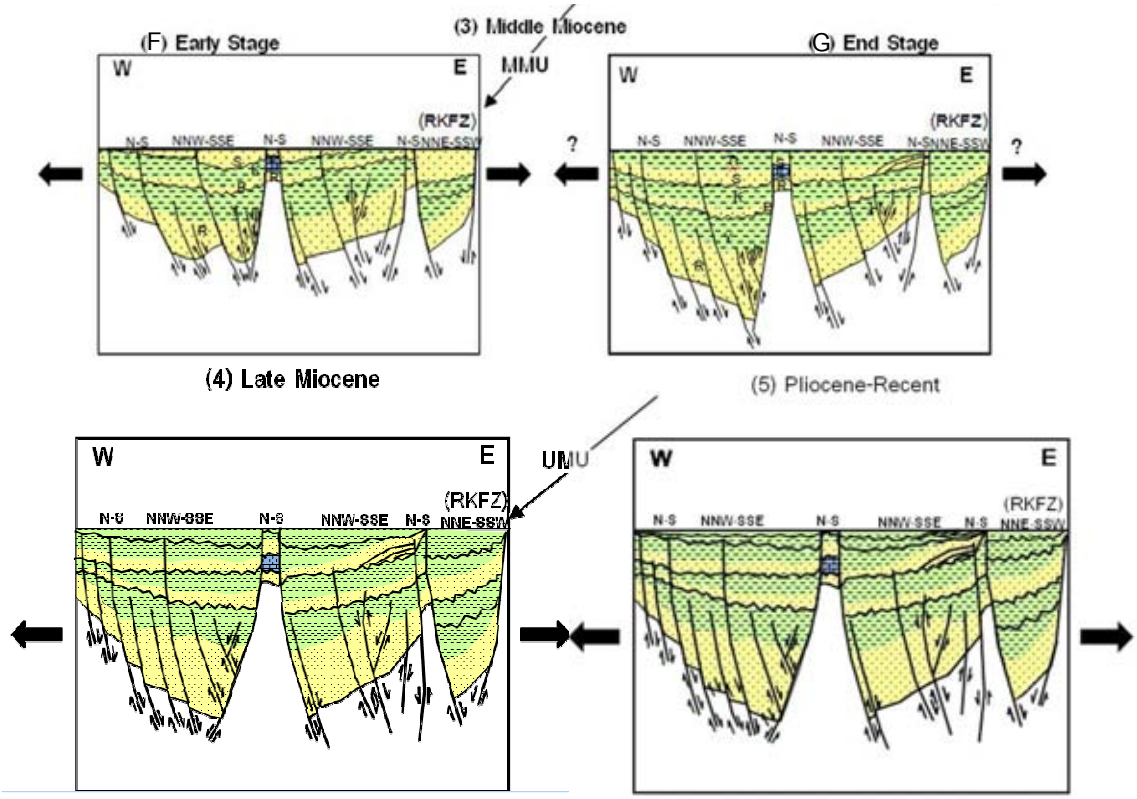

Figure 5.6 (Cont.)

minor faults that appear to continue upward to the seafloor. In the Mergui Basin, such minor faults developed along the active Ranong and Klong Marui Faults. The reactivation of these two faults uplift occurred periodically through times are believed to be related to the movement of the Mergui fault zone, which may be the consequence of the Indian plates continued movement further northward into the Eurasian plate (Mahattanachai, 1996).

The N to NNW trending Mergui Fault with the essential normal component interpreted to cut through Ranong Formation. This activity is most likely to give rise to the thickness to the west is much more than that to the east. The Ranong Fault is the left lateral strike-slip fault with high dip angle (45˚-60˚) and extendes from Ranong province into Mergui Basin. This fault runs into the Mergui Basin as a low-magnitude epicenters can be extended and linked with the RNF in Andaman sea. Also, the Ranong fault has the strike slip fault movement that creates narrow push uplift (Ranong Ridge) (Thipyopas, 2010).

The NW - SE trending Mergui and the NE-SW trending Ranong Faults clearly cuts through the Takua pa Formation to the seafloor. The Ranong Fault segment cutting seafloor sediments was found at the Ranong Ridge suggesting that both faults are still active till present. Both Ranong and Mergui Faults offset the seafloor and Thalang Formation with the vertical slips of about 30 meter and 40 meter, respectively. Additionally, as shown in Figure 5.21, the distribution of several epicenters in Andaman sea.

The active faults observed in the southern Mergui Basin formed mostly in the N-S trending (eastward dipping) faults, which can be defined as active boundaries of half grabens, while faults in northern Mergui Basin formed mostly in NNW-SSE and NE-SW (Srisuriyon, 2008) as strike slip faults.

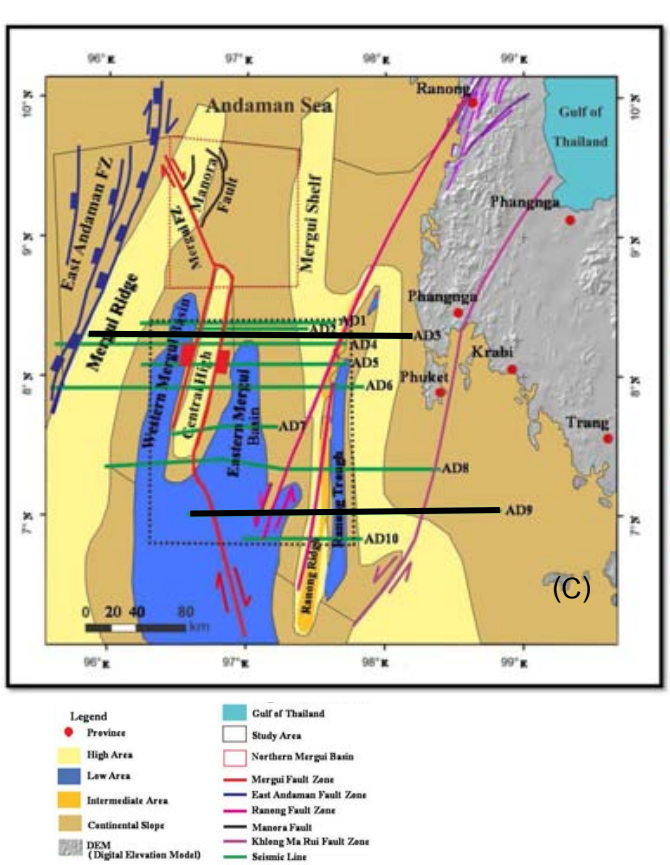

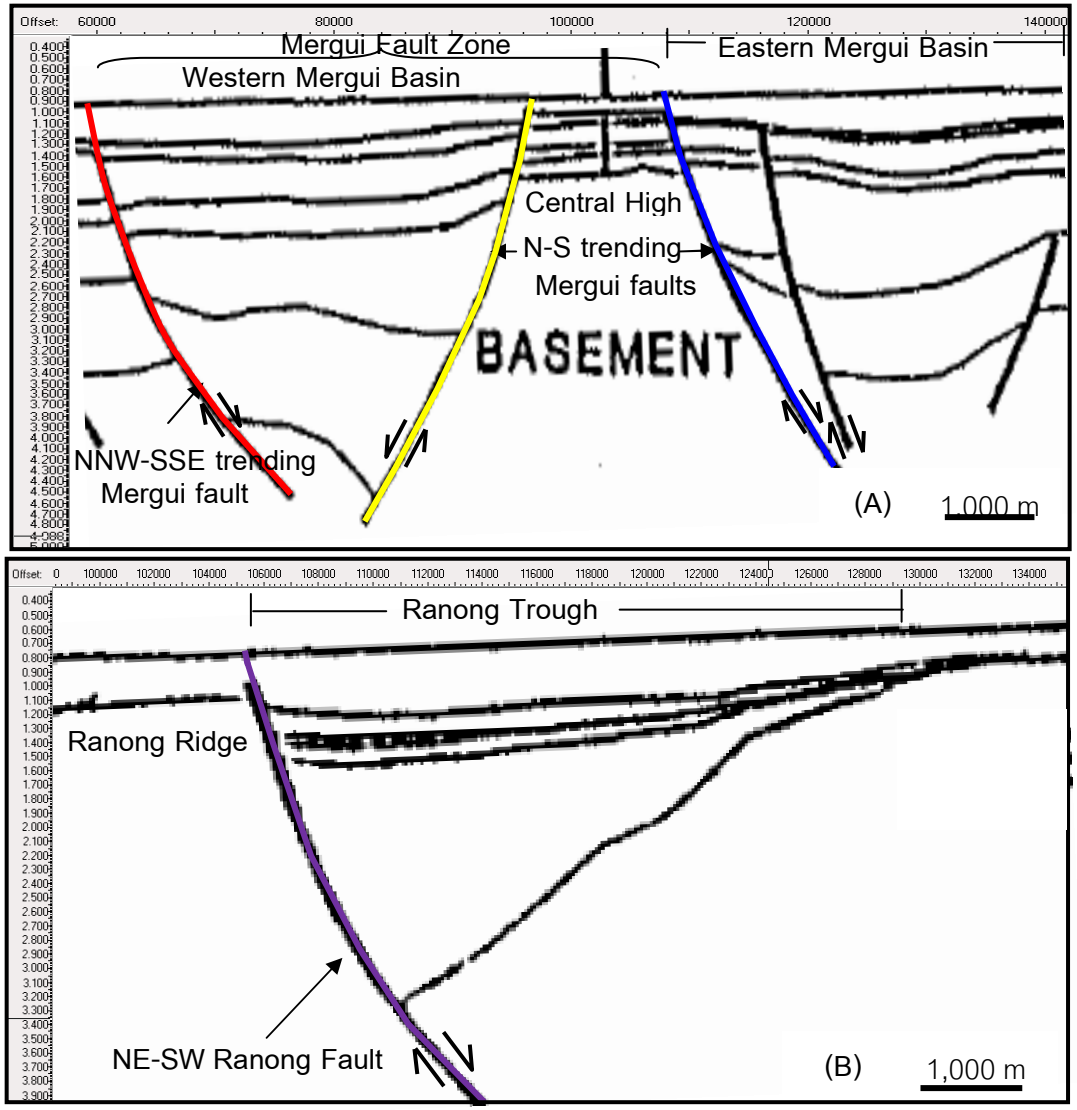

Figure 5.7 The active fault of the Mergui Fault Zone in the Mergui Basin (A) and Ranong fault which uplifting of Ranong ridge (modified Polachan, 1988).

CHAPTER VI
CONCLUSIONS AND RECOMMENDATIONS

6.1 Conclusions

Interpretation of the 2D reflection seismic profiles along with complied wire-line log data and earlier published and unpublished studies reveal that 8 formations and associated structures have been identified in the southern Mergui Basin. The oldest rocks are pre-Tertiary basement rocks, locating from 372 to 3,500 m below mean sea level and shallower in the western part of the study area. They are unconformably overlain by the oldest Tertiary sequences of the Oligocene-Lowest Miocene Ranong (±1,400 m thick) and Yala (± 1,120 m thick). These formations are marked as the base by the LTU and have been largely deposited in the shallow and deep marine environments due to successive tectonic rifting. Unconformably overlying is the Oligocene Payang (± 600 m thick), Tai (± 500 m thick), and Kantang (± 1,300 m thick) Formations, and they are in a shallow to deep marine sediments. These formations are overlain unconformably by the MMU unconformity. The Surin (± 600 m thick) and Trang (± 700 m thick) Formations which principally occurred in shallow and deep marine environments, during Middle Miocene Epoch. Younger than these two formations is Upper Miocene Thalang Formation (± 200 m thick) which deposited in the deep marine environment during post-rifting setting. The youngest formation is the Pliocene to Recent Takua Pa Formation (± 200 m thick) which has been deposited in shallow and deep marine environments.

Four major faults trends have been identified in the southern Mergui Basin. From west to east, they are (1) the N-S trending, west Mergui Fault that cut through the basement, Ranong, Payang, Tai Surin, Trang, Thalang and Takua Pa formations with the offet ranging from 25 m to 1,522 m.; (2) the N-S trending east Mergui Fault that cuts through the basement, Ranong, Payang, Tai, Surin, Trang, Thalang and Takua Pa formations with the offet ranging from 10 m to 1,033 m., (3) the NNE-SSW trending west Ranong Fault that cut through the Ranong, Trang, Thalang, and Takua Pa Formations with the maximum offset of about 2,066 m; and (4) the NE-SW trending Ranong Fault that cutting through the Ranong, Yala, Kantang, Surin, Trang, Thalang, and Takua Pa

Formations with the maximum offset of about 2,700 m. A few faults have been observed to cut through the topmost sea beds of the Takua Pa Formations. Such characteristics along with epicentral distribution in the offshore Andaman sea along the faults suggest that both Mergui and Ranong Faults are still active.

The Mergui fault displacement along the NNW-SSE direction shows high value of basement offset, the Ranong Formation and the Kantang Formation. Displacement of Ranong Formation is as high as 780 ms (TWT) in the northern area and decreases in the central area, and then increases in the southern area of 600 ms (TWT) The displacement of Kantang Formation in the northern and southern areas are as high as 200 and 300 ms (TWT), respectively. High displacement of the basement rock occurs at an averge depth of 1,400 ms (TWT), which develope from the Basement rock and cut into the Cenozoic section of the Mergui basin.

Structural evolution of the southern Mergui Basin can be subdivided into 5 stages. They are (1) Oligocene syn-rifting due to the extension tectonics and deposited marine sediments of the Ranong and Yala Formations and development of large normal faulting generating half graben depocenters as well as flower structures; (2) Thermal subsidence of the post-rifting causing early Miocene deposition of the Payang and Kantang Formations and cessation of normal faulting; (3) Inversion of normal faulting together with reactivation of strike-slip faulting due to compression tectonics causing the movements of the Ranong and associated faults; (4) Westward progradation of the Surin and Trang Formations due to extensive opening of the Andaman Sea during the Late Miocene, followed by deposition of the Plio-Pleistocene Thalang and Takua Pa Formations, and termination major of structural development, and (5) The development of active seafloor off setting since Pleistocene causing by the up to present-day reactivation of Ranong and Klong Marui active faults.

6.2 Recommendations

From this study, it is unclear to indicate when the strike-slip movement occurred definitely. Therefore, it is recommended that a further investigation should focus on detailed interpretation on the enhanced seismic survey data. The detailed interpretation

of seismic facies in the Andaman Basin, locating north of the Mergui, is also recommended to be conducted in the future.

Further, the age of the whole Mergui Basin stratigraphic formations in details need to be dated analyzed and either by paleontological dating or radiometric dating method.

REFERENCES

Achalabhuti, C. 1975. Petroleum geology of Thailand (Gulf of Thailand and Andaman Sea Summary). In Halbouty, M.T. Maher, J.C., and Lian, H.M. (Eds). Circum-Pacific Energy and Mineral Resources. American Associate of Pertroleum Geologists., pp. 147-157. Department of Mineral Resources, Ministry of Industry, Bangkok, Thailand.

Andreason, M.W., Mudfod B., and Onge, J.E.St. 1997. Geologic Evolution and Petoleum System of the Thailand Andaman Sea Basins. In proceedings of the Petroleum Systems of SE Asia and Australasia Conference May, 1997, pp. 337-350. Indonesian Petroleum Association.

Beckinsale, R.D., Suensilpong, S., Nakapadungrat, S., and Walsh, J.N. 1979. Geochronology and geochemistry of granite magmatism in Thailand in relation to a plate tectonic model. Journal of the Geological Society.136: 529-540.

Charusirisawad, R. 1996. Reprocessing of seismic data from the Mergui Basin, Andaman Sea, Thailand. Master's Thesis, Department of Geosciences, Tulsa University.

Curray, J.R., Moore, D.G., Lawver, L.A., Emmel, F.J., Raitt, R.W., Henry, M., and Kieckhefer, R. 1979. Tectonics of the Andaman Sea and Burma. In J.S. Watkins, J. Montadert and Montadert, L. (Eds). Geological and Geophysical Investigations of Continental Margins. pp. 189-198.

Curray, J.R. 2004. Tectonics and history of the Andaman Sea region. Journal of Asian Earth Science. 25: 187-232.

Dain, S.R. 1984. Structural evolution of the West Natuna Basin and the tectonic evolution of the Sunda region. In Proceeding of the Association of Petroleum Geologist of India, .14: 39-61.

Department of Mineral Fuels 2006. Petroleum assessment in Northeastern and Andaman region, Thailand. Atop Technology Co, Ltd., Bangkok, Thailand.

Department of Mineral Resources, (1996). Andaman Sea Basin Study. STS Engineering consultants Co., Ltd., Bangkok, Thailand.

REFERNCES

Department of Mineral Resources. 2007. Geology of Thailand. Thailand's Department of Mineral Resources. Ministry of Natural Resources and Environment. Bangkok.

Harding, T.P. 1985. Seismic characteristic and identification of negative flower structures, positive flower structures, and positive structures inversion. Bull. Am. Assoc. Petrol. Geol. 69: 582-600.

Hutchison, C.S. 1975. Ophiolites in Southeast Asia. Geological Society of American Bull. Geol. Soc. Am. 86: 797-806.

Hutchison, C.S. 1977. Granite emplacement and tectonic subdivision of Peninsular Malaya. Bull. Geol. Soc. Malaysia. 9: 187-207.

Khursida, P. 2002. Subsurface Geology of the Southern part of Tertiary Mergui Basin, Andaman Sea. Master's Thesis. Department of Geology, Faculty of Science, Chulalongkorn University.

Le Dain, A.Y., Tapponnier, P. and Molnar, P. 1984. Active faulting and tectonics of Burma and surrounding regions. Journal of Geophysical Research, 89. 453-472.

Molnar, P. and Tapponnier, P. 1975. Cenozoic Tectonic of Asia; effects of a continental collision. Science. 189: 419-426.

Morley, C.K. 2002. A tectonic model for the Tertiary evolution of strike–slip faults and rift basins in SE Asia. Journal of Tectonophysics. 347: 189-215.

Mukhopadhyay, M. 1984. Seismotectonics of subduction and back-arc rifting under the Andaman Sea. Tectonophysics. 108: 229-239.

Nakanart, A. and Mantajit, N. 1983. Stratigraphic correlation of the Andaman Sea. Conf. on Geol. And Min. Res. Of Thailand. Bangkok. 19-28. pp.7.

Packham, G. 1993. Plate Tectonics and Development of Sedimentary Basin of the dextral regime in Western Southeast Asia. Journal of Southeast Asian Earth Sciences. 8: 497–511.

REFERNCES

Paul, D.D. and Lian, H.M. 1975. Offshore Tertiary basins of S.E. Asia, Bay of Bengal to South China Sea. In Proceeding of the 9th World Petroleum Congress. Exploration in t he Far East outside Japan. 107-121.

Peter, G., Weeks, L.A. and Burns, R.E. 1966. A reconnaissance geophysical surveyin the Andaman Sea and across the Andaman-Nicobar Island Arc. J. Geophys. Res. 11: 495- 509.

Polachan, S. 1988. The geological evolution of the Mergui Basin, SE Andaman Sea, Thailand, Doctoral dissertation, PhD.Thesis, London University.

Polachan, S. and Racey, A. 1994. Stratigraphy of the Mergui Basin, Andaman Sea: Implications for Petroleum Exploration. Journal of Petroleum Geology. 17 (4): 373-406.

Polachan, S., Pradidtan, S., Tongtaow, C., Janmaha, S., Intarawijitr, K., Sangsuwan, C. 1991. Development of Cenozoic basins in Thailand, Marine and Petroleum Geology, 8, 84-97.

PTT Exploration and Production Public Co., Ltd. 2010. Structural Evolution and Tectonostratigraphic Correlation for the Southern Mergui Basin. Department of Geology, Chulalongkorn University, Bangkok.

Ridd, M.F. 1971. Southeast Asia as part of Gondwanaland. Nature. 234: 531-533.

Rodolfo, K.S. 1969. Bathymetry and marine geology of the Andaman Sea Basin, and tectonic implications for Southeast Asia. Bull.Geol. Soc. Am. 80: 1,203-1,230.

Sheriff, R.E. 1980. Seismic stratigraphy: International Human Resources Development Corporation. United States. America.

Shouls, M.M. 1973. Seismicity and plate tectonics in the Thaialnd-Burma-Andaman Sea area. CCOp. Newsletters. 1: 17-19.

Srikulwong, S. 1986. Structural evolution and sedimentation during the Oligocene, in the vicinity of the W9-E-1 Well, Mergui Basin, Andaman Sea, Thailand. Master's Thesis. Science in Petroleum Geology, Aberdeen University.

REFERNCES

Srikulwong, S. 2005. Potential of petroleum geology in Thailand. The Department of Mineral Fuels. Ministry of Energy. Bangkok.

Srisuriyon, K. 2008. Structural style and evolution of the northern Mergui Basin, Andaman Sea, Thailand. M.Sc. Thesis. Science in Petroleum Geosciences, Aberdeen University.

Suensilpong, S. 1977. The role of plate collision in tin mineralization in Thailand. In Proceeding of the 7th Circum-Pacific Plutonism Project meeting, Japan. pp. 9.

Suensilpong, S., Putthapiban, P., and Mantajit, N. 1981. Some aspects of tin granite and its relationship to tectonic setting. Geol. Soc. Am. Spec. Vol. 9.

Tananchai, M. 2004. Seismic Stratigraphy and Seismic Facies Analysis of the Mergui Basin, Thai Andaman Sea. M.Sc. Thesis. Science in Petroleum Geology, Aberdeen University.

Tapponnier, P., Peltzer. G., Le Dain, A. Y., Armijo, R., and Cobbold, P. 1982. Propagating extrusion tectonics in Asia: new insights from simple experiments with plasticene. Geology. 10: 611-616.

Tapponnier, P., Peltzer. G., and Armijo, R. 1986. On the mechanics of the collision between India and Asia. In Ramsey, J. G., Coward,M. P., and Ries, A. (Eds.), Collision Tectonics. Geological Society, London, Special Publications.19: 115-157.

Thipyopass, S. 2010. Paleoearthquake investigation along the Ranong Fault Zone, Southern Thailand. M.Sc. Thesis. Science in Petroleum Geosciences, Aberdeen University. Master's Thesis, Department of Geology, Faculty of Science, Chulalongkorn University.

Weeks, L.A., Harbison, R.N., and Peter, G. 1967. Island arc system in the Andaman Sea. Bulletin of American Association of Petroleum Geologists. 51: 1,1803-1,815 .